



Degree Project in Space Technology

Second cycle, 30 credits

Towards a Demisable Satellite Platform

Design for Demise State of the Art, Development Roadmap and
DRACO mission contribution

SARA SANCHIS CLIMENT



Degree Project in Space Technology

Second cycle, 30 credits

Towards a Demisable Satellite Platform

Design for Demise State of the Art, Development Roadmap and DRACO mission contribution

SARA SANCHIS CLIMENT

Date: April 21, 2025

Master's Programme: Aerospace Engineering

KTH Supervisor: Christer Fuglesang

Company Supervisor: Antonio Caiazzo

Examiner: Christer Fuglesang

Host company: The European Space Agency

(This page intentionally left blank)

Abstract

The increasing presence of space debris poses significant risks to the sustainability of space operations. ESA's Clean Space Initiative is addressing this issue through its Zero Debris approach, which aims to prevent the creation of new debris by ensuring that all future missions are designed considering a sustainable End of Life management. A key part of this is the Design for Demise (D4D) strategy, which aims to ensure that satellite components burn up during atmospheric re-entry, thereby minimising the risk of debris reaching the Earth's surface. This thesis presents a state of the art review of existing D4D strategies, analysing and comparing their effectiveness. It also evaluates current demisable technologies, taking into account their Technology Readiness Levels, applications, and how demisable they are. This evaluation links the technology to the D4D strategies, identifying how they contribute to the overall satellite demisability. Additionally, the review identifies gaps in existing research and areas requiring further technological development, to define a technology development roadmap towards achieving a demisable satellite platform.

The thesis also addresses the uncertainties surrounding on ground testing and simulations for demise evaluation. To further this, the Destructive Re-entry Assessment Container Object (DRACO) mission is explained, as it seeks to improve the understanding of the demise process by validating current demise simulation tools and on ground testing with in-flight data. DRACO will study the demise of Objects of Interest (OoI) integrated in the platform using cameras, thermocouples and spectroscopic markers. Among other things, the thesis presents the trade-off performed on how to integrate and locate the sensors and OoI within the platform. The scientific return from DRACO will contribute significantly to refining D4D strategies and improving satellite design for future missions.

Keywords: Demise, D4D, Zero Debris, End of Life management, re-entry, Clean Space, DRACO, Spectroscopic markers.

Sammanfattning

Den ökande mängden rymdskrot utgör betydande risker för hållbarheten av rymdverksamhet. ESAs Clean Space-initiativ hanterar detta problem genom sin Zero Debris-strategi, som syftar till att förhindra uppkomsten av nytt rymdskrot genom att säkerställa att alla framtida uppdrag utformas med en hållbar sluthantering i åtanke. En central del av detta är Design for Demise (D4D)-strategin, som har som mål att säkerställa att satellitkomponenter brinner upp vid atmosfärisk återinträde, vilket minimerar risken för att rymdskrot når jordens yta. Denna avhandling presenterar en översikt av den aktuella forskningen kring befintliga D4D-strategier, där deras effektivitet analyseras och jämförs. Den utvärderar även nuvarande demiserbara teknologier med hänsyn till deras teknologiska mognadsnivåer (TRL), tillämpningsområden och nedbrytningsförmåga. Genom denna utvärdering kopplas teknologin till D4D-strategierna, vilket identifierar hur de bidrar till den övergripande demiserbarheten hos satelliter. Dessutom identifierar genomgången forskningsluckor och områden som kräver ytterligare teknologisk utveckling, i syfte att definiera en utvecklingsplan för att uppnå en fullt demiserbar satellitplattform.

Avhandlingen behandlar även de osäkerheter som finns kring markbaserade tester och simuleringar för utvärdering av satelliters uppbrytning. För att adressera detta presenteras Destructive Re-entry Assessment Container Object (DRACO)-uppdraget, som syftar till att förbättra förståelsen av uppbrytningsprocessen genom att validera nuvarande simuleringar och markttester med flygdata. DRACO kommer att studera uppbrytningen av Objects of Interest (Ooi), som är integrerade i plattformen, med hjälp av kameror, termoelement och spektroskopiska markörer. Bland annat presenterar avhandlingen den trade-off-analys som utförts kring hur sensorer och Ooi ska integreras och placeras inom plattformen. De vetenskapliga resultaten från DRACO kommer att bidra väsentligt till att förbättra D4D-strategier och optimera satellitdesignen för framtida uppdrag.

Nyckelord: Demise, D4D, Zero Debris, End of Life-hantering, återinträde, Clean Space, DRACO, spektroskopiska markörer.

Acknowledgements

After almost two years of pursuing this MSc in Aerospace Engineering, four years of a BE in Aerospace Engineering at UPV, and two incredible internships, the journey feels like it has only just begun. Success is never the result of a single effort but rather the collective support, inspiration, and kindness of many. With profound gratitude, I would like to acknowledge the individuals without whom the completion of this thesis would not have been possible.

First and foremost, I express my heartfelt thanks to my parents, my sister, and Carlos for their endless love, encouragement, and belief in my abilities. Your unwavering support, patience, and understanding have been the foundation not only of my academic pursuits but also of the person I am today. Dad and Mum, I am forever grateful for the opportunities you have given me to follow my dreams and for teaching me to never stop asking questions.

I am also deeply grateful to my coworkers at ESA's Clean Space Office for welcoming me as one of their own and treating me like family. Tiago, Roxane, Jessica, Marco, Daniele, Sara, Julie, Sibyl, Andrew, Enrico, Christian, and Calumn, each of you has taught me something valuable, and I sincerely appreciate the time you invested in me. Your dedication to making space more sustainable and cleaner has been truly inspiring. A special thank you to:

Lea, for being the best "office mate" I could have wished for, for your support, our daily chats, and all the laughter we shared.

Stijn, for the D4D masterclasses and for opening doors to exciting projects.

And especially, Beatriz, for your patience, guidance, and for always taking the time to teach me, no matter how busy you were. Your encouragement gave me the confidence to tackle new challenges, going outside of my comfort zone. You gave me invaluable professional and personal advice while continuously pushing me to grow. Your dedication and generosity have left a lasting impact on me, and I am incredibly grateful for everything you have done.

I also express my profound gratitude to my thesis tutor at ESA, Antonio, who has accompanied me from the very first day. Your expertise, guidance, and support have been invaluable throughout this journey, and your passion for Clean Space has been truly inspiring.

To KTH, I extend my sincere appreciation for all the resources, facilities, and education that have shaped my academic experience. As Mahatma Gandhi said, *"Live as if you were to die tomorrow. Learn as if you were to live forever."*

A special thanks to my thesis tutor at KTH, Christer. Your prompt and thorough feedback were truly invaluable. Your support helped me shape this thesis on time, and for that, I am truly grateful.

Finally, to Andrea and Ainhoa, my besties, my second family in the Netherlands. Thank you for opening your home to me, for treating me like a sister, and for filling my days with laughter, warmth, and unconditional support. And to Martin, our intern, your company, countless shared teas, and endless encouragement made even the busiest days more enjoyable. In a world where some promises fade, friendship remains a quiet force that never overpromises and never underdelivers. Throughout this journey, your friendship has been a constant source of strength, and your support during my internship was fundamental in shaping this thesis into its final form.

Eternally grateful for the people who turned this chapter of my life into an unforgettable story,

Sara

Contents

Abstract.....	i
Sammanfattning	ii
Acknowledgements	iii
List of Figures.....	vii
List of Tables.....	x
Acronyms	xi
1. Introduction.....	1
1.1. Statement of purpose	2
1.2. Objectives	2
1.3. Socioeconomic impact.....	2
1.4. Approach	3
2. State of the art	4
2.1. Satellite development history.....	4
2.2. Current situation of debris	5
2.2.1. Sources of Space Debris	6
2.2.2. Increasing Collision Risk and the Kessler Syndrome	6
2.3. Clean Space and End-of-life management.....	7
2.3.1 EcoDesign	8
2.3.2 In Orbit Servicing	8
2.3.3 Management of End-of-Life Operations	9
2.4. Regulatory framework and guidelines	10
3. Design for Demise.....	14
3.1. Identification of critical elements for re-entry	15
3.2. Demise and Containment strategies.....	19
3.2.1. Maximise available heat	19
3.2.2. Minimise required heat.....	20
3.2.3. Optimise heat transference	20
3.2.4. Design for Containment	21
3.3. Observation campaigns	21
3.4. Re-entry modelling and re-entry demise analysis tools.....	23
3.5. Demise on-ground testing facilities	25
3.6. Prospective missions: DRACO.....	27
4. D4D ESA activities.....	29
4.1. Material level activities	29
4.1.1. Ceramics and Glasses	30

4.1.2. Metal Alloys.....	33
4.1.3. Composites	38
4.1.4 Ablative Materials	40
4.1.5 Demisability Summary of Materials	41
4.2. System level activities.....	42
4.2.1. Structural panels	43
4.2.2. Joints	44
4.2.3. Solar panels	44
4.2.3. Solar Array Deployment Mechanisms	45
4.2.4. Batteries	45
4.2.5. Electronic cards and boxes	47
4.2.7. Tanks	48
4.2.8. Thrusters.....	49
4.2.9. Balance masses	50
4.2.10. Reaction Wheels	51
4.2.11. Magnetorquers	52
4.2.12. Gyroscopes	53
4.2.13. Star trackers	53
4.2.14. Optics	55
4.3. Technology development activities.....	57
4.3.1. Structural Panels	58
4.3.2. Joints.....	59
4.3.3. SADM	65
4.3.4. Propellant tanks.....	66
4.3.5. Reaction Wheels.....	72
4.3.6. Magnetorquers	74
4.3.7. Optics	75
4.3.8. Design for Containment	77
5. D4D technology gaps and development roadmap	80
5.1. D4D gaps for fully demisable platform	80
5.1.1. Critical components with unstudied demisability.....	80
5.1.2. Critical Components Without Existing D4D Technologies	81
5.1.3. D4D Technologies Requiring Further Maturation	81
5.2. D4D proposed development roadmap	82
5.2.1. Engines and Fill and Drain Valves demise behaviour.....	83
5.2.2. Helicoils influence in demise	83

5.2.3. Antennas and Communication Payloads demise behaviour	83
5.2.4. Demisable Gyroscope	84
5.2.5. Demisable Thruster	84
5.2.6. Batteries and Electronic Cards and Boxes demise enhancement.....	85
5.2.7. Demisable Star Tracker	85
5.2.8. Demisable Balance Masses	86
5.2.9. Demisable structural panels and joints development roadmap	86
5.2.10. Demisable SADM development roadmap	87
5.2.11. Demisable Propellant tanks development roadmap	87
5.2.12. Demisable Reaction Wheels development roadmap	88
5.2.13. Demisable Magnetorquer development roadmap	88
5.2.14. Demisable Optics development roadmap.....	88
5.2.15. Design for Containment development roadmap.....	89
5.3. Scalability and mass production	90
6. D4D implementation in DRACO mission and scientific return	92
6.1 DRACO Objects of Interes	93
6.2 Spectroscopic markers characterisation	94
6.2.1 Integration of Ool: COPV tanks	95
6.2.2 Software tool PRODUCERS simulations	99
6.3 Cameras' location	103
6.3.1 Software tool EVENT SIMULATOR simulations.....	103
7. Conclusions	106
Bibliography.....	107
Appendix	113

List of Figures

Figure 1: CubeSats form factor configurations illustration [6].	4
Figure 2: Growing quantity of tracked space debris and spacecrafts operating Earth over time [10].	5
Figure 3: Illustration of the Soviet Kosmos - 1408 destruction [13].	6
Figure 4: Relationship between altitude and orbital lifetime [18].	7
Figure 5: Clean Space branches [19].	8
Figure 6: Passivation techniques [21].	9
Figure 7: Illustration of satellite demising [22].	10
Figure 8: EOL decision making process [20].	11
Figure 9: MTQ burning up in a PWT before and after the test [25].	14
Figure 10: SAR antenna from Oxford Space System [27].	18
Figure 11: LCT concept of DLR German Space Center and TESAT-Spacecom [28].	18
Figure 12: Satellite early break up fragmentation concept [29].	20
Figure 13: BUC Infrared Camera and SatCom [30].	22
Figure 14: Cluster II re-entry illustration [32].	22
Figure 15: ESA DRAMA software tool and its 5 modules.	24
Figure 16: Comparative panel of re-entry simulation testing facilities with respect to condition fidelity and setup complexity [9].	25
Figure 17: Schematic of VKI Plasmatron facility [35].	27
Figure 18: DRACO ConOps.	28
Figure 19: Silicon carbide SSiC ultra-pure – Photographs before and after testing in L2K PWT test [37].	31
Figure 20: Silicon carbide SSiC ultra-pure – Photographs before and after testing in L3K PWT test [37].	31
Figure 21: Video frames from test of Qz-HS50 in subsonic (top) and supersonic (bottom) conditions showing their ablation mechanisms [38].	31
Figure 22: Fused Silica 10 mm diameter rod demise behaviour in PWT test [39].	32
Figure 23: Video frames from test of Ze-HS30-A (top) and Ze-HS50-A (bottom) conditions showing their ablation mechanisms [38].	32
Figure 24: Zerodur demise behaviour in PWT test [39].	33
Figure 25: Aluminium alloy 7075 – Photographs before and after testing in DLR's PWT [37].	34
Figure 26: Stainless steel AISI 316 – Photographs before and after testing in DLR's PWT [37].	35
Figure 27: Titanium alloy Ti6Al4V – Photographs before and after testing in L2K DLR PWT [37].	36
Figure 28: Titanium alloy Ti6Al4V – Photographs before and after testing in L3K DLR PWT [37].	36
Figure 29: Haynes 25 demise behaviour and oxide layer collapsing in PWT test [40].	36
Figure 30: Inconel 718 demise behaviour and oxide layer collapsing in PWT test [40].	37
Figure 31: Molybdenum and Titanium screws demise behaviour in PWT test [41].	37
Figure 32: Tungsten cube demise behaviour in PWT test [41].	38
Figure 33: Average CFRP layer by layer demise in DLR's PWT test [42].	39
Figure 34: CFRP, FFRP, CF-FFtbt, CF-FFpbp after testing. On the right, a closer view of the ply-by-ply hybrid, with a clear view of the central twill flax ply near a full demise with only carbonated Flax Fibres left [9].	39
Figure 35: GFRP sheet of battery module demise behaviour in stagnation configuration in DLR's PWT facilities [44].	40
Figure 36: Behaviour of ablative materials [46].	41

Figure 37: Sensitivity analysis of demisability index respectively for factors influencing demise [47].	42
Figure 38: 4 ply CFRP Sandwich Panel Before and After Panel Removal; Elliptic Recession of Honeycomb Evident [48].	43
Figure 39: Battery Module demise behaviour in DLR's static PWT test [44].	46
Figure 40: Battery Module demise behaviour in dynamic PWT test and high-flux conditions [44].	46
Figure 41: EnMAP Electronics Card demise behaviour in DLR's PWT facilities [44].	47
Figure 42: BCM Electronics Module demise behaviour in DLR's PWT facilities [44].	47
Figure 43: 50 mm diameter nozzle of Haynes 25 demise behaviour in DLR's PWT test [40].	50
Figure 44: Whole thruster at 0 ° demise behaviour in DLR's PWT test [40].	50
Figure 45: Test RW90 events sequence from housing significant material removal to completely removed with the cage leaving the motor and flywheel (from left to right) [55].	51
Figure 46: MTQ demise behaviour in PWT test, showing the CFRP burn through, layer-by-layer Coil removal and core melt from up to down [55].	52
Figure 47: Star tracker demise behaviour in DLR's static PWT test and high-flux conditions [44].	54
Figure 48: Holes bipod demise behaviour in DLR's PWT test [39].	56
Figure 49: OHB Bolted and bonded cleat to panel joint with the temperature sensitive side at the outer panel (left) and inner panel (right) [58].	59
Figure 50: OHB two SMA bolts in a cleat joint externally mounted in PWT testing [58].	60
Figure 51: TAS Thermally Triggered Fastener Joint [58].	61
Figure 52: Absorption contrast of short and continuous CF/PEEK bolts [9].	64
Figure 53: KARMA-4 TG SADM from KDA [52].	65
Figure 54: ADS and Orbital ATK UK large Aluminium tank with its bolted halves [62].	67
Figure 55: MTA large Aluminium tank with its EPDM diaphragm [63].	67
Figure 56: Institute of Aviation small Aluminium tank after FSW [64].	69
Figure 57: PEAK small COPV tank illustration [65].	70
Figure 58: Haydale Composite solutions large hybrid composite tank illustration [64].	71
Figure 59: PEAK small COPV Krypton tank illustration [66].	72
Figure 60: Demisable RWs Rockwell Collins illustration [64].	73
Figure 61: Demisable MTQ LusoSpace illustration [68].	74
Figure 62: OHB D4C Spectrometer Thermal Guard [69].	77
Figure 63: OHB D4C Optical Bench and Mounting Solutions [69].	77
Figure 64: OHB D4C Feet/Bipods Connected by Tether [69].	78
Figure 65: OHB D4C Electronic Units in a Net/Cage [69].	78
Figure 66: DRACO Design platform concept [36].	92
Figure 67: Emission spectra of common materials in the Ool and in the markers [70].	94
Figure 68: Data-logger circumferential layer ceramic paper [72].	97
Figure 69 a and b: Thermocouple placement coordinate system and thermocouple application on Al liner, respectively [72].	98
Figure 70: PRODUCERS analysis process workflow [73].	100
Figure 71: Example EquilibriumShock Shock Layer Temperature Plot PRODUCERS [73].	101
Figure 72: Example FragmentGasEmission Indicative Radiance Plot PRODUCERS [73].	101
Figure 73: Example GenerateTimeline Object Demise Timeline PRODUCERS [73].	102
Figure 74: DDCU connectivity of a DRACO re-entry study case at around 120 km and 45 km of altitude respectively.	104
Figure 75: EVENT SIMULATOR's workflow.	104

Figure 76: DRACO simplified CAD with the FoV of the on-board cameras in green with the tanks' camera on the centre of the mid-panel looking downwards..... 105

Figure 77: DRACO simplified CAD with the tank on-board camera at the corner of the lower box of the platform. 105

Figure 78: DRACO simplified CAD with the tank on-board camera at the middle of the lower side of the mid-panel. 105

Figure 79: D4D development roadmap for a demisable satellite platform. 114

List of Tables

Table 1: ESA Space Debris Mitigation Compliance Verification Guidelines Relevant Requirements [1].	11
Table 2: Critical components for demisability and reasons.....	16
Table 3: D4D Technologies with their TRL and company that develops them.	81
Table 4: Proposed thermocouple Positions for COPV PEAK Tank.	97
Table 5: Trade-off marker integration manufacturing options.	99
Table 6: Summary of demise behaviour of components part 1.....	113
Table 7: Summary of demise behaviour of components part 2.....	113

Acronyms

ADN	Ammonium Dinitramide
ADR	Active Debris Removal
AM	Additive Manufacturing
ASAT	Anti-satellite
BBU	Ball Bearing Unit
CA	Casualty Area
CAS	Collision Avoidance Systems
CF	Carbon Fibre
CFD	Computational Fluid Dynamics
CFRP	Carbon Fibre Reinforced Polymer
CIRA	Italian Aerospace Research Centre
CoG	Centre of Gravity
COPV	Composite Overwrapped Pressure Vessel
COTS	Commercial Off-The-Shelf
CR	Casualty Risk
CSID	Clean Space Industry Days
CTE	Coefficient of Thermal Expansion
CuBe	Copper-Beryllium
D4C	Design for Containment
D4D	Design for Demise
DC	Demise Criterion
DDCU	Demise Data Collection Unit
DoF	Degrees of Freedom
DLR	German Aerospace Centre
DMA	Dynamic Mechanical Analysis
DRACO	Destructive Re-entry Assessment Container Object
DRAMA	Debris Risk Assessment and Mitigation Analysis
DSC	Differential Scanning Calorimetry
EoL	End of Life
EPDM	Ethylene Propylene Diene Monomer
ESA	European Space Agency
FAR	Flight vehicles, Aerothermodynamics and Re-entry missions engineering
FEM	Finite Element Models
FFRP	Flax Fibre Reinforced Polymer
FoV	Field of View
FPA	Focal Plane Array
FRP	Fiber-Reinforced Polymers
FSW	Friction Stir Welding
GEO	Geosynchronous Equatorial Orbit
GEU	Gyro Electronics Unit
GFRP	Glass Fibre Reinforced Polymer
H2O2	High-Concentrated Hydrogen Peroxide
IRS	Institute of Space Systems
JRC	Joint Research Centre
LCA	Life Cycle Assessment
LCT	Laser Communication Terminal
LEO	Low Earth Orbit

MMC	Metal-Matrix Composite
MTQ	Magnetorquer
OoI	Objects of Interest
PCB	Printed Circuit Board
PWT	Plasma Wind Tunnel
RACS	Roll and Attitude Control
REBR	Re-Entry Break up Recorder
RW	Reaction Wheels
SADM	Solar Array Deployment Mechanism
SAR	Synthetic Aperture Radar
SARA	re-entry SurvivAl and Risk Analysis
SDGs	Sustainable Development Goals
SDMR	Space Debris Mitigation Requirements
SERAM	Spacecraft Entry Risk Analysis Module
SESAM	Spacecraft Entry Survival Analysis Module
SiC	Silicon Carbide
SMA	Shape Memory Alloy
SRC	Static Re-entry simulation Chambers
TAS	Thales Alenia Space
TGA	Thermo-Gravimetric Analysis
TPS	Thermal Protection Systems
TRL	Technology Readiness Levels
VKI	Von Karman Institute
ZD	Zero Debris

(This page intentionally left blank)

1. Introduction

The present document describes the execution of the Master Thesis Project: “Towards a Demisable Satellite Platform”. This thesis aims to provide a state-of-the-art analysis of Design for Demise (D4D) strategies and technologies, identifying existing solutions, ongoing developments, and gaps that need to be addressed to enable the design of fully demisable satellite platforms. It assesses the current Technology Readiness Level (TRL) of demisable components and their demise compliance, and proposes a development roadmap to ensure that all components required for a demisable platform are available as Commercial Off-The-Shelf (COTS) solutions.

Since this platform aims to be in line with the European Space Agency (ESA) Clean Space Zero Debris (ZD) Approach and compliant with ESA’s Space Debris Mitigation Requirements (SDMR) [1], it also provides an overview on the space debris issue, justifying why debris mitigation strategies, including D4D, are necessary, and when are they applicable.

The uncontrolled re-entry of space debris poses an increasing risk to human safety, with a few hundreds of catalogued objects re-entering Earth's atmosphere per year. A significant fraction of their mass, typically 20 - 40%, can survive the re-entry, impacting the Earth's surface with high kinetic energy [2]. Intending to attenuate this risk, it is imperative to have demisable satellite platforms, which is the focus of this thesis.

A fundamental aspect of implementing D4D is considering mission-specific design constraints. Different satellite types use distinct components, influencing their material choices, structural configurations, and trade-off criteria. However, developing a demisable platform adaptable to multiple payloads could significantly enhance efficiency and reduce satellite development costs. A standardised approach to D4D could also facilitate SDMR compliance, promoting the sustainable use of space.

A major challenge in advancing D4D technologies is the limited availability of validation data for destructive re-entry, particularly in the 50 - 100 km altitude range, where most critical break up events occur. The Destructive Re-entry Assessment Container Object (DRACO) mission aims to provide in-situ observations of a satellite’s demise to improve our understanding of demise physics and enhance the predictive accuracy of simulation models and on-ground Plasma Wind Tunnel (PWT) testing. This thesis explores how to obtain the maximum scientific return possible from DRACO’s re-entry, focusing on sensors distribution and integration in the satellite so that the data acquired in DRACO can be leveraged to refine simulations and on-ground testing, and consequently the design and validation of demisable technologies, ensuring their effectiveness in real re-entry scenarios.

To conclude, the outcomes of this thesis hold relevance for ESA and the space industry, providing a foundation for future steps on satellite platform designs that align with space sustainability objectives. The insights gained could help improve existing spacecraft architectures, support the development of new demisable designs, and ultimately reduce the risks associated with satellites and space debris re-entry.

1.1. Statement of purpose

This Master Thesis Project examines the challenges associated with the implementation of D4D technologies and the role they play in mitigating the risks posed by space debris. Thus, the aim of the project is to develop a technology roadmap that outlines the necessary steps to achieve fully demisable satellite platforms, identifying technology gaps, assessing the readiness of existing COTS solutions and exploring how to get the most scientific return from DRACO's in-situ observations to enhance re-entry simulations and on-ground testing. This study aligns with ESA's Clean Space ZD approach, contributing to the sustainability of space operations.

1.2. Objectives

The objective of this MSc Thesis is to analyse the current state of D4D technologies, identify gaps, and define a development roadmap to ensure the availability and validation of all critical components required for demisable satellite platforms. This includes:

- Conducting a state-of-the-art review of existing D4D solutions and their TRLs.
- Mapping the technological gaps that need to be addressed to enable a fully demisable platform.
- Proposing a development roadmap to advance demise-enabling COTS components toward market readiness.
- Assessing how DRACO's in-situ re-entry data can improve simulation models and ground-based testing for demisable components validation.
- Ensuring alignment with ESA's SDMR and fostering compliance within the industry.

1.3. Socioeconomic impact

Investment in the space industry has brought technological advances for decades and has responded to social needs having an enormous impact on humanity. The rapid increase in satellites, particularly with the rise of mega-constellations, poses a significant threat to both economically and scientifically vital orbital regions, since the impact of losing these satellites would be immense on the overall economy. Furthermore, space debris re-entry is becoming more frequent, increasing also the number of surviving debris impacts in the Earth's surface. Due to this situation, ESA has called for immediate action [3].

To address these concerns, protected zones for Low Earth Orbit (LEO) and Geosynchronous Equatorial Orbit (GEO) have been established, and several mitigation strategies are under development to minimise the impact of space operations in the orbital environment, reduce the collision risk on orbit, and ensure the safety of the Earth population when re-entry takes place. D4D is one of the most promising solutions, ensuring that satellites are designed to demise upon atmospheric re-entry, thereby reducing the risk to both orbital and terrestrial environments.

Beyond improving space safety, advancing D4D technologies and defining a clear roadmap for their implementation supports several United Nations Sustainable Development Goals (SDGs) [4] by promoting environmental responsibility and sustainable resource management:

- **SDG 8. Decent Work and Economic Growth:** The influence of satellites and all their applications in the global economy is enormous. Thus, developing sustainable satellites

for which the economic investment necessary is decreased compared to the current market, allows to promote sustained, inclusive, and suitable economic growth.

- **SDG 9. Industry, Innovation, and Infrastructure:** Encouraging sustainable industrialisation in the space sector through the development of demisable technologies.
- **SDG 12. Responsible Consumption and Production:** D4D promotes sustainable practices in satellite manufacturing and disposal, implementing efficient production patterns from the economic, technologic and time perspectives.
- **SDG 13. Climate Action:** D4D takes urgent action to combat climate change and its impacts, mitigating environmental impacts by reducing space debris and ensuring a sustainable orbital environment.
- **SDG 14. Life Below Water and SDG.15 Life on Land:** D4D prevents space debris from reaching the Earth's surface, mostly in the oceans and also in land. It contributes to conserve and protect the maritime and terrestrial ecosystems and biodiversity.

Additionally, advancing D4D technologies fosters a more sustainable space economy, supports innovation, and ensures that future generations can continue to benefit from satellite services without exacerbating the current space debris crisis. This research is closely related to recent international efforts, particularly the “ESA Space Debris Mitigation Compliance Verification Guidelines” [1]. These guidelines, while not yet legally binding, are shaping the future of satellite design and the implementation of the Clean Space initiative [5], an eco-friendly approach to preserving the orbital environment.

1.4. Approach

The methodology of this thesis follows a structured approach to assessing the feasibility and development path of D4D technologies:

1. State-of-the-Art Analysis:

- Reviewing the current landscape of D4D-enabling technologies, including materials, structural design, and component integration.
- Identifying technology gaps and limitations that hinder the development of demisable satellite platforms.

2. Development Roadmap for D4D Technologies:

- Outlining the steps required to mature D4D technologies from concept to commercial availability.
- Evaluating the alignment of emerging D4D solutions with ESA's SDMR.

3. Leveraging DRACO Data:

- Examining how DRACO's in-situ observations can enhance re-entry modelling, simulation tools, and validation testing.
- Analysing which sensors to use and how to incorporate and distribute them within the satellite to get the maximum scientific return possible from the re-entry.

By structuring the thesis around these core areas, the study aims to provide a practical and actionable roadmap for the development and validation of D4D technologies, ensuring their readiness for future missions and long-term space sustainability.

2. State of the art

The increasing presence of artificial satellites in Earth's orbit has brought significant advancements in communication, navigation, and Earth observation. However, it has also led to a growing challenge: space debris accumulation. The long-term sustainability of space activities depends on effective strategies to mitigate debris generation and ensure the safe disposal of satellites at the end of their operational life.

This section presents an overview of the state of space sustainability initiatives, beginning with a brief history of satellite development and the evolution of space debris concerns. It then explores the current debris situation, emphasising the risks posed by uncontrolled re-entries and the need for enhanced D4D technologies. Furthermore, ESA's Clean Space initiative is introduced, highlighting its role in fostering eco-friendly and ZD satellite design practices. Lastly, the existing regulatory frameworks and End of Life (EoL) management guidelines are discussed providing context for the development of a roadmap toward demisable satellite platforms.

2.1. Satellite development history

Human beings have been venturing into space since the first space mission, Sputnik 1 in 1957, up to the present. Initially, satellites were developed for scientific and military purposes, but over time, their applications diversified to include telecommunications, navigation, Earth observation, and space exploration. This made satellites indispensable to humanity, supporting weather forecasting, disaster management, global connectivity and scientific research.

Throughout the 20th century, space activities were dominated by a few government agencies, including NASA, ESA, Roscosmos, and CNSA. These organisations focused on large, complex satellites with long operational lives. However, with advancements in miniaturisation, propulsion, and launch capabilities, the commercial space sector emerged. In 1999, a revolution in satellite design started with the CubeSat, designed for space exploration and research enabling academic purposes. A CubeSat is a small satellite based on a form factor of a 10 cm square cube known as unit (U). The original design was composed of a single cube (1U), which evolved to new designs usually formed by a combination of multiple cubes, as illustrated in Figure 1, forming even 27U. These larger CubeSat sizes have become more standardised and spread in the past years since they allowed science missions for a lower cost with additional volume, power, and an overall increase in capability with respect to older satellites [6].

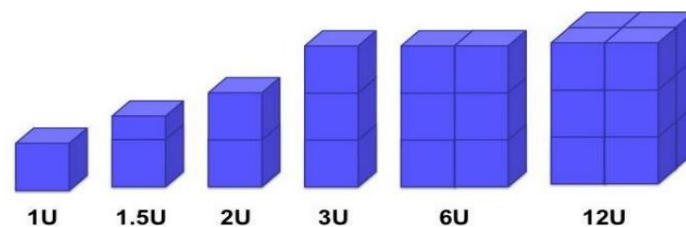


Figure 1: CubeSats form factor configurations illustration [6].

Moreover, companies like SpaceX, OneWeb, and Amazon's Project Kuiper have fuelled the growth of mega-constellations, deploying thousands of satellites to provide global broadband coverage. While this enhanced connectivity worldwide, it also drastically increased the number of objects in orbit. In fact, SpaceX at 2019, manifested its intention to put into orbit more than 4.5 times satellites this decade on its own than humans have ever launched since Sputnik [7].

The advances in satellite design and launcher capabilities present projections for future growth, however, early satellite missions paid little attention to EoL disposal, leading to a steady accumulation of space debris, including inactive satellites, spent rocket stages, and mission-related fragments. As of March 5th 2025, there are more than 11800 satellites currently operating in-orbit, and prognoses for the upcoming increase in satellites suggest that there are many more to come together with the debris associated to their launches [8].

2.2. Current situation of debris

Since the dawn of space exploration, Earth's orbits have become an invaluable resource, hosting a growing number of satellites injected to accomplish diverse functions such as communication, navigation, defence, and scientific research. In recent years, the rapid increase in satellite launches has intensified orbital congestion, particularly in LEO is illustrated in Figure 2. In just the first 24 days of 2024, 104 new satellites were launched in 14 missions. This follows an unprecedented trend from 2023, where an average of 15 launches per month deployed 200 satellites, a 200% increase since 2020 [9]. This rise in activity has led to an exponential increase in the number of objects in space, increasing the risk of collisions and uncontrolled re-entries that could pose a hazard to both space operations and Earth's population.



Figure 2: Growing quantity of tracked space debris and spacecrafts operating Earth over time [10].

The space debris population includes defunct satellites, spent rocket stages, and fragments of these. Many of these objects remain in orbit long after their functional life, contributing to high-risk congestion zones, particularly in regions where fragmentation events occurred. As of early 2024 more than 36500 catalogued debris occupy Earth's orbit. It is estimated that about 1 million debris fragments range between 1 cm - 10 cm, while a 130 million pieces are between 1 mm - 1 cm [9]. These small yet hazardous fragments further complicate space sustainability efforts.

Approximately 24% of catalogued space objects are satellites, but fewer than a third remain operational. While over 660 in-orbit fragmentation events have been recorded since 1961, most were caused by explosions or structural failures rather than direct collisions. However, as the number of active and defunct objects in orbit continues to increase, experts predict that collisions will become the dominant source of new debris in the near future [11]. Inoperative satellites now account for around 22% of the 11500 currently functioning satellites, effectively acting as uncontrolled "flying mines" that could trigger cascading debris events [9].

A major contributor to the rising debris count is the previously introduced deployment of mega-constellations, such as Starlink and OneWeb. While they bring significant benefits, their scale presents challenges for long-term orbital sustainability. As satellite lifetimes decrease and older units are replaced, a continuous flow of deorbiting debris is introduced in the space environment, increasing the risk of accidental collisions and fragmentation events.

2.2.1. Sources of Space Debris

Space debris can be generated by several mechanisms, the most significant of which include:

- Accidental failures and collisions: Satellites and rocket bodies that malfunction or lose communication control in orbit and can lead to fragmentation or high-velocity collisions.
- Explosions: Residual propellants and onboard energy sources can trigger self-ignition due to material degradation in the harsh space environment, leading to destructive explosions that release thousands of debris fragments.
- Intentional destruction: Anti-satellite (ASAT) weapon tests have been a major factor in debris creation. In 2007, the Chinese FengYun-1C ASAT test alone increased the trackable debris population by 25% [12]. Similarly, in 2021, the Russian destruction of Kosmos-1408 using a surface-launched missile produced 904 catalogued objects [13], further aggravating orbital congestion as illustrated in Figure 3.



Figure 3: Illustration of the Soviet Kosmos - 1408 destruction [13].

2.2.2. Increasing Collision Risk and the Kessler Syndrome

As debris density increases, so does the likelihood of catastrophic collisions. The probability of such events occurring is estimated to be up to four times higher than in previous decades, raising concerns about the onset of the 'Kessler Syndrome', a self-sustaining chain reaction in which collisions generate additional debris, leading to an ever-increasing cascade of fragmentation [14]. If left unmitigated, this phenomenon could make certain orbital regions unusable for future missions, jeopardising both commercial and scientific space activities.

Currently, a growing number of "conjunction events" (close approaches between operational satellites and debris) have been reported in highly congested orbital zones. This has prompted space agencies and private operators to perform frequent collision avoidance manoeuvres, but as the number of debris objects continues to rise, these manoeuvres will become operationally unsustainable. ESA and other agencies are working on automated Collision Avoidance Systems (CAS) to reduce manual intervention and improve spacecraft safety. However, the continued rise in debris means even automated systems may struggle to prevent all high-risk events [15].

As space access becomes increasingly fundamental to global infrastructure, efforts must focus on balancing technological advancements with environmental responsibility. The impact of rising launch rates and deorbiting activities from mega-constellations and reusable launch vehicles like Starship further underscores the urgency of developing more sustainable debris management solutions. To mitigate space debris generation, international organisations have established protected zones in LEO and GEO, along with new regulations aimed at reducing collision risks and ensuring safe deorbiting procedures [16].

However, despite growing concerns, recent space debris focused events, including ESA's 8th Space Debris Conference and the 2nd International Orbital Debris Conference [17], have highlighted a severe lack of coordination between scientific institutions, industry stakeholders, and policymakers. The absence of binding regulations and political reluctance to enforce stricter space traffic management policies remain significant obstacles to addressing the problem effectively. Additionally, the lack of precise small debris tracking data leads to a systematic underestimation of risks, slowing down mitigation efforts.

While natural forces such as atmospheric drag and solar radiation pressure assist in gradually clearing debris from orbit, this process is slow and inadequate for long-live objects in high-altitude orbits. The relationship between altitude and orbital lifetime is presented in Figure 4 for different mass over area ratios. A big difference can be observed between spacecraft at 500 km which deorbit naturally in around 1 year (depending on the mass over area ratio), and spacecraft at 800 km of altitude, which would require around 100 years to deorbit naturally. This stresses the influence of atmospheric drag and solar radiation forces in the deorbiting process.

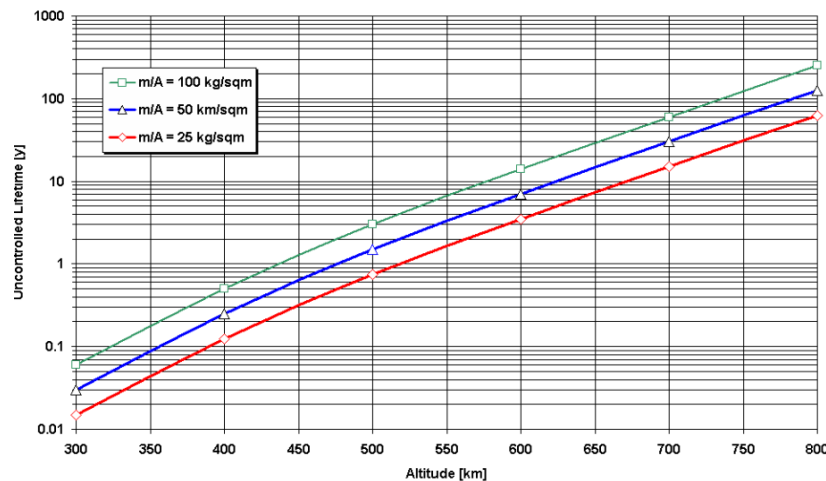


Figure 4: Relationship between altitude and orbital lifetime [18].

The combination of high-durability spacecraft materials and uncontrolled re-entry events poses an increasing risk to the human population. ESA's latest projections suggest that re-entering space debris could transition from a rare event to a near-daily occurrence, increasing the likelihood of ground casualties [9].

2.3. Clean Space and End-of-life management

To further enhance space sustainability, a set of technical and regulatory measures have been introduced under the framework of the Clean Space Initiative, an effort led by ESA. This initiative encompasses three main branches:

- **EcoDesign: Focused on minimising the environmental footprint of space missions.**
- **In Orbit Servicing (IOS) (formerly Active Debris Removal (ADR)):** Aimed at servicing satellites towards enabling circular economy and extracting large high risk debris from orbit.
- **Management of EoL Operations (formerly CleanSat):** Dedicated to ensuring satellites and other space assets comply with SDMR at the end of their service life.

A visual representation of these three branches is provided in Figure 5.

ecodesign
• REDUCING IMPACTS

**management
of end of life**
• SPACE DEBRIS REDUCTION

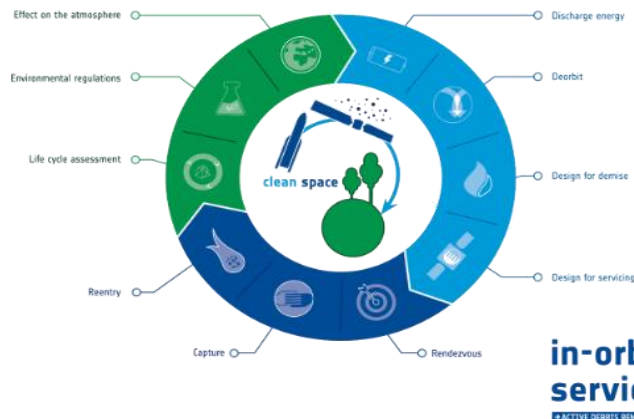


Figure 5: Clean Space branches [19].

2.3.1 EcoDesign

The EcoDesign initiative seeks to integrate sustainable practices into satellite manufacturing and operation by promoting green technologies and reducing the overall environmental impact of space activities. This involves assessing a range of environmental impact factors, including: climate change contribution, ozone layer depletion, resource consumption, toxicity to human health and ecosystems, and water and land use.

Given the complexity of these factors, a standardised evaluation method was introduced: the Life Cycle Assessment (LCA), developed by the European Commission’s Joint Research Centre (JRC) and ISO-certified. The LCA provides a quantitative assessment of emissions, resource depletion, and environmental impact, allowing engineers to optimise designs while avoiding unintended burden-shifting across impact categories.

2.3.2 In Orbit Servicing

IOS aims to extend the operational life of satellites moving them to another orbit, refuelling, manufacturing, recycling, etc. It aims to set the basis for a circular economy from 2050 onwards. Together with ADR they form ADRIOS. ADR focuses on removal of large defunct objects that pose a high risk of collision and fragmentation. As some satellites and rockets fail to comply with SDMR, ADR serves as a corrective measure to stabilise orbital environments. Concerns include:

- **Selecting optimal removal targets:** Priority is given to objects with high mass and high collision probability, particularly in densely populated orbits.
- **Legal and regulatory challenges:** Since debris objects remain the property of the original operators, their removal requires explicit authorisation and international agreements.
- **Demonstration missions:** ESA’s e.Deorbit mission, initially aimed at deorbiting the defunct Envisat satellite, has evolved into a broader IOS initiative. This now includes tasks such as satellite refuelling, component upgrades, and orbital repositioning, marking the future direction of ADR technologies.

2.3.3 Management of End-of-Life Operations

The Management of EoL Operations branch is dedicated to reducing debris production by ensuring satellites comply with SDMR through four main approaches:

- **Deorbit:** deorbiting systems execute controlled manoeuvres to transfer satellites to higher “graveyard orbits” (for GEO) or induce atmospheric re-entry (for LEO). To facilitate these manoeuvres, propulsion and drag augmentation solutions are under development:
 - Monopropellant adaptation: Advances in repressurisation systems, low-cost thrusters, and hybrid electric-chemical propulsion are improving deorbit reliability while limiting mass impact.
 - Passive deorbiting solutions: Drag Augmentation Systems like deployable sails accelerate orbital decay for small satellites at minimal cost. And electrodynamic space tethers, consisting of multi-kilometre-long conductive wires, use Earth’s magnetic field to generate a drag force, enhancing natural orbital decay.
 - Cutting-edge deorbit engines: The ArianeGroup 400N Hydrazine SCA, originally designed for Roll and Attitude Control (RACS), is now repurposed as a deorbit engine for ESA’s METOP SG spacecraft. Research is ongoing into green deorbit propulsion, utilising Ammonium Dinitramide (ADN) and High-Concentrated Hydrogen Peroxide (H₂O₂) as eco-friendly alternatives with high TRLs [20].
- **Discharge Energy:** Passivation is critical for preventing satellite explosions caused by stored energy release at the end of a mission. Passivation involves venting propellant tanks to release residual gases, and depleting battery charge to eliminate electrical energy storage risks as seen in Figure 6. Various passivation techniques are under investigation, including electrically driven valves (though they pose risks of seat leakage), and pyrotechnic (pyro) valves, which despite having lifespan limitations and Shape Memory Alloy (SMA) valves, emerge as a preferred fail-safe solution [20].

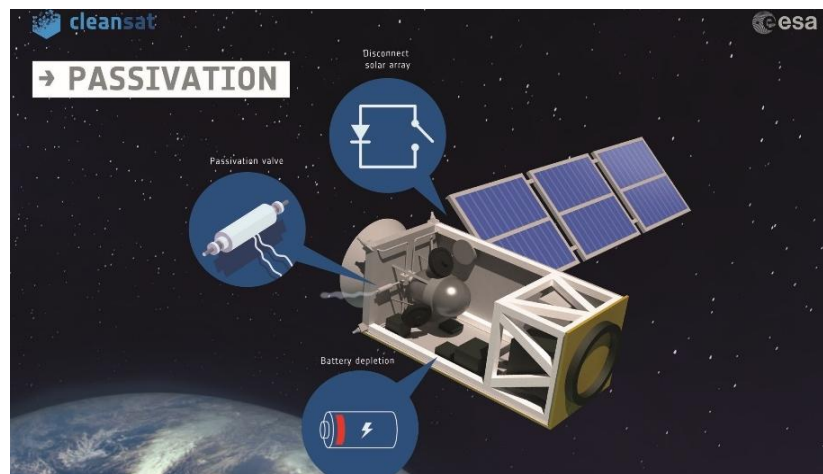


Figure 6: Passivation techniques [21].

- **Design for Demise:** The D4D concept aims to maximise spacecraft disintegration during re-entry as illustrated in Figure 7, thereby minimising on-ground Casualty Risk (CR). This approach involves:
 - Identifying non-demisable components based on material properties, mass, geometry, and thermal resilience.
 - Implementing modifications to enhance structural break up during re-entry.
 - Altering materials or repositioning them to expose them to higher heat loads.



Figure 7: Illustration of satellite demising [22].

Compared to a controlled re-entry, the D4D approach offers a cost-effective alternative for satellite disposal. However, further advancements in demisable materials and re-entry prediction tools are still required to fully optimise this technique.

- **Design for Servicing:** It aims to designing satellites to facilitate on-orbit maintenance, repair, refuelling, and upgrading, thereby extending their operational lifespans and reducing space debris. This approach ensures satellites remain functional and minimises the need for replacement missions. To be applicable, the concept requires:
 - **Modular Design:** Implementing standardised, modular components allows for straightforward replacement or upgrading of satellite parts.
 - **Servicing Interfaces:** Incorporating dedicated docking ports and standardised interfaces enables servicing spacecraft to securely attach to satellites.
 - **Refuelling Capabilities:** Designing satellites with accessible and standardised refuelling ports allows servicing missions to replenish onboard propellant.
 - **Autonomous Rendezvous and Docking Systems:** Integrating these technologies enables satellites to autonomously approach and dock with servicing spacecraft.

By incorporating these principles, satellite operators can significantly enhance mission flexibility, reduce operational costs, and contribute to sustainable space operations by mitigating the accumulation of space debris.

2.4. Regulatory framework and guidelines

Implementing Space Debris Mitigation measures is crucial to ensuring long-term sustainability in space operations. However, for these measures to be effective, they require clear and standardised guidelines. Recognising this need, major European space agencies established the *European Code of Conduct for Space Debris Mitigation* in 2004. This laid the foundation for the first *ESA Space Debris Mitigation Policy* [1], released in 2008 and periodically updated since then. These regulations serve as a benchmark for space safety and orbital debris mitigation, defining EoL strategies based on spacecraft characteristics and outlining the necessary requirements for compliance, following the rationale presented in Figure 8.

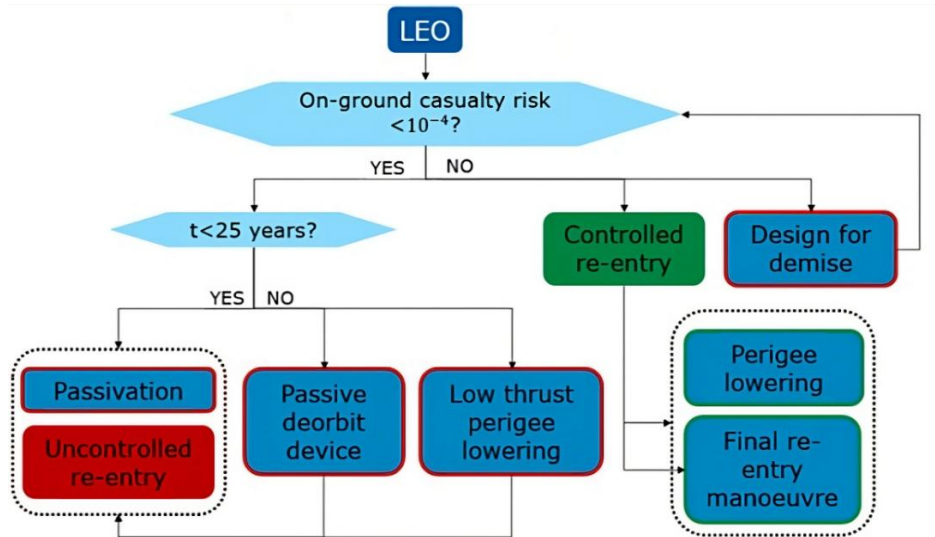


Figure 8: EOL decision making process [20].

The ESA guidelines focus on several aspects:

- Minimising debris released during normal operations, with a strong emphasis on protecting the LEO and GEO protected regions.
- Reducing the risk of on-orbit break ups and collisions by implementing passivation.
- Ensuring post-mission disposal, either by deorbiting spacecraft in a controlled manner or ensuring their natural orbital decay within an acceptable timeframe.
- Limiting Casualty Risk (CR) during both controlled and uncontrolled re-entries.

The ESA handbook "Space Debris Mitigation Compliance Verification Guidelines" [1] provides a structured approach to implementing Space Debris Mitigation policies across all phases of satellite design and operations. The most relevant requirements for this thesis are outlined in Table 1, which presents compliance verification measures established by ESA:

Table 1: ESA Space Debris Mitigation Compliance Verification Guidelines Relevant Requirements [1].

Requirement	Description	Relevance
5.2.1.a	Re-entry of space system or elements shall not result in hazards to the human population, harmful contamination of Earth's environment, and damages to assets due to: Impacting, Floating, Pressurised or explosive fragments; or Hazardous chemical or Radioactive substances.	The proposed design must consider impacting fragment characteristics to comply with SDMR.
5.2.2.a	The re-entry casualty risk shall include all impacting fragments of the space system with a kinetic energy equal to or greater than 15 J at their impact on the Earth's surface.	A proper definition of elements to consider in CR is mandatory since it is to be minimised.
5.2.3.a	Re-entry of the space system shall not create hazardous floating wrecks.	Design to minimise CR and pollution.
5.2.4.a	Pressurised fluids or explosive substances contained in surviving fragments shall not create a hazard to the human population.	Design to ensure safety from pressurised or explosive fragments.

6.1.2.3	Avoid releasing combustion products larger than 1 mm Solid Rocket Motors in LEO Protected Region.	Considered if solid rocket motors are accounted in the design.
6.2.1	Prevent any deliberate generation of space debris in Earth's orbit.	Design must not break up or generate debris intentionally in orbit.
6.2.2.1	The probability of accidental break up of a spacecraft or launch vehicle orbital stage in Earth orbit shall be less than 10^{-3} until its EoL.	In case of break up, debris will be generated, and D4D might not be practical. Must minimise break up probability.
6.2.2.3	A spacecraft or launch vehicle orbital stage, for which a controlled re-entry has not been planned, shall be passivated in a safe and controlled manner before EoL.	Since D4D is based on uncontrolled re-entries, design must consider passivation before EoL.
6.3.1.1	Ensuring by design a high probability of performing the disposal of the space system and minimising the risk of remaining in LEO or GEO Protected Regions after EoL.	To minimise interference with protected regions and ensure D4D effectiveness.
6.3.1.2	Compute the 0.9 probability of successful disposal defined in Requirement 6.3.1.1 through the appropriate assessment method.	To minimise interference with protected regions and ensure D4D effectiveness.
6.3.3.1	The orbit lifetime of the spacecraft shall be < 25 years starting from: a) Orbit injection epoch, if the spacecraft operates continuously or periodically in LEO protected region and has no capability to perform collision avoidance manoeuvres. b) End of mission epoch, if the spacecraft operates continuously or periodically in the LEO protected region and has the capability to perform collision avoidance manoeuvres. c) Epoch of the first orbit intersection with the LEO protected region within 100 years after EoL if the spacecraft or launch vehicle orbital stage operates continuously outside the LEO protected region.	Disposal time limit to minimise interference with LEO protected region. Relevant for the design characteristics definition.
6.3.3.2	The removal of a spacecraft or launch vehicle orbital stage from the LEO protected region shall be accomplished by one or more (in order of preference): a) Retrieving it safely to Earth. b) Performing a controlled re-entry with a well-defined impact footprint on the surface of Earth to limit the possibility of human casualty. c) Allowing its orbit to decay naturally in accordance with the 25-year limit for orbit lifetime.	Design according to the time limit and to ensure a safe re-entry.

	<p>d) Manoeuvring in a controlled manner to reduce remaining time in orbit to comply with the 25-year limit for orbit lifetime.</p> <p>e) Augmenting its orbital decay by deploying a device to reduce the remaining time in orbit to comply with the specified 25-year limit for orbit lifetime.</p>	
6.3.4.1	Specific re-entry safety requirements imposed contractually, voluntarily or by national or international authorities shall be identified and applied.	Re-entry safety requirements must directly affect design.
6.3.4.2	The quantifiable risks associated with a re-entry shall be less than or equal to the corresponding risk thresholds set by approving agents.	Uncertainty and dispersion in re-entry make it mandatory to identify critical items and provide a design reducing risks.
7.1	Planning activities that define the SDM actions to be performed at a high level shall start during the mission design.	SDM actions to be performed from the design phase.
7.2.1	A Space Debris Mitigation Plan (SDMP) that includes all design, manufacturing, launch, operation, and disposal phases shall be prepared.	For all design phases assessed this might be considered in a SDMP.
7.2.2	<p>As a minimum, SDMP shall contain:</p> <p>a) Applicable SDMR.</p> <p>b) Plans for addressing the applicable SDMR.</p> <p>c) Verification and validation to assess compliance with SDMR.</p> <p>d) A compliance matrix.</p> <p>e) Justifications for non-compliance.</p>	To provide an effective design it considers addressing applicable SDMR identified and verifying its compliance with these justifying the whole process.

Beyond ESA, regulatory bodies worldwide continue to refine SDM policies in response to evolving risks. A notable example is the U.S. Federal Communications Commission (FCC), which took a more stringent stance on orbital debris mitigation. In its Second Report and Order, the FCC reduced the recommended post-mission disposal timeframe for LEO satellites to just 5 years. This decision was driven by concerns over the exponential rise in collision avoidance manoeuvres required for satellite constellations and the increasing congestion of LEO [23]. ESA's 25-year rule was recently updated, recommending a reduced deorbit timeframe of 5 years for satellites launched after 2023, in line with FCC. However, this remains a non-binding recommendation, meaning compliance varies among operators. As satellite constellations expand, uncontrolled re-entry events are expected to increase significantly, potentially reaching hundreds or even thousands per month in the coming years.

3. Design for Demise

D4D is the intentional design of space system hardware in such a way that it is more easily or even entirely disintegrated during an uncontrolled re-entry to the atmosphere. Unlike controlled re-entries, which require additional mass, complexity, and cost to manage, D4D enables uncontrolled re-entry while minimising on-ground CR. As space debris mitigation policies affect vehicle design, operation, and disposal across the entire spacecraft lifecycle, D4D plays a critical role in mission and system design. Its primary objective is to ensure a safe and predictable disintegration process, reducing the risk of injury or damage on Earth to below the threshold of 1 in 10,000, as per ESA's SDMR [24].

However, D4D remains a relatively new area of study with many unresolved uncertainties. Advancements in material science, aerothermodynamics, and structural engineering are required to refine demisable technologies and ensure effective implementation. Since D4D is a multidisciplinary approach, it involves several research areas, including:

- Flight dynamics: Understanding how re-entry forces impact spacecraft break up.
- Aerothermodynamics: Modelling heating and fragmentation during atmospheric re-entry.
- Mechanical stress and fragmentation: Studying how satellites disintegrate.
- Ablation physics: Investigating material erosion and degradation at high temperatures.
- CR analysis: Predicting potential on-ground risks from surviving debris.

Three main methodologies are used to study and validate D4D principles.

- **Computational Simulations**: Simulations provide predictions of spacecraft break up dynamics, generating data on thermal loads, aerodynamic forces, and fragmentation processes. These models are fundamental for defining D4D requirements but rely heavily on material thermal properties and approximations, requiring experimental validation.
- **Ground Testing**: To enhance the accuracy of simulations, various ground-based testing facilities are used to replicate re-entry conditions:
 - Kinetic Facilities: Analyse basic break up mechanics, object aerodynamics and hypersonic shock-shock interactions.
 - Static/Auxiliary Facilities: Investigate individual material properties and ablation behaviour to build up material databases.
 - PWTs: Test material and components survivability in re-entry conditions, as shown in Figure 9, where a magnetorquer (MTQ) endures plasma-induced demise.



Figure 9: MTQ burning up in a PWT before and after the test [25].

- **Flight Experimentation:** Since ground tests cannot fully replicate real re-entry environments, in-orbit flight experiments are critical for validating both simulations and on-ground testing. These experiments provide in situ fragmentation data, heat flux profiles and structural break up dynamics.

Moreover, D4D strategies can be classified into two categories:

- System-Level Design: Modifications applied to entire spacecraft structures, influencing overall disintegration patterns.
- Equipment-Level Design: Targeted adaptations for specific components, such as reaction wheels, propellant tanks, and magnetorquers.

These approaches involve material substitution, optimised structural geometries, and the development of dedicated subsystems to enhance demisability. For example, current estimations place spacecraft break up between 80 and 75 km altitude. However, since the break up process is highly chaotic, a D4D goal is to initiate disintegration at a higher altitude (85 - 90 km). Promoting an early break up, which would be a System-Level design D4D strategy, ensures that internal components are exposed sooner, accelerating their demise through increased aerodynamic heating and ablation.

The ultimate objective of D4D is to achieve a "zero-casualty-risk" for the mission, where all the components fully or partially ablate before reaching the Earth's surface. According to ESA guidelines, this would imply reaching a level of ablation that ensures that any surviving debris has an impact energy below 15 J [1]. However, significant challenges remain, primarily due to gaps in re-entry heat flux and fragmentation data, uncertainty in real-world re-entry physics, and limitations in current ground testing capabilities. Continuous research efforts are needed to refine computational models, testing methods, and flight validation strategies, ensuring the development of robust, cost-effective, and reliable D4D technologies for future space missions.

3.1. Identification of critical elements for re-entry

In the context of D4D, ensuring both the break up of the system and the demise of all equipment fragments is necessary to maintain a CR below 1 in 10,000, as required for all space missions that re-enter Earth's atmosphere. To achieve this, critical elements that have been observed to survive re-entry or fragmentation in past missions have been identified, to focus D4D efforts on their redesign to promote complete disintegration.

A demise index defines a component's ability to ablate under re-entry conditions. Traditionally, studies focused on survivability, but D4D efforts prioritise mass loss and fragmentation. The ballistic coefficient (β),

$$\beta = m / (C_D \times A)$$

Equation 1: Ballistic Coefficient

where m is mass, C_D is the Drag Coefficient and A the cross-section area, plays a major role in demise. When β is low, it opposes airflow resistance, thus favouring demise. When β is high, it leads to higher heat flux absorption, thus enhancing ablation. However, in the orbital phase, a high β prolongs orbit lifetime, affecting debris mitigation strategies.

Apart from β , demise is also highly influenced by the type of material, as they present distinct demise behaviours. As a summary, Ceramics and High-melting-point metals resist demise with steady-state thermal properties; metals such as Aluminium, Stainless Steel and Titanium Alloys present diverse behaviours but all form oxidation layers that influence demise; and Fiber-Reinforced Polymers (FRPs) undergo fibre spallation, ply separation, and matrix pyrolysis.

In total, 9 material properties have to be considered to define the Demise Criterion (DC) as

$$DC = f[T_m/T_{degrad}, C_p(T), \chi_{cat}(T), \theta_{cy}, \varepsilon(T), H_f(T), k(T), E(T), \sigma_{fail}(T)]$$

Equation 2: Demise Criterion [9].

where:

- T_m : Melting temperature
- T_{degrad} : Degradation temperature
- $C_p(T)$: Specific heat capacity
- $\chi_{cat}(T)$: Surface catalycity
- θ_{cy} : Char yield
- $\varepsilon(T)$: Emissivity
- $H_f(T)$: Heat of fusion
- $k(T)$: Thermal conductivity
- $E(T), \sigma_{fail}(T)$: Mechanical properties

It is to be noted that $\chi_{cat}(T)$ is a temperature dependent parameter that indicates how much energy of atomic species recombination is absorbed by the surface, directly influencing the total heat transfer transmitted to the surface. θ_{cy} is the amount of material left over after being subjected to high temperature pyrolysis (applicable for composites). And $\varepsilon(T)$ is the ratio of the energy radiated from the surface of a material over that radiated from a black body (known as a perfect emitter), both at the same temperature, wavelength and viewing conditions. An optimal material for demisability should exhibit low melting temperature, specific heat, heat of fusion, char yield and surface emissivity, coupled with high thermal conductivity and surface catalytic activity to facilitate fast heat diffusion and promote mass loss through chemical reaction [9].

Therefore, considerations that could be derived from this criterion are, firstly, that retrograde orbits increase re-entry velocity. Secondly, that enhancing demise conditions and material selection should favour low melting points, high thermal conductivity, and high surface catalytic activity for efficient mass loss. Critical elements in spacecraft design must be analysed carefully to promote disintegration upon re-entry. Materials like stainless steel, titanium, silicon carbide, and composites have low-demise-capability and require targeted D4D strategies. Being aware of which equipment is critical from the demise perspective, enables to consider this matter early on in the design process and to focus on the components that will have the highest impact in reducing the CR. Components have varying levels of criticality during re-entry, depending on their material composition, structural properties and exposure to heat flux as summarised in Table 2.

Table 2: Critical components for demisability and reasons.

Component	Criticality	Key Factor
Batteries	Low-Medium	Steel casing, multiple cells
Electronics Card	Medium	High-temperature GFRP
Fill & Drain Valve	High	Titanium construction
Gyroscope	High	Titanium housing

MTQ	Low	Magnetic core (higher melting point than steel)
Propellant Tank	High	Titanium construction
Reaction Wheel Shaft	Medium	Steel material, multiple objects
Reaction Wheel Flywheel	High	Steel material, multiple objects
Solar Array	Low	Low ballistic coefficient
Structural Panels	Low	Low ballistic coefficient (demise in fragments)
Mirrors (Zerodur)	Medium	Zerodur material
Mirrors (Silicon Carbide)	High	Ceramic material
Thrusters	Medium	Inconel material
Optical Payload Fixings	High	Invar/Titanium materials
Solar Array Drive Mechanism	High	Steel central shaft
Star Tracker	High	Titanium parts
Lenses	High	Silica material

More details about the reasons for some of the elements more prone to surviving re-entry are hereby presented.

- **Propellant Tanks:**
 - Observed to survive re-entry intact, as in Sentinel-1, other missions and simulations
 - Often made from Titanium, a material highly resistant to fragmentation and ablation.
 - Typically located near the Centre of Gravity (CoG) and shielded by structural elements, reducing exposure to high temperatures.
 - Present a high area-to-mass ratio that makes the tank decelerate fast after being released from the spacecraft.
 - Account for ~20 % of total on-ground CR [26].
- **Reaction Wheels (RWs):**
 - Survive re-entry due to their dense metallic composition and minimal fragmentation.
 - Consist of multiple subcomponents: case, flywheel, and motor, each with different criticality levels.
 - The Ball-Bearing Unit (BBU) remains shielded for a significant part of the re-entry, delaying its exposure to heat flux.
 - Major contributor to CR, up to 40% [26].
- **Magnetorquers:**
 - Typically, small spacecraft carry three MTQs, most of which survive re-entry.
 - Constructed with Stainless Steel ballast mass, which withstands high temperatures.
 - Exposure to heat flux occurs late in re-entry, delaying demise.
 - Mass-dependent survivability: <5 kg objects often demise, whereas >50 kg objects reach ground [26].
 - Can contribute up to 10% of the total CR [26].
- **Batteries:**
 - Commonly demisable depending on the material of the case of the battery and the accommodation point of the battery inside the satellite.
 - Mass-dependent survivability: small cells batteries demise completely from most release altitudes, whereas large cells show lower demisability, posing a risk.
 - The re-entry conditions can cause thermal runaway, leading to an explosive or combustion-based reaction which might result in generation of fragments.

- **Synthetic Aperture Radar (SAR) Antenna** (see Figure 10):
 - Highly uncertain fragmentation behaviour.
 - Central panel survives due to delayed exposure, while lateral wings are exposed earlier and demise.
 - Separation altitude of central panels is critical: higher altitude leads to lower Casualty Area (CA).

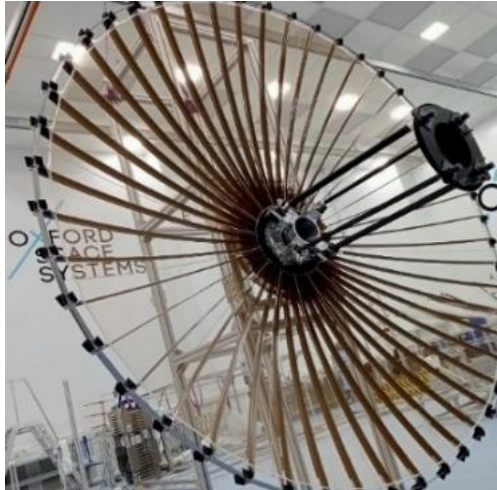


Figure 10: SAR antenna from Oxford Space System [27].

- **Laser Communication Terminal (LCT)** (see Figure 11):
 - Simulations indicate entire LCT units survive in one piece.
 - Critical non-demising parts include Ceramic mirrors, Titanium/Invar optical fixings, Ceramic truss structures and Titanium mounting feet.
 - Unlike platform components, LCT elements prioritise performance over demisability, requiring dedicated mitigation strategies.

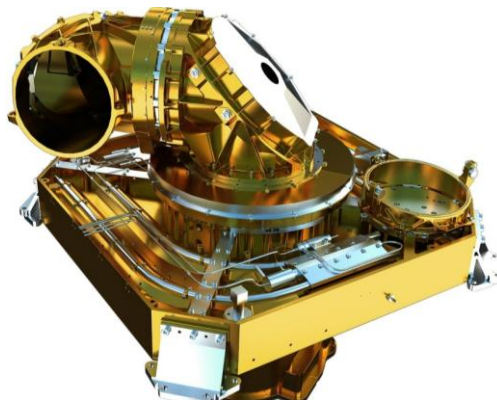


Figure 11: LCT concept of DLR German Space Center and TESAT-Spacecom [28].

Demise critical elements can be grouped in three categories based on break up behaviour. This enables to choose which demise strategy (presented within Section 3.2) to implement:

- Items that fragment into smaller pieces: Their survivability depends on heat exposure timing, leading to high uncertainty in final ground impact risk, i.e. SAR central panels.
- Items that either fully demise or survive intact: Since exposure for these elements occurs late in re-entry, it leads to a stepwise variation in CR, i.e. MTQs.
- Items that never demise: Survivability is linked to high melting temperature materials and massive structures, leading to minimal variation in CR, i.e. Propellant tanks or RWs.

3.2. Demise and Containment strategies

To enhance the demisability of a spacecraft upon atmospheric re-entry, different strategies can be implemented. D4D strategies can be classified into four main categories:

- **Maximise Available Heat:** Ensuring that the spacecraft and its components experience the highest possible thermal loads during re-entry.
- **Minimise Required Heat:** Reducing the energy necessary to break up or vaporise.
- **Optimise Heat Transference:** Enhancing thermal conductivity and exposure to ensure that all spacecraft elements receive sufficient heat to demise.
- **Design for Containment:** Implementing measures to prevent the widespread dispersal of surviving debris if complete demise is not possible.

Each of these strategies plays a distinct but complementary role in enhancing re-entry safety. Their implementation requires a multidisciplinary approach. No single method can guarantee complete spacecraft demise upon re-entry; instead, a combination of thermal optimisation, material selection, structural design, and containment measures must be carefully integrated into the spacecraft architecture.

3.2.1. Maximise available heat

A fundamental principle of spacecraft demise is to increase the heat flux experienced by individual components. By ensuring critical components are subjected to extreme temperatures for an extended period, the probability of their demise can be significantly improved. Key approaches to maximising available heat include:

- **Geometric Considerations:** The shape of an object affects the way it interacts with the atmosphere. Components with sharp edges and flat surfaces, such as rectangular plates or cylindrical bodies, are more likely to experience high stagnation-point heating. In contrast, streamlined shapes such as spheres or cones may dissipate heat more efficiently, potentially reducing their exposure to extreme temperatures.
- **Ballistic Coefficient Optimisation:** β (previously introduced in Section 3.1) determines how an object decelerates and heats up during re-entry. Components with a lower β tend to slow down earlier, exposing them to prolonged heating at higher altitudes. Conversely, denser objects may descend more rapidly and retain enough kinetic energy to survive the re-entry and impact on ground. Careful design modifications, such as increasing the exposed surface area of critical components, can help optimise their re-entry profile.
- **Mass Redistribution Strategies:** Placing high-mass-density elements (e.g. RW, batteries, or MTQs) in more exposed locations ensures that they encounter severe heating earlier in the re-entry sequence. Components located at the periphery of the spacecraft structure will be more likely to demise than if shielded within the spacecraft's core.
- **Use of Exothermic Reactions:** Certain material interactions, such as the oxidation of Silicon Carbide or the Thermite reaction, can generate additional heat within structural components, accelerating their demise. While this technique has yet to be widely adopted in spacecraft design, it presents a potential avenue for future research.

3.2.2. Minimise required heat

Equally important to increasing available heat is reducing the energy required for satellite components to demise. Some materials and structures inherently require much higher temperatures to melt or ablate, making them more likely to survive re-entry. The following strategies can improve demisability by lowering the necessary heat input:

- **Material Selection:** High melting point materials such as Titanium alloys, Stainless Steel and Tungsten are more likely to survive re-entry than lower melting point alternatives like Aluminium, or high-performance thermoplastics. Where feasible, spacecraft elements should be designed using materials with lower melting points to enhance demise.
- **Structural Mass Reduction:** Reducing mass of critical components lowers their thermal inertia, allowing them to reach demise temperatures quicker. Techniques such as thinning structural panels, incorporating lattice structures, or using lightweight composites e.g. Carbon Fibre Reinforced Polymers (CFRPs) can help enhance demise.
- **Advanced Manufacturing Techniques:** Satellite structures often use metal components inherently resistant to heat. Alternative manufacturing processes, such as 3D printing (additive manufacturing), sandwich structures, or Metal-Matrix Composites (MMCs), can introduce porosity and reduce the overall density of components enhancing demisability.

3.2.3. Optimise heat transference

Even if enough heat is available during re-entry, some satellite components may survive because they do not efficiently conduct or absorb this thermal energy. To address this issue, various techniques can be used to improve heat transfer and ensure that all critical elements reach temperatures sufficiently high for demise:

- **Enhancing Conductive Heat Paths:** Components with poor thermal connectivity e.g. isolated RW, may survive re-entry because heat does not transfer efficiently through their structure. Using metallic contact points, welded joints, or thermally conductive interfaces can help distribute heat more effectively throughout the satellite.
- **Encouraging Early Break Up:** If a satellite stays intact for too long during re-entry, some components may be shielded from direct heating by the structure. Introducing predefined weak points, frangible joints, or controlled break up mechanisms as in Figure 12, ensures that components separate early, maximising their exposure to high-temperature airflow.
- **Venting/Perforation:** Hollow components i.e. bipods, may resist demise due to their insulating properties. Adding venting holes, perforations or structurally weak sections, hot gases can penetrate and thus enhance heat absorption and demise.

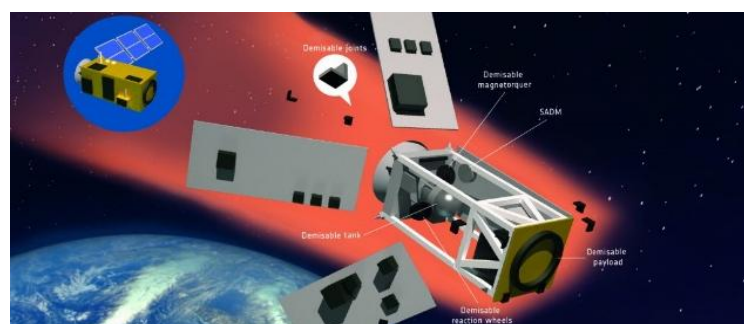


Figure 12: Satellite early break up fragmentation concept [29].

3.2.4. Design for Containment

In cases where complete demise is not achievable, Design for Containment (D4C) strategies aim to reduce the risk of debris dispersal and impact with populated areas. This approach is important for dense, high melting point components such as Tungsten RW, optical parts and large battery packs, which are known to survive re-entry. Containment strategies include:

- **Component Regrouping:** Instead of allowing single high-risk components to separate and disperse unpredictably, the satellite standard architecture design can be modified so that these elements remain clustered together, reducing dispersion on ground.
- **Attachment and Retention Mechanisms:** Brackets, tethers, or reinforced enclosures can be used to keep surviving debris together. While this does not ensure full demise, it reduces the likelihood of scattered fragments causing harm.
- **Protection:** Sometimes, heat-resistant coatings, ablation layers or mechanical shields can be applied to critical components to avoid exposing certain elements to the heat flux.
- **Encapsulation:** A mechanical containment implements a dedicated device to enclose elements surviving re-entry. It can be done through partial or total encapsulation.

3.3. Observation campaigns

Re-entry physics remains an area with significant unknowns and uncertainties. The complex interactions between atmospheric composition, velocity, shape, material properties, and aerothermomechanical loads make it challenging to predict accurately the demise of space objects during re-entry. While computational models and ground-based experiments provide valuable insights, they cannot fully replicate the dynamic conditions experienced during re-entry.

Observing re-entry events in real time is crucial for refining the understanding of fragmentation, heating conditions, and survivability of space debris. These observations enhance the accuracy of re-entry simulations. Over the decades, numerous observation campaigns have been conducted, using a combination of ground-based tracking, airborne monitoring, and in-situ instrumentation to capture re-entry data. Re-entry studies have evolved from analysing recovered space debris to sophisticated real-time monitoring efforts. Several missions have contributed valuable in-situ and observational data:

- OREX (1994, JAXA): Provided early data of re-entry conditions with onboard instruments.
- ESA's Atmospheric Re-entry Demonstrator (ARD, 1998): A controlled re-entry experiment designed to test Thermal Protection Systems (TPS) and break up dynamics.
- STS-96 (1999, Space Shuttle Discovery): Enabled high-fidelity monitoring of controlled re-entry conditions.
- ATV-1 to ATV-5 (2008–2015): ESA's Automated Transfer Vehicle missions, equipped with Re-Entry Break up Recorder (REBR) capsules, provided data on spacecraft fragmentation. Specifically, the Re-entry SatCom capsule used in ATV-5 which can be seen in Figure 13, worked like an aircraft-style 'black box' to store images and transmit them to Earth once the break up of the vessel took place via an Iridium satellite link.

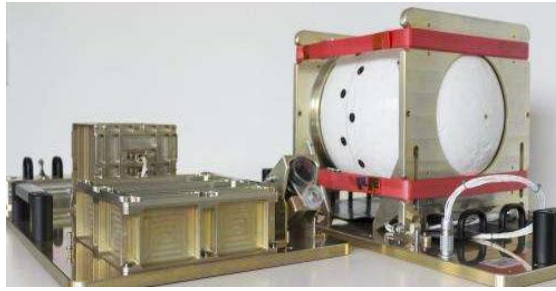


Figure 13: BUC Infrared Camera and SatCom [30].

The campaign for Cygnus OA-6 re-entry in 2016, sought to combine airborne tracking with in-situ monitoring via an REBR-W capsule. Unfortunately, data transmission failures possibly due to battery issues, radiation interference, or impact damage, prevented data recovery. Similarly, the QARMAN CubeSat aimed to record uncontrolled re-entry data with a novel cork-based heat shield. However, contact was lost due to an unexpectedly prolonged orbital lifetime caused by a solar activity that was lower than anticipated, delaying its re-entry by nearly two years [9].

The most recent observation campaign performed by ESA was the re-entry of a Cluster satellite module, which was part of ESA's Cluster II mission. The module underwent uncontrolled atmospheric re-entry on January 7, 2024, with its final descent occurring over the Pacific Ocean near Easter Island [31]. The re-entry of this module, illustrated in Figure 14, was particularly relevant as it involved a dedicated airborne observation campaign aimed at studying the physical and chemical processes occurring during satellite re-entry. Using an instrumented aircraft this campaign sought to capture high resolution data on plasma formation, fragmentation events, and aerosol generation. The Easter Island airborne observation campaign of Cluster II is a crucial step in advancing the understanding of re-entry physics.



Figure 14: Cluster II re-entry illustration [32].

Previous analysis of spectroscopic and thermal imaging data suggests that:

- The sequence of structural failure followed expected aerodynamic loads, with initial break ups occurring at similar altitude thresholds (~75 - 80 km).
- The aerosol production from re-entry debris is an area of active study, with early indications that some of the material interactions with the upper atmosphere may have transient environmental effects.

Data collected from this campaign is currently being processed and will provide further insights into the evolution of spacecraft fragmentation under atmospheric re-entry conditions. Such studies are fundamental to improve space debris mitigation policies and refine satellite EoL deorbiting strategies.

3.4. Re-entry modelling and re-entry demise analysis tools

Space re-entry modelling encompasses the simulation and analysis of an object's behaviour as it re-enters a planet's atmosphere from space. This process involves the study of complex multi-physics interactions, where an object transitions from a near-vacuum environment into an increasingly dense fluid at hypervelocity (Mach > 5). Due to the extreme conditions involved, re-entry modelling requires expertise in multiple disciplines, including atmospheric physics, flight dynamics, aerothermodynamics, material science, and structural engineering.

Interest in re-entry modelling grew significantly during the early years of space exploration in the 1960s, as human spaceflight and satellite missions became a reality. The necessity to safely return astronauts and spacecraft from orbit, accelerated the development of predictive models for re-entry conditions. The moon race further drove advancements in re-entry planning, requiring precise trajectory control and heat shielding technologies.

Over time, re-entry modelling has evolved beyond human spaceflight applications to include the controlled destruction of space debris. The increasing number of satellites in orbit has raised concerns about the risks posed by uncontrolled re-entries. Consequently, modern re-entry analysis focuses on optimising spacecraft designs for maximum demisability while ensuring compliance with international guidelines on CR mitigation.

Re-entry modelling relies on different atmospheric, aerothermodynamic, and material ablation models, each with varying degrees of accuracy and maturity. A challenge lies in modelling demise of composites, particularly FRPs, whose behaviour during re-entry remains less well understood compared to bulk materials like metals or ceramics. Current demise models are primarily validated through recovered debris and limited re-entry observations, leading to inherent uncertainties in their predictions. Current space missions must assess re-entry scenarios to select an appropriate EoL strategy, which generally falls into one of three categories:

- **Controlled Re-Entry:** Requires significant propellant reserves and precise manoeuvring to direct the spacecraft into a designated area (e.g. the South Pacific Ocean Uninhabited Area). This method is costly and complex but ensures maximum safety.
- **Assisted Re-Entry:** A trade-off between controlled and uncontrolled re-entry, where a de-orbit manoeuvre lowers the perigee to increase atmospheric drag, accelerating decay. This was successfully demonstrated with the Aeolus mission in July 2023.
- **Uncontrolled Re-Entry:** Relies on natural orbital decay due to atmospheric drag. This approach is the simplest but inherently risky, as re-entry location predictions have significant uncertainties. It is here where the application of D4D has the highest benefits.

To assess the demisability of spacecraft components, several simulation tools have been developed, categorised into two main approaches:

- **Object-Oriented:** represents a spacecraft as an assembly of simple geometric primitives (e.g. spheres, cylinders, cones) connected via hierarchical relationships. Fragmentation events occur based on altitude thresholds or physical triggers such as heat flux, temperature, dynamic pressure, or load factor. Aerodynamics are modelled using 3-Degrees of Freedom (DoF), while aerothermal analysis is simplified based on object-specific heat transfer properties. The advantage of this approach is computational efficiency, making it suitable for rapid design iterations. Common software tools in this category include DRAMA/SARA (ESA), DEBRISK (CNES), DAS (NASA), and ORSAT (NASA).

- **Spacecraft-Oriented:** employs a more detailed, panelised geometry representation, similar to Finite Element Models (FEM). The aerothermodynamic analysis is conducted using 6-DoF simulations, capturing aerodynamic forces and structural responses. Fragmentation is determined based on stress and structural integrity. While this provides higher fidelity results, it demands greater computational resources and longer processing times. Representative tools include SCARAB (HTG-ESA) and PAMPERO (CNES) [33].

Since this MSc thesis has been developed within an internship at ESA, the European tool DRAMA (Debris Risk Assessment and Mitigation Analysis) presented in Figure 15, has been used and will be explained in more detail, leveraging direct access to ESA expertise. The DRAMA suite includes five modules, with SARA (re-entry SurvivAl and Risk Analysis) being particularly relevant for assessing satellite demisability and CR. SARA integrates two computational models:

- SESAM (Spacecraft Entry Survival Analysis Model): Computes the aerothermodynamic forces (drag, lift, side forces) acting on individual spacecraft components.
- SERAM (Spacecraft Entry Risk Analysis Module): Evaluates the likelihood of component survival based on heat transfer and ablation processes.



Figure 15: ESA DRAMA software tool and its 5 modules.

For demise modelling, SESAM and SERAM adopt a lumped-mass approach, relying on temperature-dependent material properties such as: density, specific heat capacity, melting temperature, emissivity coefficient and thermal conductivity [33]. For metallic, ceramic, and polymeric materials with isotropic properties, these models yield reasonably accurate results. However, FRPs present additional challenges due to their anisotropic structure and complex failure modes under high-temperature and high-stress conditions.

Despite significant advancements in re-entry simulations, several uncertainties persist:

- **Material Characterisation:** The response of several materials to extreme aerothermal loads is not yet fully understood. For example, for FRPs, the current Charring Material Ablation model, which describes the two-step process of pyrolysis and surface ablation, does not fully capture additional effects such as mechanical erosion and spallation.
- **Fragmentation Dynamics:** Predicting the precise break up altitude and fragmentation pattern of a spacecraft is complex due to dependencies on structural integrity, thermal gradients and aerodynamic forces.
- **Aerothermodynamic Forces:** The simplified aerodynamic coefficients used in object-oriented models introduce errors in trajectory and heating predictions, especially for irregularly shaped debris.
- **Computational Limits:** While high-fidelity models exist, their computational demands restrict practical use in large-scale debris risk assessments.

Improving re-entry modelling tools is critical for ensuring compliance with debris mitigation regulations and optimising spacecraft D4D. Continued research efforts, including conferences and workshops such as the Flight vehicles, Aerothermodynamics and Re-entry missions engineering (FAR) Conference, Clean Space Industry Days (CSID) or the Space Debris Risk Assessment and Mitigation Analysis Workshop, highlight the growing need for refined modelling.

3.5. Demise on-ground testing facilities

Reproducing on ground the conditions experienced during atmospheric re-entry is a formidable challenge. It requires sophisticated and costly equipment capable of withstanding and replicating high-temperature, high-pressure, and high-velocity environments. Despite this, ground-based testing is indispensable for material selection, component validation, and the overall assessment of a satellite demise upon re-entry. An illustration of the various testing methods related to demisability characterisation considering the setup complexity and the re-entry conditions fidelity can be observed in Figure 16.

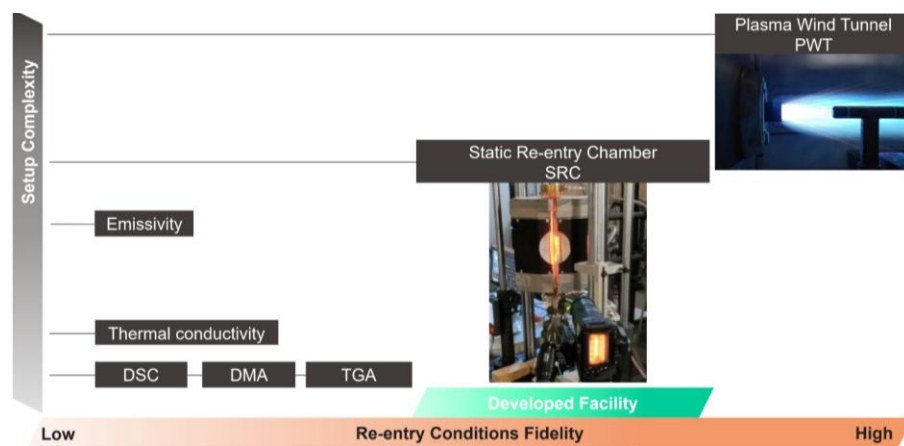


Figure 16: Comparative panel of re-entry simulation testing facilities with respect to condition fidelity and setup complexity [9].

Laboratory scale experimental techniques are commonly used to characterise thermal and mechanical properties of materials under high-temperature conditions. These methods include:

- **Thermo-Gravimetric Analysis (TGA):** measures the mass loss of a material as a function of temperature and time under controlled conditions. This helps determine decomposition temperatures, oxidation rates, and the onset of material ablation. By analysing weight loss trends, researchers can infer material stability at high temperatures and assess the likelihood of demise during re-entry.
- **Differential Scanning Calorimetry (DSC):** is used to study thermal transitions of materials, such as melting, crystallisation, and decomposition. By measuring heat flow as a function of temperature, DSC provides information on phase changes and heat capacity, necessary for understanding how materials behave under the extreme thermal loads faced during re-entry.
- **Dynamic Mechanical Analysis (DMA):** evaluates the mechanical properties of materials as a function of temperature, frequency, or time. This method is particularly useful for assessing the viscoelastic behaviour of polymers and composite materials, which are widely used in spacecraft structures. By measuring storage and loss moduli, DMA helps predict how structural components will respond to cyclic mechanical stresses during re-entry.

Furthermore, emissivity and thermal conductivity measurements are important for modelling heat transfer in satellite materials. Emissivity determines how efficiently a material radiates heat, which helps predicting temperature evolution during re-entry. Techniques such as laser-based radiometry and infrared thermography are often used to measure spectral and total emissivity at high temperatures. Moreover, thermal conductivity tests, including laser flash analysis and steady-state methods, provide data on how efficiently heat propagates through a material.

Laboratory-scale techniques complement large-scale re-entry testing by providing material properties, allowing for better predictive modelling and informed material selection before conducting more complex and costly tests. For these higher fidelity tests two categories exist:

- **Static Re-entry Chambers (SRC):** are designed to subject materials and components to controlled environments that mimic the thermal and pressure loads at re-entry. By adjusting parameters such as temperature, pressure and mechanical stress, researchers can investigate the thermophysical and thermomechanical responses of materials under conditions analogous to atmospheric re-entry. These facilities are particularly valuable during the early stages of material selection due to their relatively smaller size, ease of operation and lower operational costs compared to dynamic testing. Moreover, SRCs allow transient environmental conditions within a single test run, simulating the varying conditions experienced during actual re-entry. As of now, Aerospace & Advanced Composites GmbH in Austria operates a publicly accessible SRC facility [34].
- **Dynamic Experiments – PWT:** also known as plasmotrons, where high-enthalpy plasma gas flows are directed onto test samples. This setup simulates the aerothermodynamic loads experienced during re-entry, enabling the evaluation of materials, assemblies, or equipment under high-fidelity steady-state conditions. Demise characterisation using this method typically requires multiple tests runs under correlated conditions to recreate the real re-entry. In Europe, several centres are equipped with PWT facilities:
 - **Institute of Space Systems (IRS)** in Stuttgart, Germany: has been actively involved in testing various materials for demise characterisation. For instance, ATMOS Space Cargo conducted a test campaign at IRS on heat shield materials.
 - **Von Karman Institute for Fluid Dynamics (VKI)** in Brussels, Belgium: VKI operates PWT facilities that contribute to the study of aerothermodynamic phenomena related to re-entry conditions. The schematics can be seen in Figure 17.
 - **German Aerospace Center (DLR)** in Cologne, Germany: DLR's facilities have been used for various re-entry simulation tests, including studies on material demisability and satellite component behaviour during re-entry.
 - **Italian Aerospace Research Centre (CIRA)** in Capua, Italy: CIRA operates the Scirocco PWT, one of the largest PWT facilities, used for testing spacecraft materials and components under simulated re-entry conditions. Notably, ESA's QARMAN CubeSat underwent testing in this facility, enduring six and a half minutes of simulated atmospheric re-entry conditions.

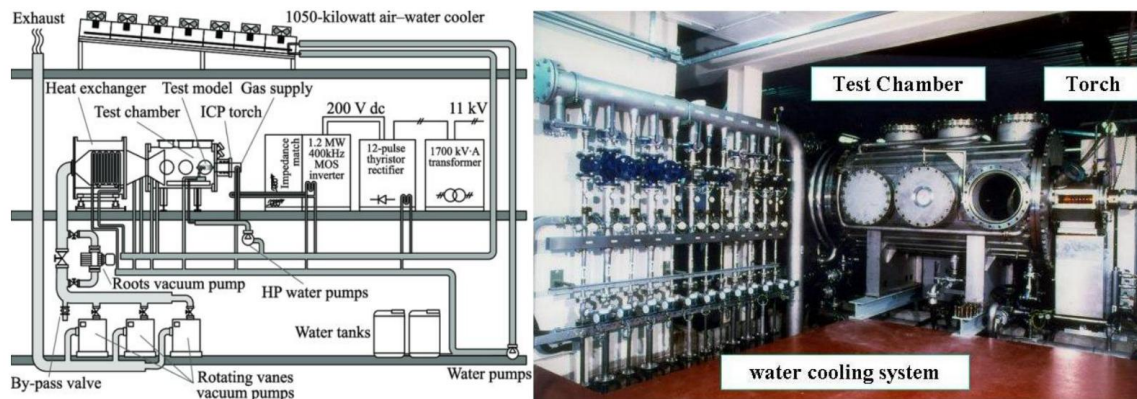


Figure 17: Schematic of VKI Plasmatron facility [35].

The choice between static and dynamic testing depends on various factors, including the specific objectives of the test, the desired fidelity to actual re-entry conditions, and resource availability. Static tests in SRCs are advantageous for early-stage material screening due to their lower complexity and cost. They allow for controlled and repeatable testing environments, making them suitable for assessing material properties under simulated re-entry conditions. However, they may not fully replicate the dynamic aspects of re-entry, such as the aerothermal loads resulting from high velocity atmospheric interaction.

In contrast, dynamic tests using PWTs provide a higher fidelity simulation of the re-entry environment by replicating the aerothermal loads at re-entry. These tests are essential for evaluating the integrated behaviour of materials and components under conditions that closely mimic real scenarios. The complexity and cost of PWT tests are higher compared to SRC tests, but the data obtained are crucial for validating numerical models and verifying the demisability or survivability of spacecraft materials and designs during re-entry.

Advancements in testing methodologies have led to innovative approaches that enhance the representativeness of ground-based tests. One such development is the integration of mobile holders, such as rotating cylinders, within PWT setups. This aims to simulate the tumbling or spinning attitudes of re-entering objects, providing a more accurate representation of the aerodynamic conditions during re-entry. The continuous development and enhancement of these facilities, particularly in Europe, contributes to the safety of space missions, ensuring that materials and components demise as required.

3.6. Prospective missions: DRACO

DRACO mission represents a critical advancement in our understanding of satellite demise during atmospheric re-entry. Scheduled for launch in 2027, DRACO, whose ConOps is presented in Figure 18, is designed to provide unique in-situ observations of the destructive processes that satellites undergo as they re-enter Earth's atmosphere. Weighing approximately 150 kg and comparable in size to a standard washing machine, DRACO is designed to emulate the characteristics of typical LEO satellites. Unlike conventional satellites, DRACO will lack propulsion and navigation systems to authentically replicate uncontrolled re-entry conditions. The spacecraft will be equipped with an array of 200 sensors and four cameras, all connected to a capsule designed to withstand the extreme conditions of re-entry. This capsule will collect and transmit data on temperature, pressure, structural stress and ablation experienced during the satellite's re-entry [36].

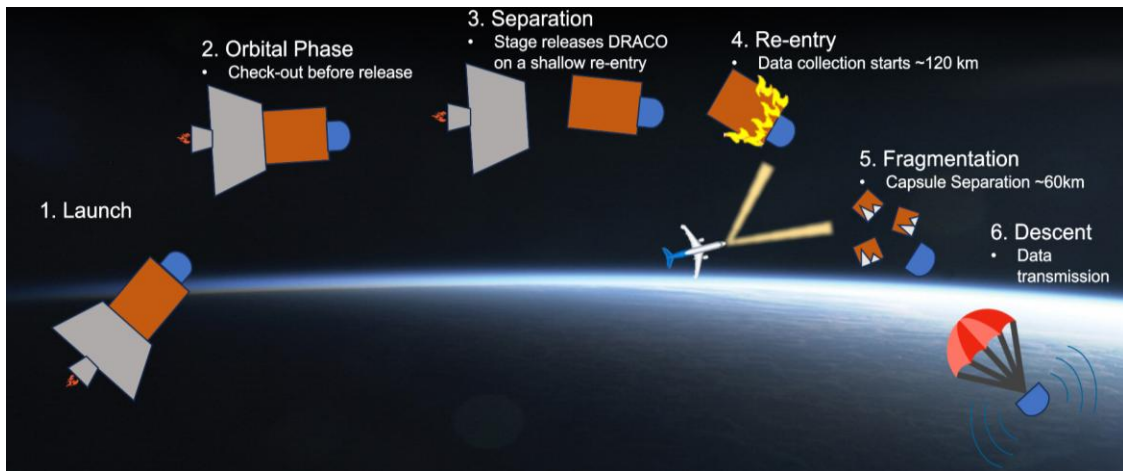


Figure 18: DRACO ConOps.

The primary objective of the DRACO mission is to obtain empirical data that will significantly enhance the accuracy of current re-entry predictive models. So far, our understanding of satellite break up processes during re-entry has been constrained by the limitations of ground-based experiments and observational data. Ground facilities often struggle to replicate the exact conditions of re-entry, such as the high velocities and complex aerodynamic interactions. By capturing real-time data during an actual re-entry event, DRACO aims to bridge this knowledge gap, offering insights that are unattainable through ground tests and simulations alone.

With a more precise understanding of the physical processes involved in satellite demise, engineers and scientists can improve the design of satellites to ensure more predictable and safer re-entries. This mission aligns with ESA's "Zero Debris" initiative, which aspires to tackle the generation of new space debris by 2030. By informing the development of technologies and strategies that facilitate the demise of satellites upon re-entry, DRACO contributes to global efforts aimed at mitigating the generation of space debris, thereby enhancing the long-term sustainability of space operations.

4. D4D ESA activities

This section presents the work conducted within ESA activities related to D4D, focusing on the behaviour of materials and components during atmospheric re-entry, and the technologies developed to enhance their demise. The content in this section draws upon a combination of publicly available literature, ESA led research initiatives, internal technical assessments, and insights from ongoing development activities. Where applicable, specific references have been included, while some information is based on ESA's internal expertise and mission experience.

A fundamental aspect of designing spacecraft for improved demise is understanding how different materials and components behave when exposed to extreme thermal and mechanical loads during re-entry. The way a material demises depends on its thermophysical properties, including melting and boiling points, thermal conductivity, and oxidation resistance. Similarly, spacecraft components such as propellant tanks, structural panels, and optical instruments, have complex geometries and multi-material compositions that influence their fragmentation and demise behaviour. The selection of an effective D4D strategy requires a detailed assessment of these properties and behaviours. Therefore, this section is divided into three main parts:

- **Material Level Activities:** This subsection explores the influence of material properties on demise behaviour, including a State of the Art (SoA) on existing knowledge about commonly used aerospace materials. It also highlights recent ESA activities that provided new insights into less characterised materials.
- **System Level Activities:** In this subsection, the focus shifts to spacecraft components, analysing how their geometry, assembly methods, and interactions with other parts influence demise. This includes an SoA of component behaviour and recent studies led by ESA that improved the understanding of critical satellite elements.
- **Technology Development Activities:** The last subsection discusses technologies designed to enhance demise using demisable materials, structural modifications and alternative design approaches. The SoA of these technologies is presented, followed by a discussion of recent advancements made through ESA activities.

ESA activities refer to research and development projects, experimental campaigns, and studies funded or coordinated by the ESA to advance space technology and ensure compliance with regulations such as SDMR. Within the context of D4D, these activities aim to improve the predictability of spacecraft demise, identify high risk components, and develop solutions to reduce CR. By establishing a thorough understanding of material and component behaviour and assessing the latest technological advancements, this section lays the groundwork for identifying optimal D4D strategies and integrating them into satellite design.

4.1. Material level activities

The space environment presents unique challenges that dictate material selection for satellite structures and components. When considering D4D, material properties become key in ensuring demise during re-entry and minimising the risk of surviving debris. One of the strategies is minimising the heat required for ablation by replacing conventional materials with alternatives that have lower melting temperatures, reduced emissivity, or lower specific heat of fusion.

Many components incorporate materials with high resistance to thermal degradation, including Titanium, Stainless Steel, Tungsten, Molybdenum, and Composites. Additionally, materials used in optical payloads, such as Glasses, present challenges due to their thermal stability. D4D studies focused on understanding the demise behaviour of these materials and identifying alternative ones that maintain mechanical performance while enhancing demisability.

Recent research led by ESA focused on refining the understanding of material demise through PWT and SRC tests. These investigations have contributed to updates in the ESTIMATE material database, improving the accuracy of spacecraft demise predictions. The following sections provide an overview of recent findings on the demisability of Glasses, Metals and Composites.

4.1.1. Ceramics and Glasses

Ceramic and Glass materials are widely used in space applications due to their hardness, chemical stability, and high thermal resistance. These properties make them essential for components exposed to extreme temperatures such as TPSs, heat shields and high-temperature coatings. However, these same properties are counterproductive for demise since they have high ablation resistance. Some applications and their demise implications include:

- TPS: to prevent atmospheric re-entry heating and not required for a demisable platform.
- Windows and optical components: often used in payloads, like camera lenses and substrates for telescope mirrors of e.g. Silicon Carbide.
- Solar cells cover glasses: Thin Silica or Silicate glass sheets used to protect solar cells. They pose minimal risk for demise due to their low thickness.

Aiming to enhance demisability, Ceramic and Glass materials should be avoided except in cases where their presence is mandatory e.g. solar cell cover glasses or high precision payloads. Unlike metals, which predominantly undergo melting and oxidation during re-entry, Glasses degrade through surface viscosity changes, thermal fracturing, and molecular recombination. Their low catalytic efficiency leads to reduced heat flux input, making standard ablation models unreliable in predicting their demise. PWT tests have contributed to refine the demise models for Ceramic and Glass materials, including Silicon Carbide (SiC), Fused Silica, and Zerodur.

Silicon Carbide

SiC is a well-known material for high-temperature applications and a candidate for non-ablative heat shields due to its very low demisability. This is attributed to its extremely high melting point, high spectral emissivity, and oxidation resistance (in high temperature tests, only slow oxidation has been observed). To better understand SiC behaviour during atmospheric re-entry, dynamic tests in DLR's L2K PWT have been conducted using two sample types: a cylindrical sample under constant heat flux and a cubical sample under variable heat flux.

The cylindrical sample resisted thermal shocks well, showing no cracking despite a high heating rate (see Figure 19). The cubical sample under variable heat flux exhibited a controlled temperature increase, making it an ideal test configuration for future brittle material studies. Moreover, pyrometer measurements confirmed that SiC behaves as a near-grey body, but a thin silicon dioxide layer formed on the surface during exposure. This layer potentially reduced heat flux to the sample by altering surface catalytic properties or introducing thermal resistance [37]. In the end, despite high heat flux exposure, no significant demisability was observed, confirming that SiC retains its structural integrity under re-entry conditions.

Further testing in a higher heat flux regime (L3K PWT) also showed no material loss (see Figure 20), even under constant heat load conditions. Although slight surface passivation occurred due to oxidation [37], the results reinforce that SiC can be considered non-demisable.

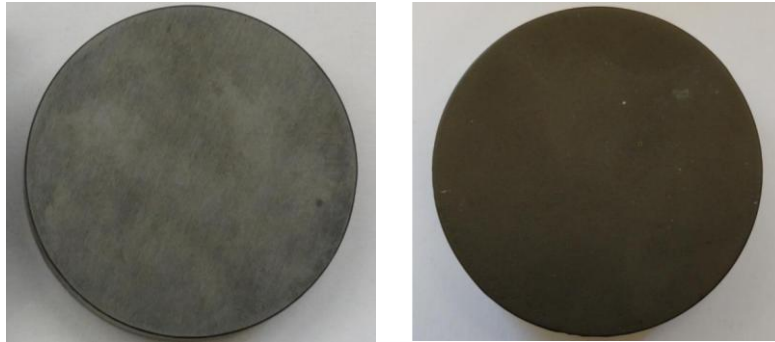


Figure 19: Silicon carbide SSiC ultra-pure – Photographs before and after testing in L2K PWT test [37].



Figure 20: Silicon carbide SSiC ultra-pure – Photographs before and after testing in L3K PWT test [37].

Silica

Silica, or Qz-HS50-A, was tested in the VKI Plasmatron at subsonic and supersonic conditions, showing that depending on the velocity regime, the same material can present different ablation mechanisms, as seen in Figure 21. While the subsonic case is slower and more uniform over the sample surface, the localised heating and the high stagnation pressure of the supersonic case squeeze the material to a flat surface. Nonetheless, none of the cases studied demise in the necessary time conditions of an atmospheric re-entry.

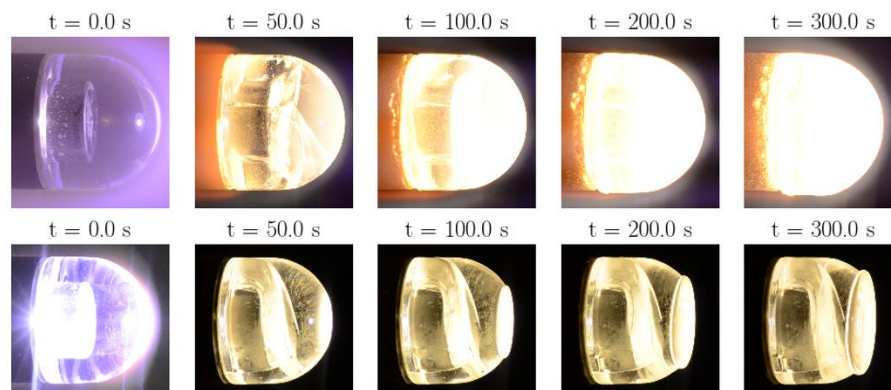


Figure 21: Video frames from test of Qz-HS50 in subsonic (top) and supersonic (bottom) conditions showing their ablation mechanisms [38].

Moreover, Fused Silica is a common optical material used in space applications due to its high thermal stability and resistance to chemical degradation. Its demise behaviour is primarily driven by surface viscosity changes rather than conventional melting or ablation. Tests were performed at the PWT of DLR on three cylindrical samples (optical windows) of 3 mm, 6 mm and 10 mm of diameter under high heat flux conditions.

- The 3 mm sample showed rapid deformation, indicating a threshold size for viscosity driven failure [39].
- The 6 mm sample had minor deformation, suggesting limited heat penetration effects.
- The 10 mm sample remained structurally intact confirming that larger structures maintain mechanical integrity for longer times (see Figure 22).

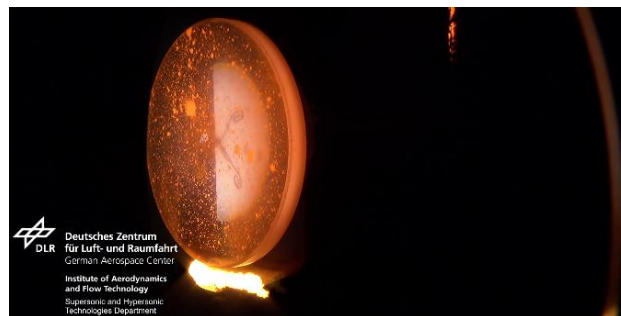


Figure 22: Fused Silica 10 mm diameter rod demise behaviour in PWT test [39].

These tests on Fused Silica optical windows confirmed its low catalytic efficiency, which reduces the effective heat flux compared to fully catalytic materials. It is to be noted that this effect must be accounted for in demise simulations to avoid overpredicting its demisability.

Zerodur

Zerodur, a glass-ceramic material produced by Schott, is widely used in telescope mirrors and space instruments due to its near-zero thermal expansion and high thermal stability. These properties impact its demise, leading to a degradation more delayed than for standard glasses.

Specifically, Ze-HS30-A and Ze-HS50-A were tested in the VKI Plasmatron. For the first one, ablation started after 60 s, while the second presented sample shrinks and a fast ablation after 80 s due to technical issues in the radiometer used for the probes which made these results not reliable. The results obtained in another test are presented in Figure 23, in which onset boiling was detected around 40.3 s for the first material and 4 s for the second [38]. As in the previous case, none of the Zerodur samples demised in the studied timeframes, which makes it a non-suitable material for demise processes.

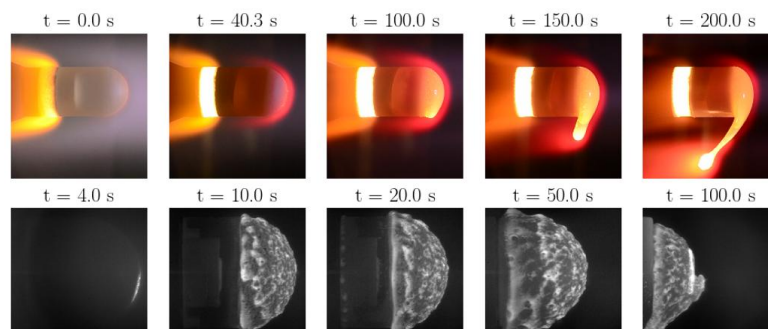


Figure 23: Video frames from test of Ze-HS30-A (top) and Ze-HS50-A (bottom) conditions showing their ablation mechanisms [38].

Zerodur has been recently further studied in DLR's PWT via several tests (see Figure 24). In this case, tests revealed that it presented delayed surface softening, with degradation occurring only at higher temperatures than initially expected. Moreover, like Fused Silica, Zerodur's low catalycity resulted in a lower heat flux input than predicted by standard demise models. Material loss was primarily due to shear failure of the softened surface layer, but overall, Zerodur retained its structural integrity longer than conventional glasses [39]. Zerodur's model on ESTIMATE now accounts for its non-catalytic nature and high surface viscosity to improve simulation accuracy.

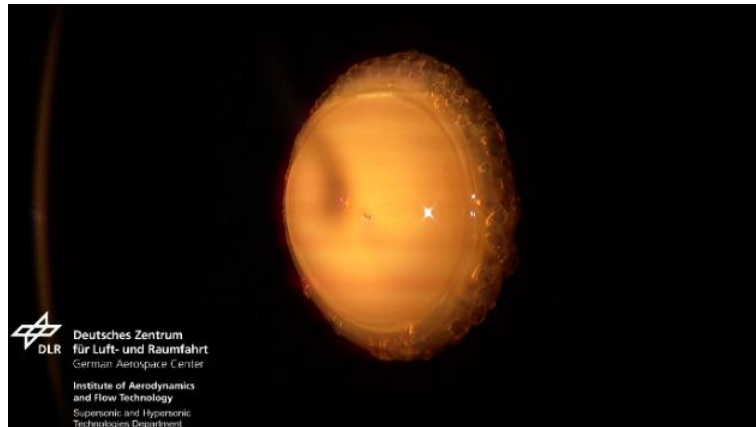


Figure 24: Zerodur demise behaviour in PWT test [39].

4.1.2. Metal Alloys

Metal alloys are the most used materials in spacecraft structures due to their strength, corrosion resistance and ease of fabrication. However, their demisability varies significantly depending on their melting points, oxidation behaviour, and thermal properties. Some metals present rapid demise due to low melting points, while others survive re-entry, requiring design modifications or alternative material choices to enhance spacecraft disposal. They are categorised in different families, each with unique properties influencing their demise behaviour:

- **Aluminium Alloys:** Characterised by low melting points and high demisability.
- **Titanium Alloys:** Possess high melting temperatures and a high specific enthalpy of fusion, making them non-demisable. Normally used in propellant tanks and structural components.
- **Steels:** Exhibit high-temperature resilience, leading to poor demise characteristics. Often found in RW and MTQs.
- **Nickel and Copper Alloys:** Used in electrical components, heating elements, and coatings. Nickel-based alloys, in particular, tend to survive re-entry due to their oxidation resistance.

To enhance demise, use of Titanium and Steel should be minimised, prioritising instead Aluminium-based alternatives where feasible. In cases where re-entry data is unavailable, databases such as ESTIMATE provide baseline material properties. However, due to the limited characterisation of oxidation and ablation at re-entry conditions, approximations are often required. For instance, emissivity values are typically available for unoxidised surfaces but less well defined for ablated materials. A baseline emissivity of 0.8 is generally assumed, supported by experimental observations. Additionally, oxidation heat release and surface catalycity remain at default values (0 and 1, respectively) unless experimental results indicate otherwise.

The demise behaviour of alloys from the four families previously named is presented in detail below. Recent studies have examined the demisability of previously uncharacterised metallic alloys, including Haynes 25 and Molybdenum, while refining existing models for Inconel 718 and Tungsten. Other metal alloys' demise behaviour will not be characterised in this thesis as they are considered either less common in space applications, lacking demise characterisation or non-critical from the demise perspective.

Aluminium Alloy 7075

Different Aluminium Alloys families (e.g. 2xxx, 6xxx, and 7xxx series) have distinct mechanical and thermal behaviours. AA7075 is in the 7xxx series, commonly used in space applications due to its excellent mechanical properties and relatively low weight. It is composed of Aluminium, Zinc, Magnesium and Copper, providing high strength but lower corrosion resistance than other Aluminium alloys. Moreover, its high thermal conductivity leads to a rapid heat distribution.

PWT tests on AA7075 at DLR facilities showed that it has a rapid softening and deformation rather than immediate melting. The high thermal conductivity of the alloy resulted in a low temperature difference across the sample, causing it to weaken uniformly and deform instead of breaking apart. Key findings include:

- Softening was observed after ~24 s, with a major deformation occurring just 4 s later [37] (see Figure 25 to compare the sample before and after testing).
- The highest recorded temperature was 608 °C, below the liquidus point (635 °C) [37] but high enough to significantly reduce the material's rigidity.
- An oxide layer was formed, containing molten Aluminium until mechanical failure, rather than allowing immediate material dispersion, hence delaying full material break up.



Figure 25: Aluminium alloy 7075 – Photographs before and after testing in DLR's PWT [37].

AA7075 is thus a generally demisable material, and components made of it, such as CubeSat structures and RW housings, tend to fail due to shear rupture of the oxide layer rather than complete melting.

Stainless Steel AISI316L

AISI 316L is a corrosion-resistant Stainless Steel alloy widely used in space for structural components, tanks, and RWs. Its high temperature resistance makes it suitable for load bearing elements but also influences its demise. Its low thermal conductivity affects how it heats up and melts, typically resulting in prolonged structural integrity before breaking apart; and its emissivity changes significantly at demise due to oxide formation, affecting thermal measurements.

Unlike Aluminium, AISI 316L melts progressively, with surface material liquefying while the core remains solid for an extended period. On PWT tests performed on AISI 316L samples on DLR's PWT facilities, it was observed:

- Liquid Steel spilling over ~25 s, but the overall shape remained intact [37] (see Figure 26).
- High emissivity due to oxide formation caused discrepancies in spectral pyrometer readings, requiring an emissivity adjustment to 1 for accurate results.
- The two-color pyrometer recorded a peak temperature of ~1420 °C, aligning well with the expected melting range of 1375 °C (solidus) and 1400 °C (liquidus).

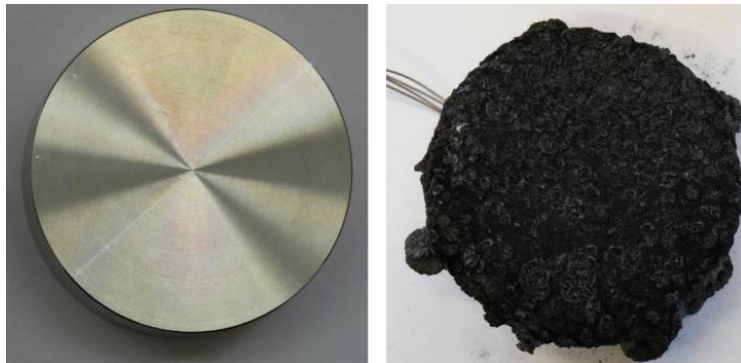


Figure 26: Stainless steel AISI 316 – Photographs before and after testing in DLR's PWT [37].

These results indicate that AISI 316L undergoes a gradual demise process, with liquid metal dripping away while structural integrity is retained for some time. The slow heating and melting behaviour suggest limited break up during atmospheric re-entry, being critical for demise.

Titanium Alloy Ti6Al4V

Ti6Al4V is extensively used in spacecraft structures, thrusters, and re-entry vehicle components due to its high strength, heat resistance, and oxidation resistance. However, its reactivity at high temperatures affects its demisability, sometimes leading to unexpected chemical interactions (such as being prone to alloying reactions and oxide/nitride formation). Moreover, it has a low thermal conductivity that leads to steep temperature gradients.

Several PWT tests have been conducted on Ti6Al4V. The results from DLR facilities showed unique thermal behaviour, with minimal material loss at lower heat fluxes (1.2 MW/m², see Figure 27) but rapid degradation at higher fluxes (2.3 MW/m², see Figure 28). Critical findings include:

- Pyrometer data suggested a surface temperature plateau around 1630 °C [37], close to the expected melting point, 1660 °C.
- At higher heat fluxes, rapid material loss began at the edges first, progressing inward.
- Oxidation and interaction with molecular and atomic Nitrogen played a significant role, affecting emissivity and temperature readings.
- At 2.3 MW/m² samples demised significantly faster, with earlier structural disintegration than expected.

These results indicate that Ti6Al4V demise behaviour is highly sensitive to both temperature and environmental conditions. While it resists melting at moderate heat fluxes, it can break apart rapidly under extreme heating, though it is still considered a non-demisable material for satellite atmospheric re-entry designs. It is to be noted that the formation of Titanium nitride and Titanium dioxide layers impacts thermal emission, affecting how demise occurs in different atmospheric compositions.



Figure 27: Titanium alloy Ti6Al4V – Photographs before and after testing in L2K DLR PWT [37].

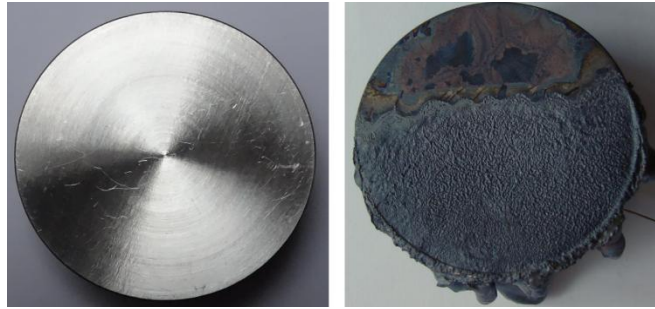


Figure 28: Titanium alloy Ti6Al4V – Photographs before and after testing in L3K DLR PWT [37].

Haynes 25

Haynes 25 is a cobalt-nickel-chromium alloy that serves as a reference material for high-temperature applications. PWT tests demonstrated notable differences between thin (3 mm) and thick (20 mm) samples. While thin samples melted at the datasheet-defined temperature, thick ones exhibited delayed demise due to the formation of a protective oxide layer. This oxide layer acted as a thermal barrier, containing the molten core and delaying structural collapse [40]. Other results from these tests include:

- The protective oxide layer (see Figure 29) of thick samples, delayed structural failure despite exceeding the melting temperature by 200 °C.
- Samples withstood heat fluxes above 970 kW/m², highlighting the role of oxidation in inhibiting demise [40].
- Unlike other metals, melting was not observed at the edges (where heat flux was highest) but instead at the central region, indicating localised internal melting.

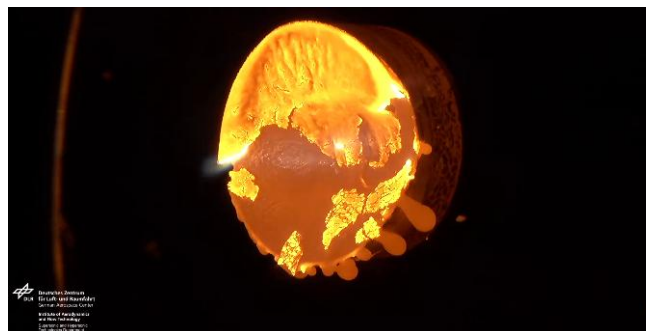


Figure 29: Haynes 25 demise behaviour and oxide layer collapsing in PWT test [40].

These findings highlight the complex oxidation and thermal behaviour of Haynes 25 during atmospheric re-entry. The results emphasise the need for further investigations into oxide layer formation and its impact on spacecraft demise.

Inconel 718

Inconel 718, a widely used nickel-chromium alloy, exhibits similar oxidation-driven inhibition effects. It was tested at DLR PWT facilities, revealing its demise is largely dictated by the formation of a protective oxide layer. To align predictive models with experimental data, models for demise simulations implement an artificial increase in latent heat of fusion. However, experimental demise rates were still slower than model predictions, highlighting the need for further refinements. The most relevant observations regarding Inconel 718 demise include:

- The oxide layer provided partial protection, but unlike Haynes 25, it was less resistant to melting, leading to some material ejection (see Figure 30).
- Unexpectedly, test samples exhibited early failure of fasteners, despite the main structure remaining intact [40]. This suggests that additional factors, such as localised stress concentrations or oxidation effects, play a role in the demise process.



Figure 30: Inconel 718 demise behaviour and oxide layer collapsing in PWT test [40].

Molybdenum

Molybdenum was investigated as a potential material for bolts in containment designs due to its exceptional high temperature stability. Comparative PWT tests on M8 and M4 Molybdenum and Titanium screws mounted on a Titanium plate in DLR facilities showed:

- Titanium bolts melted at similar rates, while Molybdenum bolts exhibited significantly delayed melting, as it can be seen in Figure 31.
- Molybdenum's high melting point and oxidation resistance reinforced its classification as a non-demisable material.



Figure 31: Molybdenum and Titanium screws demise behaviour in PWT test [41].

Given these results, the use of Molybdenum in spacecraft components should be carefully assessed. In cases where complete demise is required, alternative materials with lower melting points should be considered to enhance spacecraft demisability. Moreover, it showed potential for D4C applications.

Tungsten

Tungsten is commonly used in thrusters and RW due to its high density and extreme melting temperature. However, these properties are detrimental from the demise perspective. PWT tests at DLR facilities evaluated its oxidation-driven material loss, resulting in:

- Approximately 1 mm of surface loss was observed due to vaporised Tungsten oxide formation [41] (see Figure 32).
- Despite oxidation-driven degradation, overall structural integrity remained largely intact.



Figure 32: Tungsten cube demise behaviour in PWT test [41].

These results reinforce the necessity of incorporating fragmentation-promoting strategies for Tungsten components to enhance re-entry demisability, and its potential use for D4C.

4.1.3. Composites

Composite materials are widely used in the space sector due to their high strength to weight ratio, tailored mechanical and thermal properties, and excellent structural performance. They are typically made of reinforcing fibres embedded in a polymer matrix, with different fibre types providing varying characteristics. In the space sector, composites are mostly used for structural components, TPS, and propellant tanks overwrap. However, their demise behaviour varies significantly depending on their composition. Some composites, particularly CFRPs, exhibit high heat resistance and slow degradation, being undesirable for satellite demise. Others, such as Flax Fibre Reinforced Polymers (FFRPs), have demonstrated improved demisability.

A factor influencing composite demise is the interplay between matrix pyrolysis and fibre oxidation. While some materials experience early decomposition, the remaining fibre structure can act as a thermal shield, significantly delaying break up. Recent studies focused on optimising composites for improved demisability by modifying their matrix properties and fibre configurations. The next subsections discuss composite families and their re-entry behaviour.

CFRPs

CFRPs consist of Carbon Fibres (CFs) embedded in a polymer matrix, offering high stiffness, low weight, and excellent heat resistance. Their matrix materials typically include epoxy or phenolic resins, which decompose at high temperatures. However, even after matrix pyrolysis, the remaining CF retain their structural integrity and can act as an ablative thermal shield, hindering demise. This is confirmed by recovered debris from re-entering spacecraft in which CFRPs often survive intact.

They have a high strength to weight ratio and low thermal expansion. Moreover, the matrix decomposition occurs through pyrolysis, and the CFs have a low oxidation rate. To better understand their demise, CFRPs have been studied in several PWT tests. The results confirmed that CF acts as a thermal shield (preventing complete demise), and that high heat flux exposure led to a convective blockage due to extreme outgassing. This prevented heat from reaching the material surface, delaying component break up (see Figure 33). But overall, that CFRPs demise behaviour is determined by the layer-by-layer ablation of the matrix and fibres used.

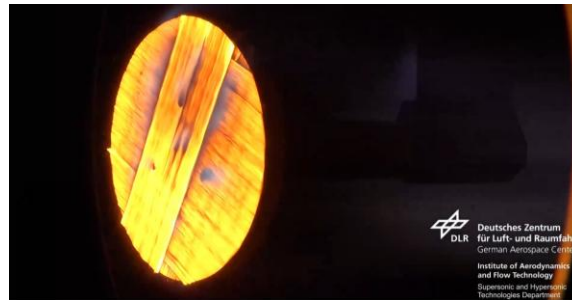


Figure 33: Average CFRP layer by layer demise in DLR's PWT test [42].

Alternative CFRPs designs have been investigated to enhance demisability. Discontinuous fibre reinforcement (cut-CF) improved demisability by promoting fibre spallation and mechanical break up [9]. Furthermore, specific CFRP matrix compositions (e.g. L20/EPH960) showed improved demise due to low char yield, as demonstrated in DLR PWT tests [43]. Other ideas to increase CFRPs demisability include exposing laminate edges to encourage spallation and designing components for early exposure to the heat flux to accelerate failure.

FFRPs

FFRPs are a bio-based alternative to CFRPs, using Flax Fibres instead of CFs. FFRPs have been studied due to their improved thermal decomposition properties. They have comparable mechanical properties to CFRPs, higher demisability due to lower char yield and improved mass loss behaviour at high heat fluxes. PWT tests (PWK4) performed on FFRP samples confirmed significantly higher demisability than CFRPs. Infrared thermography and optical spectroscopy reinforced rapid decomposition and mass loss.

Besides, alternatives to increase their demisability have also been explored, such as adding AlMg fillers, which, as seen in PWT tests in IRS facilities, further improved demise by facilitating matrix breakdown. The AlMg integration in FFRP allows a 4 % improved ablation rate and a 17 % higher [9] proportion of demised plies. Other tested options consisted of a hybridisation of CF and Flax Fibre tow by tow and ply by ply. Compared to CFRP, the tests showed that hybrids improve demise greatly with more than 60% (tow-by-tow) and 200% (ply-by-ply) higher ablation rates respectively [9] (see Figure 34).

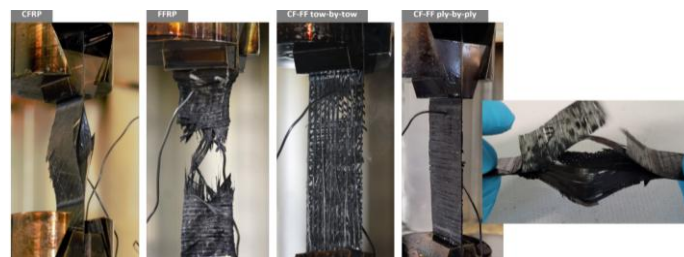


Figure 34: CFRP, FFRP, CF-FFtbt, CF-FFpbp after testing. On the right, a closer view of the ply-by-ply hybrid, with a clear view of the central twill flax ply near a full demise with only carbonated Flax Fibres left [9].

GFRPs

Glass Fibre Reinforced Polymers (GFRPs) consist of Glass Fibres embedded in a polymer matrix. They are used for electronic housings and battery modules due to their electrical insulation and mechanical durability. They also have moderate thermal resistance and require further investigation to refine material models. To address this, PWT tests have been conducted to characterise GFRPs demise behaviour and develop an equivalent metal proxy model to improve re-entry simulations. These tests are different than other material tests as they were conducted directly on the parts made of GFRP instead of material testing samples.

The tests results showed that GFRP has a delayed mass loss at moderate heat fluxes, with no immediate fragmentation (especially on battery modules where rotational motion accelerated break up). At moderate heat fluxes, surface melting was observed, though with high viscosity preventing material loss, while at higher fluxes, the viscosity decreased sufficiently to have material flow, leading to mass loss above ~ 1200 °C [44]. However, fragmentation was not instantaneous, and in cases where no substantial mass was present, the material deformed rather than disintegrated into small fragments. When tested separately in a stagnation configuration, GFRP sheets exhibited early delamination and warping, followed by material bending and partial melting (see Figure 35) at high heat fluxes. Alternatively, at low heat fluxes, GFRP fibres sintered, forming a protective layer that inhibited further demise [44].



Figure 35: GFRP sheet of battery module demise behaviour in stagnation configuration in DLR's PWT facilities [44].

4.1.4 Ablative Materials

Ablative materials are designed to withstand extreme aerothermal heating by charring and sublimating. They use an ablative layer on the surface so that the aerothermal heat chars a resin held by fibres into a carbonaceous mass with relatively low strength, resulting in the vaporisation of the char. As a result, it appears a new layer with a higher density, capable of absorbing six times as much heat as boiling water. In other words, the ablative material can absorb energy through latent heat during melting or evaporation and sensible heat with temperature rise. At the same time, it thickens the thermal boundary layer, reducing the incident heat flux on the surface [45].

In this process, the ablative layer dissipates heat by sacrificing the removal of surface material using polymeric materials. These polymeric ablatives present high heat shock resistance, low density, good mechanical strength and good thermal insulation capabilities; and can be divided into non-charring materials (the gas evolution from the polymeric ablatives interferes with the convective heat transfer from the atmosphere to the material surface, forming a volatile monomer leaving no solid residue) and charring polymer materials (the solid residue formed on the surface of the ablated material provides thermal insulation for the underlying virgin material, as illustrated in Figure 36) [45]. The most used ablatives are Phenolic Impregnated Carbon Ablator (PICA) and Silicone Impregnated Reusable Ceramic Ablator (SIRCA) [46].

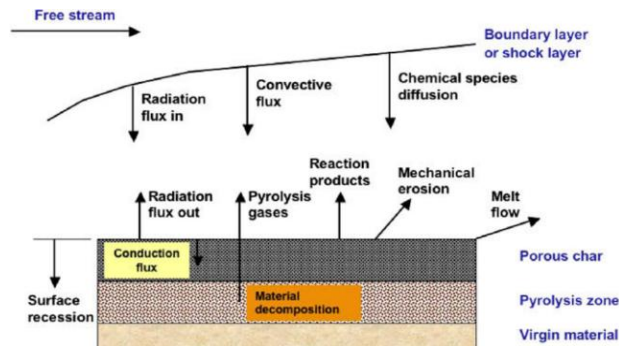


Figure 36: Behaviour of ablative materials [46].

The use of ablative materials is thus concentrated in TPS and heat shields, making them unsuitable for demise purposes. As ablative materials are counterproductive to D4D objectives, it is not recommended to include them in a satellite that has demisability as one of its objectives.

4.1.5 Demisability Summary of Materials

Material selection plays a critical role in demise during atmospheric re-entry. The demisability of materials is mainly defined by their effective heat of ablation and demise threshold, being this the temperature at which a material begins to lose mass through outgassing, active oxidation, erosion or removal of a molten phase. Otherwise, the effective heat of ablation is the ratio of the incident heat flux to the mass loss rate over a given surface area measured for an ablative material under extreme aerothermodynamic heating conditions relevant to atmospheric entry.

According to the test results presented in the previous subsections, the main conclusion is that high-temperature-resistant materials exhibit delayed ablation, while low melting point alloys and composites tend to fragment and disintegrate more predictably, thereby reducing the risk of surviving debris. Therefore, a general classification of the materials demisability can be:

- **High Demisability Materials:** Such as Aluminium alloys, due to low temperature thresholds and rapid ablation. Shear rupture of the oxide layer leads to material break up.
- **Low Demisability Materials:** Titanium, Stainless Steel, Nickel, Molybdenum, Tungsten, SiC, Fused Silica and Zerodur due to high melting points and slow degradation. Ablators also present poor demisability.
- **Low Demisability but allowing for modifications:** CFRPs and GFRPs conventional designs present low demisability. However, alternatives such as FFRP, hybridisation and micropower insertion have shown promising demisability enhancement while maintaining good structural integrity in the research performed so far.

The material properties define the fundamental response to extreme heating, but the structural context determines how this response occurs during re-entry. Consequently, beyond characterising material demisability, it is also essential to assess the demise behaviour of components within the system. The following section will focus on this aspect, examining the demisability of components. While material substitution can be an effective strategy for enhancing component demisability, practical constraints such as structural requirements, mechanical performance, and manufacturing limitations may restrict its feasibility. Therefore, a holistic approach, integrating both material characterisation and structural assessment, is necessary to develop effective D4D strategies.

4.2. System level activities

While material selection is a fundamental factor influencing demisability, it is not the sole cause of the demise behaviour of a component. This behaviour is strongly dependent on the component integration within the overall structure. Factors such as shape, width/radius, aspect ratio, thickness, positioning within the platform, mechanical connections, and thermal interactions with adjacent components influence heat transfer dynamics and affect the onset and progression of demise.

In order to assess component demisability, it is essential to quantify the relative influence of these factors. A sensitivity analysis was conducted in the past to evaluate their impact on the demisability index, which quantifies the fraction of mass lost during re-entry. The results of such analysis, presented in Figure 37, highlight the dominant role of material selection in determining demisability. However, for components where material substitution is impractical due to structural or functional constraints, modifying the thickness and overall dimensions significantly influence demisability.

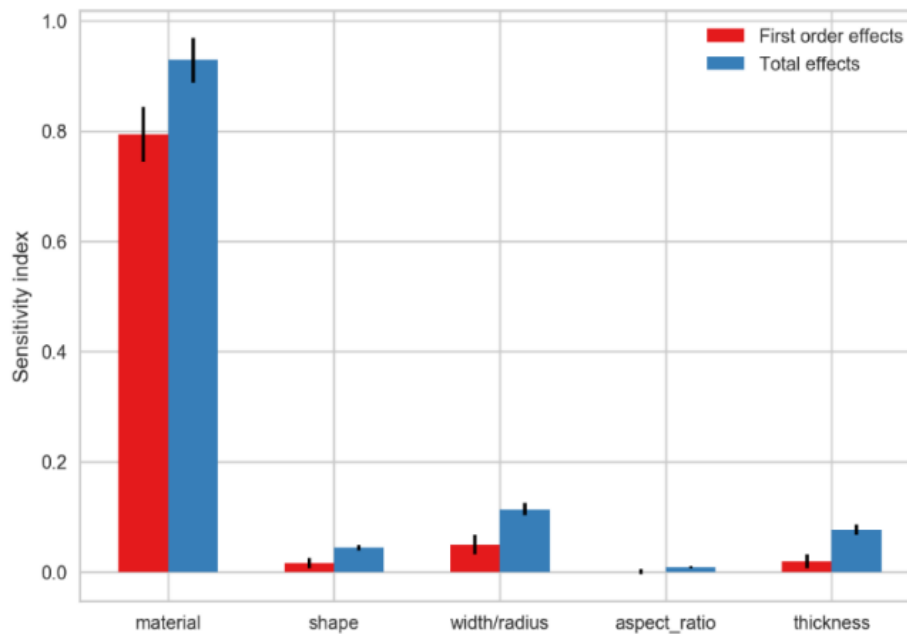


Figure 37: Sensitivity analysis of demisability index respectively for factors influencing demise [47].

Conversely, the survivability index is most strongly influenced by both thickness and material properties, with a notable degree of interaction between design parameters. The sensitivity analysis further indicates that, in the case of survivability, the total effects of multiple parameters combined exceed the first order effects of any single variable [47]. This suggests coupling effects between design parameters must be carefully considered when studying components demise.

Given these findings, the following section will analyse the demisability of critical spacecraft components identified in Section 3.1. aiming to provide an understanding of their behaviour during re-entry and to outline potential design strategies that enhance controlled demise while balancing structural and functional requirements. Particular focus will be placed on structural panels, mechanical joints, solar panels, batteries, electronic cards and boxes, propulsion system elements (including tanks and thrusters), as well as attitude control hardware (such as RWs, MTQs, gyroscopes, and star trackers). Additionally, the demisability of optical components, including mirrors, fixings, bipods, and baffles, will be examined.

4.2.1. Structural panels

Structural panels, often made of metallic or composite materials, undergo complex failure mechanisms due to extreme aerodynamic heating, mechanical stresses, and material-specific degradation processes. The break up and demise process largely depends on the panel material, core structure, and connectivity to the spacecraft body.

Honeycomb sandwich panels, commonly used in space due to their high strength to weight ratio, present different demise and break up sequences depending on the material composition:

- Aluminium honeycomb sandwich panels consist of Aluminium face sheets bonded to an Aluminium core with a film adhesive. In re-entry, the adhesive softens and peels early in the process, leading to a rapid loss of structural stiffness [48]. This early detachment enhances demise, allowing fragments to heat up and burn away more efficiently.
- CFRP honeycomb panels show delayed failure due to the high heat resistance and low in-depth conductivity of CFRP. In stagnation tests, CFRP panels with 3D-printed cores exhibited increased thermal inertia, delaying core collapse. The honeycomb structure compressed over time, squeezing molten Aluminium laterally while retaining structural integrity within an oxide layer (see Figure 38) [48].

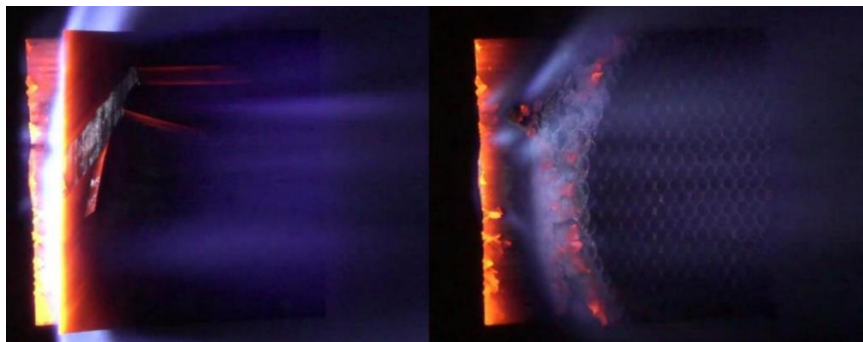


Figure 38: 4 ply CFRP Sandwich Panel Before and After Panel Removal; Elliptic Recession of Honeycomb Evident [48].

The demisability of structural panels themselves is typically not an issue. The point here is that the earlier these panels demise or fly away, the earlier the internal components of the satellite will be exposed to the heat flux, enhancing the demise of the overall platform. Therefore, promoting the early break up of structural panels would be an ideal strategy to apply in a demisable platform. Apart from changing the material to lower melting point options, other alternatives to enhance demisability consist of using **panel-free** and **closure panel-free** designs. The first option removes external structural panels to directly expose internal spacecraft components to atmospheric heating but poses significant system-level challenges, such as radiation shielding and load-bearing constraints. Closure panel-free designs, on the other hand, eliminate non-load-bearing closure panels while retaining primary load-bearing structures, enhancing the exposure of internal components while maintaining some system integrity [49].

Other options to increase demise include using **break out patches** and **topology optimisation**. Break out patches in panels can be implemented as cut-outs or localised areas of reduced core density to promote early failure. These cut-outs improve demisability but may require additional thermal control or radiation shielding. Topology-optimised panels leverage Computational Fluid Dynamics (CFD) and Additive Manufacturing (AM) to create geometries that channel heat flux effectively [9]. By designing structures with smaller curvature radii, convective heat transfer is enhanced, accelerating material degradation and break up.

4.2.2. Joints

Structural joints connect the panels of a satellite, ensuring mechanical integrity throughout the mission. During atmospheric re-entry these joints undergo extreme thermal and mechanical stresses, ultimately leading to their failure and break up. The way these joints fail plays a crucial role in the demise of the spacecraft and the exposure of internal components to the heat flux.

Standard structural joints typically consist of cleats, screws and washers, which secure panels together. The effectiveness of these joints in maintaining structural integrity diminishes as mechanical loads and aerodynamic heating intensify during re-entry, where their failure is influenced by a combination of thermal and mechanical loads. Analysis performed show that joint failure is not solely dictated by temperature but also by the distribution of forces across the spacecraft structure [50]. Simulations using the SAMj and SCARAB tools have provided insights into the forces experienced by structural joints at varying altitudes. It has been observed that joint forces range between 6 - 10 N, which is consistent with SAMj model predictions. Additionally, rotational dynamics affect the load paths experienced by individual joints, influencing their break up sequence and altering the timing of structural panel separation [48].

To promote earlier break up, demisable joints have been proposed as an alternative to conventional designs. They are designed to fail at lower temperatures or reduced mechanical loads, expediting panel separation and increasing the exposure of internal components to the heat flux. Several approaches have been investigated for enhancing joint demisability, including:

- **Material Substitution:** Replacing conventional screws with Aluminium alternatives has been considered as a means to promote earlier joint failure. However, while Aluminium screws possess a lower melting point, their mechanical performance is inferior to e.g. Titanium, requiring careful assessment of their structural feasibility.
- **Modified Joint Designs:** Integrating 3 -printed cleats and space qualified damping rubbers could introduce controlled structural weakening without compromising integrity.

In conclusion, the integration of demisable joints into satellites presents several design challenges. While the objective is to induce earlier joint failure, this must be achieved without compromising overall structural integrity and mission performance.

4.2.3. Solar panels

Solar panels are fundamental for satellite power generation, typically comprising materials such as CFRP for structural parts, Aluminium honeycomb cores for support and a very thin coating layer of a Ceramic/Glass material to protect them. Understanding their behaviour during atmospheric re-entry is essential for assessing demisability and associated CR.

In re-entry simulations and PWT testing, the CFRP front layers exhibit rapid, sequential ablation. This layer-by-layer degradation exposes the underlying materials to direct aerodynamic heating. Following the ablation of CFRP layers, the Aluminium honeycomb core melts swiftly from front to back. Notably, the melting progresses without early side melting, indicating minimal influence from lateral heat flux. It is to be noted that in certain tests, one of the six CFRP layers remained in front of the molten Aluminium core, and it is unclear whether these layers were expelled during re-entry or detached post-demise [37]. On solar cells' fragmentation behaviour, their early separation from the solar panels due to aerodynamic forces is common in re-entry.

The demisability of solar panels could be increased using features that encourage early fragmentation, such as intentional weak points. However, as their criticality is very low and mostly due to the structural support elements that compose them i.e. CFRP sheets and Aluminium honeycomb core, it is considered that they do not require to be redesigned to promote demisability. The focus is on structural panels using these components, and when technological advancements are available they could be used in solar panels if necessary to slightly reduce CR.

4.2.3. Solar Array Deployment Mechanisms

The Solar Array Deployment Mechanism (SADM) plays a critical role in the deployment and stabilisation of solar panels during spacecraft operations. These mechanisms include drive shafts, bearings, gears and stepper motors, often made from a combination of Aluminium alloys (AA7075), Stainless Steels (AISI 316), and other high-strength materials. Since understanding their demisability of these components is essential to ensure compliance with SDMR, several PWT testing campaigns have been performed [51] [52]. The tests comprised full scale unit assessment and targeted assessments on critical parts such as the inner mandrel, crown wheel, main bearing, and preload nut. To complement experimental results, numerical modelling was performed using SCARAB and DRAMA tools. The most relevant observations for demise were:

- Early detachment of minor Steel components, indicating a progressive failure of fastening mechanisms under high heat flux.
- Penetration of flow in the driveline cavity, leading to localised heating and accelerated melting of internal structures.
- Onset of melting followed by re-solidification in components such as the preload nut, potentially altering the final break up process.
- Variation in emissivity between Aluminium and molten Steel, affecting thermal measurement accuracy during peak heating phases [52].

Test results confirmed that while parts of the SADM are expected to demise, it is non demisable as a whole and uncertainties remain due to re-solidification, fragmentation behaviour of high strength Steel components and influence of cavity heating on structural integrity.

4.2.4. Batteries

Batteries are a crucial component in satellite power systems, designed to store and supply energy throughout the mission. Given their structural and chemical composition, their behaviour during atmospheric re-entry can present challenges. In particular, the presence of Steel casing affects their demisability, and internal chemical reactions such as thermal runaway may influence heating and fragmentation. Assessing the demise of batteries is complex due to limited full-scale testing opportunities, making accurate material modelling essential for predicting their behaviour in simulations. From the PWT testing performed, the main conclusions are:

- Influence of Casing Material: The demisability of battery cells is primarily dictated by their casing, which provides structural integrity but increases the likelihood of survival during re-entry. Tests showed that the melting of the Steel casing occurs at flux levels of approximately 300 kW/m^2 , revealing internal cell layers [53]. Conductivity within the cell is relatively low due to its layered structure, meaning that the casing may reach melting temperatures even when equilibrium temperature predictions suggest otherwise.

- Fragmentation and Structural Failure: Battery fragmentation is strongly influenced by the failure of the surrounding GFRP structure. Tests on battery modules (of 16 cells between two GFRP sheets) demonstrated that GFRP recession occurs at approximately 1200 °C, initiating the detachment of cells [44]. In static tests corner cells heated more quickly due to their prolonged exposure to plasma flow (see Figure 39). As GFRP deteriorated, corner cells detached first, followed by the outermost rows of the battery. Once detached, the exposure of single cells to high heat flux increases the probability of complete demise.



Figure 39: Battery Module demise behaviour in DLR's static PWT test [44].

- Thermal Runaway and Charge State Effects: Cells at different charge levels (fully charged at 4.2 V, discharged at ~1 V, and passivated at ~0.5 V) exhibited thermal runaway in the fully charged state. However, despite accelerating the rate of heating, thermal runaway was not found to be a determining factor for demise, as all cells eventually reached a common thermal equilibrium under identical flux conditions [53].
- Rotation Effects on Battery Fragmentation: In dynamic testing, two rotational speeds, 0.3 Hz and 2 Hz, were assessed to analyse centrifugal effects on fragmentation. At 0.3 Hz, the break up was driven by GFRP sheet degradation, with limited cell demise. However, at 2 Hz, fragmentation occurred at a faster rate due to increased centrifugal forces, leading to earlier cell exposure and enhanced heating effects [44] (see Figure 40). These results indicate that higher spin rates can accelerate the demise process.



Figure 40: Battery Module demise behaviour in dynamic PWT test and high-flux conditions [44].

Given the observed fragmentation and heating behaviour, a potential strategy to improve spacecraft battery demisability could be to **enhance GFRP fragmentation** as its failure defines the cell exposure and subsequent demise. For example, modifications to increase its degradation rate (e.g., **optimised material composition** or **pre-designed structural weak points**) could improve break up behaviour and enhance demisability. Summarising the conclusions from these tests, small cell batteries are expected to fully demise from most relevant re-entry altitudes, while larger cells exhibit reduced demisability, posing a higher CR. The demise process is driven by GFRP fragmentation and rotation effects significantly influence break up behaviour, with higher spin rates leading to accelerated fragmentation and increased heating exposure.

4.2.5. Electronic cards and boxes

The assessment of electronic components' demisability presents unique challenges due to their material composition, structural configuration, and thermal response during re-entry. Electronic assemblies typically consist of a combination of metallic and composite materials, each with distinct thermal and mechanical behaviours under extreme aerothermal conditions. The main factors influencing the demise of electronic components include the thermal response of Printed Circuit Boards (PCBs), the shielding effect of external housings, and the failure mechanisms of internal components.

To characterise these effects, PWT testing was conducted on several representative electronic components. The EnMAP Electronics Card presented significant softening and deformation, undergoing oscillatory motion in the plasma flow. Localised delamination was observed at the board's edges, where heat exposure was most intense (see Figure 41). Failure occurred along the pivot line, although complete material demise was not achieved [44].

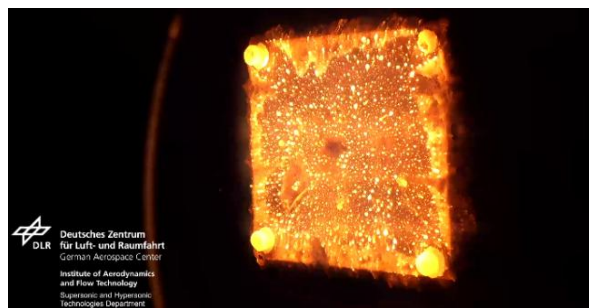


Figure 41: EnMAP Electronics Card demise behaviour in DLR's PWT facilities [44].

For the PD Electronics Card, componentry remained attached to the PCB despite significant oscillations. Delamination at the leading edge increased heat exposure, eventually leading to full demise at approximately 1200 °C, as the softened material flowed from the board [44].

The BCM Electronics Module showed an alternative failure mode. The cabling detached early on, while the module itself remained largely intact until the aluminium housing reached its melting point. At this stage, the enclosure began to warp, leading to tearing and cracking at its edges. The aluminium housing eventually failed catastrophically, but the internal electronic cards remained mostly intact, with the rear card experiencing a delayed demise due to thermal shielding from the front card (see Figure 42).

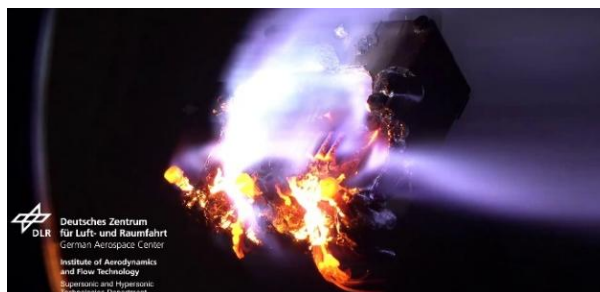


Figure 42: BCM Electronics Module demise behaviour in DLR's PWT facilities [44]

Similarly, for the PCDU Electronics Card, the Aluminium housing provided initial shielding, delaying the onset of material degradation. Upon removal of the housing, the card presented oscillatory bending and failed near its mounting points [44]. Demise was observed mainly in the rear section due to greater exposure to direct heating.

Given the observed low inherent demisability of GFRP-based PCBs, potential strategies were explored to enhance the demise of electronic assemblies during re-entry:

- **Material substitution:** Replacing GFRP by Aluminium would improve demisability; however, this is impractical due to industry-standard reliance on GFRP-based PCBs.
- **Pre-designed failure points:** Introducing deliberate weak points within the fiberglass cloth arrangement could promote earlier fragmentation, though implementation is constrained by functional and environmental requirements.
- **Dimensional optimisation:** Reducing PCB size may improve demise behaviour, but feasibility is limited by design constraints and electronic system requirements.
- **Enhanced mechanical failure mechanisms:** Investigating methods to promote higher-force material tearing could accelerate structural failure. However, further static facility testing is required to validate these mechanisms.

In summary, the research [44] showed that Aluminium housings initially shield internal electronics but eventually fail catastrophically, exposing PCBs to direct heating. GFRP-based PCBs have poor demise behaviour, with oscillatory bending as the dominant failure mode. Certain components, particularly transformers, present high survivability and pose a CR if not adequately addressed. Additionally, higher heating (~1200 °C) is required to achieve the complete demise of electronic cards. Further research into controlled failure mechanisms is recommended to enhance the demise potential of electronic while maintaining functional integrity during operations.

4.2.7. Tanks

Titanium propellant tanks are known to be highly resistant to demise due to the high melting temperature of Titanium alloys. Analysis of nominal and Monte Carlo simulation results confirms that Titanium tanks generally survive re-entry intact. The main factor contributing to their survivability is their material composition, with Titanium's high temperature resistance making it undemisable under nominal re-entry conditions. Consequently, the only viable approach to reducing the CR associated with tanks is through **material substitution**.

Finding a suitable demisable material that meets the stringent chemical compatibility and pressure requirements of propellant tanks is a major challenge. Various alternatives have been explored, including Steel and Aluminium tanks, as well as Composite Overwrapped Pressure Vessels (COPVs). However, simulation studies indicate that Steel tanks, as well as Titanium or Steel liners within COPVs, do not fully demise upon re-entry [49]. This severely limits the selection of materials that can effectively reduce CR of propellant tanks.

PWT tests were conducted to assess in more detail the demise of CFRP overwrapped Titanium tanks [54]. The tank samples tested lasted significantly longer than CFRP material samples due to the higher ablation resistance of Titanium, approximately five times greater. The observed demise process involved the endothermic decomposition of the epoxy matrix, which contributed to a heat sink effect and transpiration cooling. The CFRP overwrap exhibited minimal ablation, with CF remaining in place until they gradually burned at a rate dictated by the available oxygen. Unlike typical layer-by-layer ablation, only small fibre fragments were ejected. The Titanium liner melted only after the ablation front reached the Titanium surface. Unlike standalone Titanium, which remains largely intact at low heat fluxes during LEO re-entry, the

additional heat required for the demise of the overwrapped Titanium liner, appeared to originate from the chemical enthalpy released by the reaction of CFRP with atmospheric oxygen [37].

Given the limitations of material selection, additional strategies have been considered to improve the demise characteristics of propellant tanks:

- **Material and Manufacturing Process Substitution:** Tanks of fully demisable materials such as Aluminium-Lithium alloys or demisable COPVs of Aluminium liner [54].
- **Thermite Coating:** Applying a thermite-based coating to enhance in-orbit break up. However, initial studies indicate potential system impacts due to added mass [49] and failure and explosion risks.
- **Pyrotechnic Tank Cutting:** Employing a controlled pyrotechnic device to fragment the tank into smaller, more demisable sections upon re-entry. Simulations suggest that cutting a Titanium tank into 20 fragments significantly improves demise characteristics [49]. However, using these technologies to promote demise poses a high risk of failure, specifically when applied to pressurised components such as tanks, even if they are expected to be passivated before performing the cutting.

4.2.8. Thrusters

Thrusters are among the most challenging components to model in demise simulations due to their complex internal structure and material composition. They contain multiple subcomponents, each with distinct thermal and mechanical responses during re-entry. PWT testing demonstrated that the lower half of the thruster is significantly more prone to demise than the upper section, due to differences in material thickness and internal potting behaviour.

To investigate the thermal response and failure modes of thrusters during re-entry, five Ariane Group 1 N thrusters were subjected to controlled testing under various conditions. One thruster was disassembled into four parts to assess the demisability of each component. Another one was split into two halves to examine differential material response. Three intact thrusters were tested as complete systems to evaluate overall demise behaviour. Additional tests were conducted on thruster piping, including various sizes [40]. The results from these tests are:

- Thruster piping does not pose a CR despite being made of Titanium, as its low mass and small size lead to a rapid demise. Additionally, the thruster heatshield demises quickly once its melting temperature is reached, due to its relatively low mass.
- The large inlet section of the thruster showed delayed demise due to internal potting material outgassing, which acted as a thermal barrier. Conversely, the small inlet section presented higher resistance to demise, with only localised surface melting observed.
- The Nozzle behaviour varied depending on the material and dimensions:
 - A small Inconel 718 nozzle (20 mm diameter) showed melting along the rim, with a strong oxide layer formation that influenced material recession [40].
 - A large Inconel 718 nozzle (50 mm diameter) had a similar degradation pattern, indicating scalability effects in demise behaviour.
 - In contrast, a large Haynes 25 nozzle presented a significantly delayed demise, as the formation of an oxide layer increased structural resistance [40], reducing material motion and deformation as it can be seen in Figure 43.

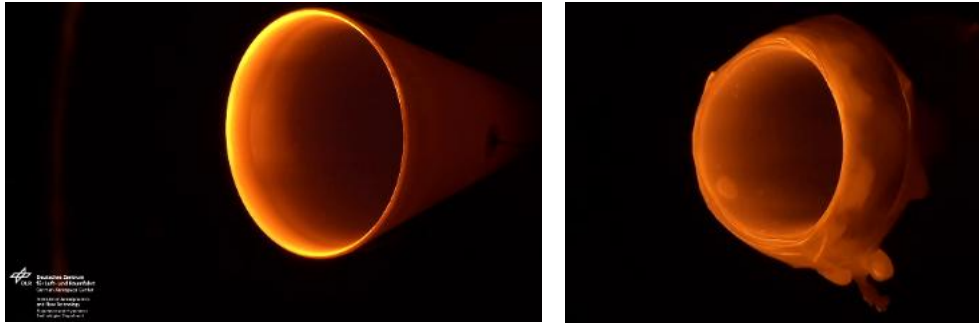


Figure 43: 50 mm diameter nozzle of Haynes 25 demise behaviour in DLR's PWT test [40].

- Lower and upper thruster sections behaved differently:
 - The lower half of the thruster demised more rapidly, particularly under high heat flux conditions, leading to significant material loss.
 - The upper half had a slow demise due to its thicker material and the thermal effects of potting material outgassing [40], which altered heat transfer dynamics.

These tests results indicate that thruster demise highly depends on material composition, internal potting effects, and structural configuration. The lower half of the thruster is more prone to early failure, whereas the upper half exhibits greater survivability due to potting outgassing and increased material thickness (see Figure 44). Additionally, nozzle material selection plays a crucial role, with Inconel 718 demonstrating progressive degradation and Haynes 25 showing enhanced thermal resistance due to oxide layer formation. These results emphasise the need for accurate modelling of thruster subcomponents in simulations and suggest that alternative design approaches, such as **material selection**, **internal structural modifications**, or **controlled failure mechanisms**, could enhance the demisability of future thrusters designs.



Figure 44: Whole thruster at 0 ° demise behaviour in DLR's PWT test [40].

4.2.9. Balance masses

Balance masses are dense structural components used to adjust a satellite's centre of mass and ensure proper attitude control. Due to their high mass and composition, balance masses can survive atmospheric re-entry, posing a potential CR. Their demisability is principally defined by material selection, exposure conditions, and mass distribution.

Balance masses are typically made of high-density non demisable materials, such as Stainless Steel. However, balance masses made of aluminium have been observed to fully demise, demonstrating the potential benefit of switching to more demisable materials when feasible in early stages of satellite's design.

Moreover, the fate of a balance mass during re-entry is strongly influenced by its size and location within the satellite. Smaller balance masses (< 20 kg) or those positioned externally tend to demise, while larger masses (> 20 kg) are more likely to survive [54]. Based on simulation results, a satellite with a 50 kg internal balance mass resulted in a single surviving fragment upon re-entry, while three external balance masses (totalling 13 kg) on the same satellite fully demised, indicating that external placement enhances heating and demise potential [49].

To improve the demisability of balance masses and reduce CR, potential strategies include:

- **Material Selection:** Using Aluminium instead of Steel increases demisability while reducing mass [54]. However, this may impact volume constraints due to Aluminum's lower density.
- **Mass Distribution:** Instead of a single large mass, divide balance masses into multiple smaller masses held together in a demisable container [54]. This enhances exposure to high temperatures and promotes earlier fragmentation.
- **Alternative Manufacturing Techniques:** Introducing layered materials or sintered structures can accelerate structural failure and demise [49].
- **External Placement:** Relocating balance masses to the exterior of the spacecraft increases heat exposure [49], accelerating their thermal response and reducing survivability.

4.2.10. Reaction Wheels

RWs are critical components in satellite attitude control systems, and play a significant role in CR. The entire RW90 reaction wheel, composed of an Aluminium housing and a Copper-Beryllium (CuBe) flywheel and the flywheel alone at a higher heat flux, were tested to assess its demise behaviour at controlled heat flux conditions. The aim was to examine the fragmentation sequence and thermal response of the RW components, providing data for demise modelling.

The PWT tests confirmed the staged demise of RW90. The housing failure started with the first surface finish changes of the housing at 60 s, followed by cracks and tearing in the Aluminium oxide layer at 94 s, with the first significant material removal at 130 s (see Figure 45 left). Finally, the front housing face detached at 147 s, exposing internal components. The internal Aluminium cage and ring melted sequentially, with the motor remaining intact due to its Steel parts acting as a heat sink. Moreover, the Aluminium housing and cage were completely removed by 612 s [55], leaving just the motor and flywheel (see Figure 45 right). The motor housing survival suggests a need for further study, particularly regarding heat sink effects and potential design optimisations.

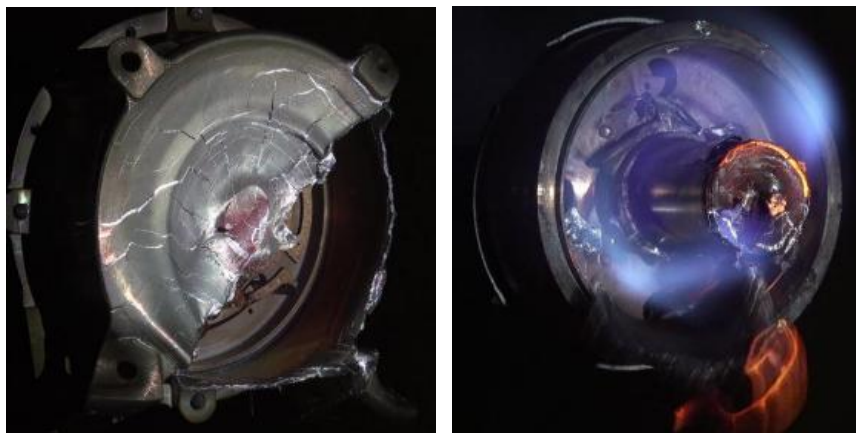


Figure 45: Test RW90 events sequence from housing significant material removal to completely removed with the cage leaving the motor and flywheel (from left to right) [55].

For the PWT tests on the CuBe flywheel under high heat flux, it was observed that at 200 kW/m², the flywheel reached thermal equilibrium, demonstrating nearly isothermal behaviour due to CuBe's high conductivity. At 300 kW/m², initial melting was observed at the rim at 320 s, with liquid material movement at 360 s. Then, the centre of the flywheel melted at 389 s, leading to structural collapse at 398 s [55]. Other PWT tests indicate that Stainless Steel inertia rims and motor assemblies typically survive re-entry [49].

Results confirm that a simplified failure model effectively represents the demise process of RWs with an Aluminium housing and less demisable interior components. The **CuBe flywheel** demonstrated significantly improved demisability compared to Stainless Steel alternatives, supporting its selection for debris reduction. Other D4D techniques that could improve RWs demisability include **substituting the material of the inertial rims with Aluminium** and **using glued or laminated Stainless Steel components** [49].

4.2.11. Magnetorquers

MTQs are commonly used in satellite attitude control systems and typically consist of an Aluminium or CFRP housing, Copper windings, and a ferromagnetic core. Their demisability during atmospheric re-entry is of particular interest due to their potential for reaching ground.

According to PWT tests, the housing of the MTQ, when made of CFRP, burns through at a heat flux of 542 kW/m², significantly faster than anticipated and following a layer-by-layer ablation process. The Copper windings, due to their insulation layers, do not behave as a solid mass but instead exhibit low net conductivity, leading to an altered thermal response (see Figure 46). The core of ferromagnetic Steel melts at approximately 749 kW/m² [53]. PWT tests showed that epoxy-based potting compounds have significant survivability, potentially affecting the overall demise [55]. Given the observed high survivability of potting materials, additional tests without the CFRP housing are recommended to isolate its contribution to the overall demise.



Figure 46: MTQ demise behaviour in PWT test, showing the CFRP burn through, layer-by-layer Coil removal and core melt from up to down [55].

SCARAB and SAMj simulations suggest that MTQs frequently survive re-entry, particularly in cases where they are released late in the trajectory and have limited exposure to high heat flux. However, higher fidelity models accounting for the high aspect ratio of MTQs indicate that previous simulations tend to underpredict heat flux by approximately 40% [54], suggesting greater potential for demise than initially assessed.

To enhance the demisability of MTQs, several D4D options can be explored:

- **Alternative Core Materials:** Replacing ferromagnetic Steel with Nickel alloys could lower survivability, but keeping magnetic performance might be challenging.
- **Dimensional Adjustments:** Modifying the length and thickness of the core could alter its thermal response, potentially increasing its susceptibility to demise.
- **External Mounting:** Positioning MTQs in more exposed areas would increase their exposure to high heat fluxes during re-entry. The systems-level impact of external mounting is minimal, but it should contemplate potential electromagnetic compatibility and thermal considerations such as thermal cycling effects. However, while placing MTQs externally enhanced demise characteristics in DEBRIS simulations, the overall reduction in CA is relatively minor given the low likelihood of MTQ survival [54].

4.2.12. Gyroscopes

Gyroscopes are part of spacecraft attitude control systems and provide measurements of angular velocity. However, their robust design and material composition pose significant challenges to demisability. Notably, gyroscopes often consist of multiple sub-components, including Gyro Electronics Units (GEUs) with GFRP cards and Fused Silica sensor coils.

Simulations and PWT testing indicate that gyroscopes represent a considerable CR, with three or more sub-components expected to survive re-entry and impact on ground across various release altitudes. The mean CA associated typically exceeds 2.5 m² [40]. The primary contributors are the GEU cards of GFRP due to the material's resistance to thermal degradation. Moreover, the Fused Silica sensor coils are also unlikely to demise owing to their material properties, but their low mass and large volume result in a predicted kinetic energy below 15 J [40] (compliant with SDMR). Similarly to other components, to enhance demisability of gyroscopes, some strategies to be considered include:

- **Material Substitution:** Replacing GFRP in GEU cards with more demisable materials. This substitution should be carefully evaluated to not compromise functionality and performance.
- **Component Redesign:** Modifying the design of gyroscope components to promote early fragmentation. This approach requires analysis to balance structural integrity during operation with demisability during re-entry.

4.2.13. Star trackers

Star trackers are high precision optical instruments used for spacecraft attitude determination, incorporating sensitive optical and electronic elements. Due to their compact and robust design, their demisability varies significantly depending on size, structural composition, and material properties. While small star trackers demonstrate a higher probability of demise, larger units are more likely to survive re-entry, posing a potential CR.

To assess the demisability of star trackers, it is necessary to know the structural elements that conform them and how they behave separately:

- Focal Plane Array Housing and Optical Barrel: typically made of Titanium, and thus resistant to demise.
- PCBs: potential CR, depending on heat exposure and fragmentation behaviour.
- Lenses: commonly made of Borosilicate glass, which exhibits viscous deformation under high temperatures rather than shattering.

Given the varied thermal and mechanical responses of these components, experimental tests were conducted under both static and dynamic PWT conditions on large (Base: 80 mm², Barrel: 38 mm Ø) and small (Base: 40 mm², Barrel: 19 mm Ø) star tracker mock-ups [44] evaluating their fragmentation behaviour, material degradation, and exposure to heat flux.

In the dynamic tests, the large mock-up (with a 0.1 Hz rotation rate) presented an even heat distribution, with localised hot spots forming on the barrel due to shock impingement. The base to barrel bolts failed, likely due to helicoil deterioration, leading to structural detachment but no complete demise. For the small mock-up (with a 2 Hz rotation rate), centrifugal effects increased but did not lead to a complete demise. Here, bolts failed under the first heat flux condition similarly to the large mock-up, indicating a potential weak point in fragmentation behaviour.

In the static tests, for the large mock-up the initial heating led to shock wave impingement on the cylindrical barrel, also creating localised hot spots. Furthermore, the base's small length scale had high localised heating, reaching a steady-state temperature with no immediate demise. At higher heat flux conditions, melting initiated at the barrel tip and shock impingement locations, leading to partial demise. Since the Borosilicate glass lenses were inside the barrel, they deformed and slowly escaped, suggesting a viscous flow mechanism rather than fragmentation, reducing their potential CR [44]. Finally, the front section of the barrel demised, whereas the rear section remained intact, even under elevated heat flux (see Figure 47).



Figure 47: Star tracker demise behaviour in DLR's static PWT test and high-flux conditions [44].

For the static tests on the small mock-up the heating behaviour was similar to the large model, with shock induced localised hot spots at the base. Steady state was kept across four heat flux conditions, preventing immediate demise. At 580 kW, melting began at the base and propagated to the barrel, leading to partial structural loss, likely due to shock wave effects [44].

The results highlight that star tracker demisability is highly dependent on size and material selection. Therefore, larger star trackers pose a higher CR, as full demise is not guaranteed under standard re-entry conditions. Titanium components (optical barrel, focal plane housing) are highly resistant to demise, and even if it was observed that the shock-wave heating influences local melting, it still does not guarantee a full demise of these components. It is to be noted that

heliocoil failure mechanisms remain uncertain, presenting a knowledge gap to predict fragmentation behaviour. On the positive side, glass lenses exhibit a viscosity-driven escape mechanism, suggesting lower CR than previously assumed.

To enhance the demisability of star trackers, several modifications were explored:

- **Material Substitution:** Investigating alternative materials for Titanium components could improve demisability; however, such changes must be carefully assessed for their impact on performance and durability.
- **Promoting Early Break up:** Encouraging earlier fragmentation could improve demise, but further research is required to quantify its effectiveness. If beneficial, demisable inserts or heliocoils could be designed to facilitate break up.
- **Size Reduction:** While reducing the size of star trackers could enhance demisability, this option is not feasible for missions requiring high accuracy attitude determination.

4.2.14. Optics

Optical components are integral to various spaceborne payloads, playing a crucial role in observation, imaging, and guidance systems. However, their demisability presents unique challenges due to the use of high melting point materials, complex geometries, and their structural integration within the satellite. Their demise behaviour is influenced by several factors, including material composition, mass distribution, shielding effects, and structural fixings connecting the payload to the platform.

The demisability of optical payloads is not uniform across components. Certain elements, such as ceramic optical benches or cryo-cooler assemblies, are particularly critical due to their high thermal resistance. Other components, such as bipods and A-frames, serve as structural connectors, directly impacting the fragmentation sequence of the payload. Conversely, elements with a higher potential for material substitution or those that do not significantly affect the overall break up process are less critical. Due to the variety of optical components, this section presents the demise characteristics of mirrors, lenses, optical fixings, bipods, thermal focus, baffles, focal plane arrays, and active and adaptive optics.

Mirrors and Lenses

Mirrors within optical payloads vary significantly in terms of material composition, size, and mounting configuration, leading to diverse demise behaviours. Results obtained in DRAMA simulations indicate that while smaller mirrors generally demise, larger ones, especially those constructed from highly resistant materials such as Silicon Carbide, tend to survive re-entry. A critical factor influencing mirror demise is the type of mounting, as rigid connections can lead to entire assemblies reaching ground intact [56] [57]. D4D techniques, such as **material substitution** (e.g. CFRP-coated mirrors) and **containment**, have shown promise in improving demisability while maintaining optical performance but require further investigation.

Similarly, lenses, particularly those made from Fused Silica or other high temperature resistant optical materials, present significant survivability risks. DRAMA analyses suggest that while some smaller lenses fully demise, larger ones often remain intact. **Material substitutions**, such as lightweight optical polymers or demisable composite glasses, could enhance demise potential [57]. Another approach involves the use of **adhesive joints** that promote early fragmentation, reducing the likelihood of intact lens assemblies reaching the surface.

Optical payload fixings

Structural elements securing optical components, e.g. A-frames and brackets, significantly impact the overall fragmentation sequence of optical components. The survivability of Titanium and Invar-based fixings presents a challenge. Studies indicate that **Aluminium or CFRP-based fixings** can enhance fragmentation. Additionally, **weakening at interface points** and the use of **AM** have been identified as potential strategies for early separation and reducing CR [56].

Bipods

Bipods are structural elements that support mirrors and other optical assemblies. Typically manufactured from high melting point materials such as Titanium, bipods have complex geometries with small structural features that influence their heating and fragmentation during re-entry. Their structural integrity and melting characteristics determine both their individual demise and their impact on the break up of the overall payload.

To evaluate the demise behaviour of bipods, a baseline Titanium bipod designed to support an 8 kg mirror was tested in DLR's PWT facilities. The results indicated that the primary mode of demise was melting, with structural cutouts failing first and initiating early fragmentation. Contrary to standard predictive models, which approximate bipods as simple box structures, the experimental results demonstrated a more progressive fragmentation process, influenced by localised heating effects and material thinning in critical regions [39].

In addition to the baseline assessment, alternative bipod designs produced via AM were tested to determine their viability as more demisable configurations. The key findings from these investigations are summarised as follows:

- **Hollow Bipod:** By reducing overall mass, this design showed accelerated demise compared to the baseline. The lower thermal inertia contributed to faster heating and earlier structural failure.
- **Perforated Bipod (Holes Bipod):** Adding holes significantly increased heating rates, resulting in leg demisability occurring concurrently with the failure of the cutouts (see Figure 48) [39]. This design demonstrated the highest improvement in demise performance, altering the fragmentation sequence and enhancing overall break up efficiency.
- **Reduced Holes Bipod:** While this design showed an improvement over the baseline bipod, its demise performance was inferior to that of the fully perforated one. The partial redistribution of heating led to a moderate enhancement in fragmentation behaviour but did not achieve the same level of effectiveness as the holes bipod.



Figure 48: Holes bipod demise behaviour in DLR's PWT test [39].

These findings highlight the potential of **AM** and **topology optimisation** for improved demisability. This way, structural components such as bipods can be tailored to promote earlier break up, contributing to a more controlled and predictable re-entry behaviour.

Thermal focus

Thermal focus units are critical for maintaining optical performance but introduce additional demisability concerns. Their structural components, often made of metallic or ceramic materials, present varied responses to atmospheric re-entry. The re-design of these units using **lower melting point materials** or **modular construction techniques** has been suggested to enhance demise potential. The structural frame of the thermal focus unit can also be optimised to promote early break up, thereby reducing the likelihood of large debris reaching ground [57]. Other ways to promote the early break up of thermal focus include using the **size effect**, for example, designing it in 3 small parts instead of a big one.

Baffle

Baffles serve as stray light suppression mechanisms. Depending on their material composition, often Aluminium, CFRP, or composite structures, their likelihood of demise varies. Results from DRAMA simulations indicate that Aluminium based baffles typically fragment during re-entry, while CFRP ones may survive if shielded [57]. Designing baffles for controlled fragmentation, through **perforations** or **integrated break lines** may enhance demisability.

Focal plane array

The Focal Plane Array (FPA) is a critical component from the demise perspective due to its compact design and use of highly resistant materials, such as Silicon Carbide and Fused Silica. Results from DRAMA simulations show that FPAs often survive re-entry intact. D4D strategies to enhance their demisability include using modular design approaches for a controlled break up such as **changing the area-to-mass ratio** e.g. reducing the size by 20% using more highly aspheric optics, and the **use of alternative materials** that maintain optical performance while enhancing demisability [57]. Additionally, **containment** strategies, have shown potential in mitigating impact risks, although they require further investigation.

Active and adaptive optics

Active and adaptive optics present additional complexities due to their reliance on very precise components including actuators and deformable mirrors. These components often use materials with high resistance to thermal degradation. DRAMA findings suggest that while some smaller actuators may demise, larger assemblies require targeted redesign efforts. Potential D4D techniques include **material substitution** for actuators, the adoption of **lightweight composite support structures**, and **modular assembly** approaches to ensure early separation and demise.

4.3. Technology development activities

To achieve a demisable satellite platform, it is not only essential to identify components that pose a risk of survival during re-entry but also to develop alternative designs that enhance their demise. This section presents an overview of the technologies that have been or are currently being developed under the D4D framework with ESA to address these challenges. The re-entry behaviour from non-demisable elements identified in Section 4.2., has been used as a baseline to lead the design modifications to enhance demise presented in this section.

This section provides an analysis of the demisable designs developed for satellite subsystems including structural panels, mechanical joints, SADM, chemical and electric propulsion tanks, RW, MTQs, optical elements, and D4C solutions. For each technology, the design principles, most relevant modifications for enhancing demise, and demisability

performance are discussed, highlighting the extent to which they mitigate re-entry risks. The demisability of these technologies has been evaluated through a combination of numerical simulations and on ground testing, to verify that proposed solutions effectively reduce the risk of surviving debris. Furthermore, their TRL is examined, offering insight about its maturity and feasibility for integration into future satellites.

4.3.1. Structural Panels

To promote early exposure of the internal elements of a satellite during re-entry, demisable structural panels have been developed through a collaboration between EPFL, Bcomp, and RUAG, and through a PhD research initiative. The technology achieved TRL 5, with a full-scale demonstrator required for TRL 6 validation in accordance with ECSS-E-HB-IIA standards.

Aiming to promote both early structural break up and complete demise during re-entry, the panels used FFRP due to its higher ablation rates compared to conventional CFRP. Other options to enhance demisability of side panels (not primary structures due to a weight penalty) were explored, including the ones identified in Section 4.2.1., specifically:

- **Hybrid Reinforcement:** Incorporation of CF and flax fibres in a ply-by-ply configuration to balance structural strength with enhanced demise behaviour.
- **Thermally Conductive Fillers:** Integration of Aluminium-Magnesium (AlMg) micropowder in the matrix to improve thermal conductivity and reduce convective blockage.
- **Pre-cut CF Prepregs:** Implementation of cut-CFRP layers to promote controlled ply separation and fragmentation upon re-entry.
- **Structural Topology Optimisation:** Removal of the top sheet and honeycomb core in non-load-bearing areas, reinforcing the bottom sheet with powerRibs, allowing for early ingress of plasma heat flux [9].

The structural panels were subjected to various testing methods to assess their demisability and structural performance under re-entry conditions. The most relevant results are:

- The CF-FFpbp hybrid presented earlier fracture at lower temperatures than CFRP, stiffness to mass ratios comparable to Aluminium and CFRP, and superior vibration damping, particularly in higher frequency modes.
- Flax hybridisation increased ablation rates by 1.5 to 3 times [9].
- Pre-cut CF layers facilitated early ply separation, whereas continuous CF experienced late stage failure.
- The addition of AlMg micropowder advanced the onset of demise by ~ 15 °C, accelerating fragmentation [9].

The results indicate that demisable structural panels can be viable alternatives to traditional ones. The CF-FFpbp hybrid panel, particularly with AlMg integration, demonstrated enhanced ablation rates, improved thermal conductivity, and predictable ply separation, making it a promising candidate for demisable satellite structures. Further full-scale testing and integration into satellite platforms will be necessary to advance these technologies to TRL 6 and beyond.

4.3.2. Joints

As part of ongoing efforts to enhance the controlled demise of satellites during atmospheric re-entry, companies such as OHB, Thales Alenia Space (TAS), ADS, HTG, EPFL, RUAG, BComp and INVENT have been working to develop demisable or controlled break up joint designs.

Demisable Joints Developed by OHB

Bolted and bonded Cleat

One of the designs by OHB is a **bonded cleat** that replaces the bolted cleat/panel joint by directly bonding the cleat to the panel. This way, the joint is only connected via **adhesive** connection and not by form fit. The cleat is made of AA7075 or CFRP, and the adhesive is Scotchweld 9323. A thin layer of adhesive is applied on the cleat side, connecting the lateral panels and shear web. This design does not require weakening of the potting material and can be adapted to edge inserts, through spool inserts and surface inserts.

The expected failure mode during re-entry is a detachment of the cleat due to weakening of the adhesive as soon as its transition temperature is reached, and/or when there is delamination of the panel face skin. The detachment temperature can potentially be adjusted by choosing the right adhesive to fit the desired point of temperature driven failure. As it can be seen in Figure 49, one side of the cleat is bonded directly onto the panel, while the other adjacent panel is bolted to the cleat. It is to be noted that the bonded side of all cleats shall be on the same side of the satellite to enable the detachment of a panel during re-entry. This joint design reached TRL 8, and the release of the cleat was estimated between 103 - 98 km of altitude [58].

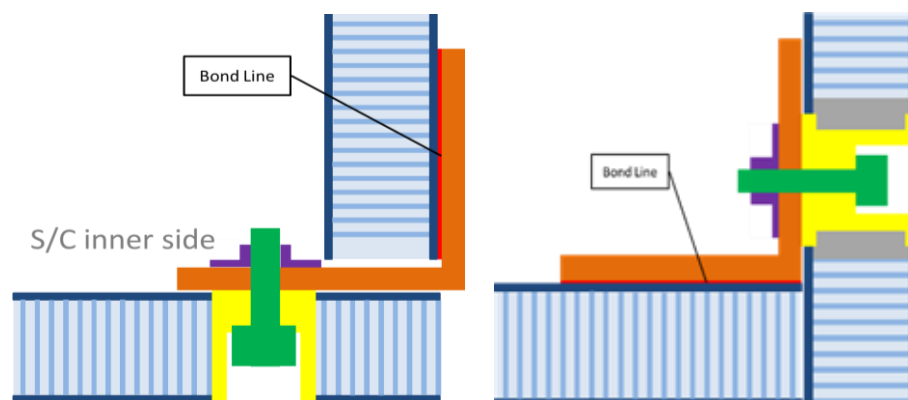


Figure 49: OHB Bolted and bonded cleat to panel joint with the temperature sensitive side at the outer panel (left) and inner panel (right) [58].

Adhesively Bonded Demisable Joint

OHB developed another adhesively bonded joint that replaces traditional rivets or welded sections. This **adhesive** incorporated **self-igniting particles to the potting material**, allowing to adjust the ignition temperature. The adhesive degrades rapidly when exposed to temperatures above 400 °C, allowing the joint to fail. At this point, connected panels and components separate, promoting early break up and increasing exposure to heat flux. The design reached TRL 4 and showed promising results, but safety has still to be proven. This design provides a predictable and gradual failure mechanism, promoting a stepwise break up sequence, but at the same time it is sensitive to environmental conditions, which may affect adhesive degradation predictability.

Composite Insert

In this concept the conventional insert is replaced by a **composite** one of CFRP, to lower its failure temperature and thus also that of the bolted joint. When comparing the melting temperatures of common Aluminium alloys (502 - 638 °C) to the failure temperature of the thermoplastic used as the matrix for this CFRP insert (~ 340 °C), an earlier failure of the joint during re-entry is expected [58]. The expected failure mode during re-entry is a deterioration of the insert, which should allow the bolt to be pulled through the thread of the insert. This would then release the joint.

This design reached TRL 5, however, no gains in demise were observed, and changes are necessary in terms of construction and materials. For both the CFRP/CFRP material combination tested in a SRC and the Aluminium/Aluminium one tested in the PWT no failure of the bond line was observed. Instead, the sandwich panel lost integrity. The CFRP cleat and Aluminium face skin combination did not fail as well, which can be explained by the thermal shielding effect of the CFRP cleat.

For the Aluminium material combination with constant trajectory and heat fluxes, the panel and cleat joint broke up slightly earlier than the conventional insert connection. Here, the failure occurred within the bond line. In the end, no improvement in the overall demise behaviour was observed when using the composite insert technology [58], which stayed solid despite a decomposition of the matrix.

SMA bolts

OHB developed **SMA bolts** to offer a controlled release mechanism for demisable joints, using SMA phase transformation to induce failure at a predefined temperature. The SMA bolt has a cylindrical SMA actuator that elongates and fractures the bolt upon reaching its trigger temperature (180 - 200 °C) [58]. The bolts can be mounted internally (shielded, delayed activation) or externally (exposed, earlier break up).

A PWT test campaign assessed SMA bolt demisability at representative re-entry conditions. Two SMA bolts in a cleat joint were tested, externally mounted for maximum heat flux exposure (see Figure 50). Tests confirmed early and predictable SMA activation, leading to structural disassembly before the material failure. Based on the results, the break up altitude would be between 80 - 90 km, fulfilling the aimed early fragmentation [58]. While the technology is mature (TRL 7), uncertainties remain to ensure fracture occurs before SMA degradation. Further optimisation is required to refine activation reliability across different re-entry scenarios.

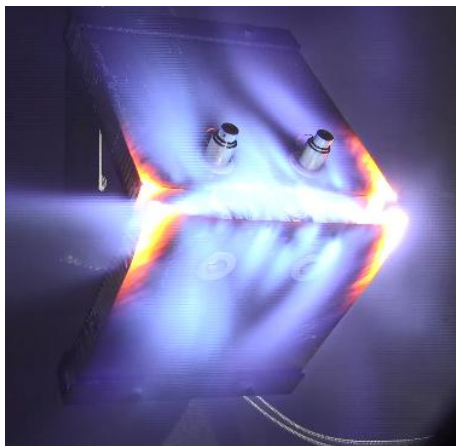


Figure 50: OHB two SMA bolts in a cleat joint externally mounted in PWT testing [58].

Demisable Joints Developed by Thales Alenia Space

Thermally Triggered Fastener Joint

To enhance early satellite break up, TAS designed a fastener release system using SMA. The joint uses Aluminium inserts and **SMA thermal triggers**. The SMA based fasteners deform and release when exposed to high re-entry temperatures (~ 600 - 700 °C). The fastener failure leads to the break up of the external structure of the satellite, exposing inner components earlier to the heat flux. The SMA material initially selected was the Zinc based alloy EZACTM. However, BABBIT material was finally selected as it showed better performance [58].

A schematic view of the joint and its integration in an external panel, particularly a lateral-to-lateral panel connection, is presented in Figure 51. During the operational life, the demisable washer (blue item) acts as usual washer in the joint assembly also composed by two cleats and a screw (orange item). During re-entry, due to the aerothermodynamic loads, the washer would heat very fast, reaching the melting point earlier than the other items of the joint assembly. Near the washer melting temperature, it can either demise by ablation or break due to the structural loads as near melting point the washer structural performances become very low. Once the washer has demised, the cleats can have a mutual shift due to the hole in one of them (light-green item) eventually leading to the joint dismantlement [58].

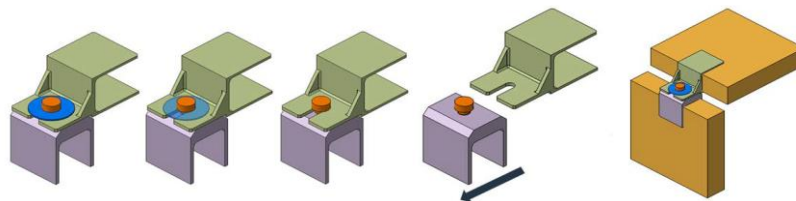


Figure 51: TAS Thermally Triggered Fastener Joint [58].

According to simulations and PWT campaigns, these joints promote break up at 75 - 80 km of altitude. In all tests, demise of the washer was achieved, with its melting temperature preliminary being 400 °C for EZACTM and 250 °C for BABBIT [58]. The melting of the washer did not always result in a separation of the joint itself during the test since the aerodynamic forces maintained the panels in position. It is worth mentioning that the washer always demised before relevant damage to both cleats and panels was seen, especially in the case of BABBIT washers. The joint reached TRL 6, and its effectiveness from the demise perspective is considered high, allowing for quick panel separation and enhancing overall demise.

Demisable Joints Developed by Airbus Defence and Space

ADS has researched several concepts for joints that promote early break up of satellites during re-entry while maintaining structural integrity during launch and operation. The designs focus on two principles: (i) the use of predetermined breaking points within the main axial load path and (ii) the use of shape connections with dividable clamps for disconnection. All the concepts reached low TRL, specifically 2/3 [59].

(i.1) ADS Bolt with Internal Actuator

This concept uses an **internal SMA actuator** instead of pyrotechnic booster loads. The SMA is compressed and secured within a Titanium housing with a predetermined breaking point. As the Titanium housing has low thermal conductivity, it reduces the heat flux into the actuator during re-entry. Upon reaching the austenite start temperature the SMA elongates, fracturing the housing and disconnecting the structural connection. It is to be noted that the low wall thickness used at the predetermined breaking point implies manufacturing challenges [59].

Regarding demise, the break up of the satellite structure occurs due to the controlled failure at the predetermined breaking point. There were challenges to ensure a uniform material failure due to strict tolerances, and the design complexity limited feasibility for further development.

(i.2) ADS Bolt with External Actuator and Dual Thread Interfaces

To address the manufacturing constraints of the internal actuator concept this design locates the **SMA actuator externally**, housing a cylindrical bolt inside the mechanism. This improves heat absorption during re-entry. Upon actuation, the SMA elongates, applying force on a predetermined breaking point within the bolt, leading to structural separation. The wall thickness for this concept is greater, enhancing manufacturability and reducing costs [59]. However, the increased clamping length creates potential bending moments, requiring structural validation.

Considering demise, the earlier exposure of this concept to the heat flux during re-entry ensures timely structural failure. This predetermined breaking point ensures predictable fragmentation but requires verification of notch integrity under launch and operational loads.

(i.3) ADS Bolt with External Actuator and Insert Interface

This concept further optimises the **SMA external actuator** placement by integrating a **modified sandwich panel insert**. The SMA is directly exposed to the external environment, enhancing heat absorption. To prevent unintentional preloading, the bolt and insert incorporate a shape locking mechanism. The bolt square cut geometry transmits torque without stressing the breaking point, and integrated lock wires prevent space debris generation in case of accidental actuation [59].

Regarding demise, the direct exposure of the actuator increases heat absorption, promoting faster break up. However, the complex assembly procedures require precise tolerances.

(ii.1) ADS Pin Puller Concept

This mechanism uses a **bending SMA actuator** that restores its original shape upon heating, **pulling a pin** from a recess to trigger separation. The actuator's large flat surface enhances heat absorption, supporting an efficient break up mechanism. This design avoids using predetermined breaking points, ensuring consistent load transmission. However, it has the potential risk of mechanical jamming due to fretting, requiring surface treatments [59].

On the demisability considerations, the break up depends on the actuator force overcoming frictional resistance, therefore, extensive testing is required to validate the force output under varying conditions. In the end, the design complexity and force limitations led to the discontinuation of this concept.

(ii.2) ADS Clamped Interface Concept

Inspired by upper-stage separation mechanisms, this design has **two clamped interfaces** held together by a preloaded bolt. The **SMA actuator**, upon heating, ruptures the bolt when reaching the breaking point, releasing the clamps and achieving separation. Here, the load transmission path is separated from the actuator mechanism, so the actuator placement has to be optimised for heat absorption during re-entry [59]. Moreover, the bracket integration eliminates additional mounting hardware requirements.

Considering demise, this separation mechanism would ensure complete structural break up according to the research performed, but its high manufacturing complexity and mass constraints were considered a limiting factor to adopt it as baseline.

(ii.3) ADS Clamped Interface with Radial Bracing

This variant refines the **clamped interface** concept by incorporating **radially braced clamps**. A preloaded notched bolt secures the mechanism, which, upon **SMA** actuation, releases the clamps and enables separation. This concept uses a clamp angle that has been minimised to optimise load transmission, as well as surface treatments to mitigate friction and prevent adhesion at vacuum conditions. Similarly to other concepts, lock wires secure the released components to prevent debris generation [59].

Regarding demise, using this optimised break up sequence would promote structural break up. The component mass and impact energy are below the critical thresholds, confirming demisability of this design. On the other hand, the high manufacturing costs and complex tolerances require additional development efforts.

Demisable Joints Developed by HTG

HTG Thermite based Joint

The integration of **thermite-based pyrotechnic charges** into demisable joints has been investigated to enhance structural break up during re-entry. Thermites, known for their exothermic reactions, provide a controlled and localised heat source. Their inclusion in spacecraft structural elements, particularly in bolted or mechanically interconnected joints, has the potential to improve fragmentation sequencing and increase the overall demise efficiency.

HTG's demisable joints incorporate thermite directly within their structure, targeting heat application at critical connection points. Two integration strategies have been considered:

- **Embedded Thermite Chambers:** Thermite is enclosed within the joint structure in cavities designed for that purpose, ensuring a controlled reaction environment.
- **Structural Infusion:** Thermite materials are directly incorporated in the joint composition, enabling self-contained reactivity upon reaching thermal thresholds.

Given the high energy density and exothermic output of thermites, the selected compositions must align with the joint's mechanical integrity and ignition requirements. Al-Fe₂O₃ has been identified as the optimal composition due to its high heat release, low gas production, and material availability [60].

Tests in L2K PWT and simulations were conducted to assess the performance of thermite enhanced joints in a re-entry environment. In the PWT, localised melting was observed in joints incorporating thermite, and thermocouple readings confirmed that ignition timing has a high impact on material break up [60]. It is to be noted that thermite formulations were tested for repeatable ignition in controlled conditions and the separation of activated primer and standard thermite significantly improved ignition reliability. On the simulations side, the results validated that heat transfer efficiency and ignition altitude are key parameters influencing break up altitude.

The TRL reached for thermite joints was low (TRL 2/3), but findings that will define future development were obtained. The ignition time is critical, with later-stage ignition having higher effectiveness in melting joint materials and preventing premature burnout at high altitudes. Moreover, activated thermite primers enabled ignition within a controlled temperature range of 450 - 800 °C. Challenges were observed, especially for loose thermite powders, which require physical separation barriers to ensure ignition reliability, and pelletised thermite formulations, despite showing potential, require mechanical reinforcement to withstand launch loads.

Demisable Joints Developed by EPFL, RUAG and Bcomp

EPFL, RUAG and Bcomp short CF/PEEK bolts

The development of demisable bolted fasteners by BComp and RUAG, with the collaboration of a PhD student from EPFL, focuses on composite alternatives to traditional metal fasteners. Conventional Stainless Steel, Ti6Al4V, and AA7075 bolts have limited demise potential. To address this, **CF/PEEK composite fasteners**, reinforced with either continuous or short CF (see Figure 52), have been developed. Leveraging lower melting temperatures (~350 °C) and brittle fracture, these bolts promote earlier separation.

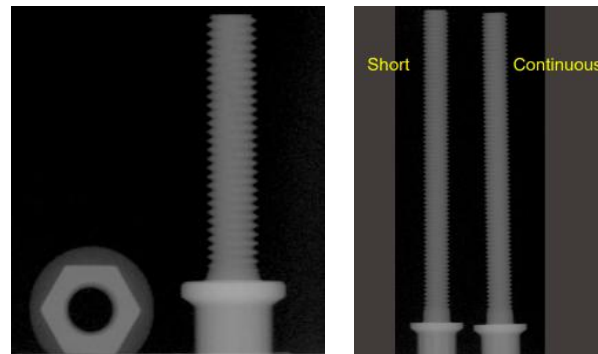


Figure 52: Absorption contrast of short and continuous CF/PEEK bolts [9].

The composite fasteners integrate Hexcel IM7 CF within a PEEK matrix to ensure high mechanical performance, damping and self-locking properties while maintaining space qualification standards. Two reinforcement types were studied:

- Continuous CF/PEEK: high strength but behaves similarly to metallic bolts at re-entry.
- Short CF/PEEK: Custom-developed to promote early break up.

For manufacturing, a **Composite Flow Moulding** was used. This is an injection moulding technique producing non-homogeneous fibre distribution preferring longitudinal orientation. Testing showed that **short CF bolts** retained over 95 % of the strength of continuous CF bolts while achieving up to 300 % improvement in shear strength compared to Stainless Steel [9]. Mechanical and thermal tests were conducted to assess the performance of these bolts:

- Tensile & Shear Tests: Short CF bolts performed comparably to continuous CF, with high mechanical integrity.
- Torque Clamp & Fatigue Tests: Confirmed the fasteners meet structural requirements.
- SRC Tests: Short CF bolts exhibited earlier separation at lower temperatures (~500 °C reduction in loosening onset [9]) compared to Stainless Steel.
- Failure Mode Analysis: Short CF bolts fracture cleanly.

Replacing fasteners with short the CF/PEEK ones, break up initiates at lower temperatures. The reduced mechanical resistance post-demise onset enables earlier and faster disassembly of the satellite structure, increasing its overall demise. These bolts have reached TRL 5/6 [9].

Demisable Joints Developed by INVENT

INVENT is developing demisable primary structure joints for future LEO satellite communication platforms. This activity aims to understand the demise behaviour of different joint designs and their key influencing factors. The project, initiated in September 2024 is now defining technical requirements and selecting joint concepts for PWT testing. Afterwards, it will refine designs based on test results. No further information is yet available.

4.3.3. SADM

As explained in Section 4.2.3. traditional SADM designs contain elements with high likelihood of survival during re-entry, requiring the development of demisable alternatives. This subsection presents the efforts undertaken to enhance the demisability of SADM designs through material modifications, structural adaptations, and early break up strategies. Two parallel development activities have been conducted by KDA and DLR to enhance the demise of these mechanisms.

KDA KARMA - 4/5 TG

The demisable SADM concept developed by KDA aims to enhance break up during re-entry using Aluminium screws, with the goal of reaching TRL 6 within the year. The project involved high-fidelity assessments using simulations in SCARAB, and PWT campaigns.

Simulations predict that the KDA KARMA-4 TG SADM (see Figure 53) fully demises from an average release altitude of 78 km [52]. The use of **Aluminium and demisable joints for housing fasteners** significantly improved overall demisability, particularly when the release trigger temperature was sufficiently low. Several PWT tests were conducted to validate the numerical predictions, focusing on both the full SADM assembly and individual critical components where:

- The twist capsule was confirmed to fully demise.
- The gearbox, motor, and final shaft successfully separated during demise.
- The crown wheel demised while attached to the inner mandrel.
- The main bearing was confirmed to demise, although with minor fragment separation.



Figure 53: KARMA-4 TG SADM from KDA [52].

In the full SADM test, the mechanism fully demised after 3 min of exposure, without requiring repositioning of the sample. Further numerical studies confirmed that:

- Using Aluminium screws for SADM housings significantly improved demisability.
- SCARAB database simulations indicated demise from a release altitude of 76 km (5% significance level).
- ESTIMATE database results slightly shifted this value to 80 km (5% significance level).

To further improve demisability, demisable screws were analysed using thermal triggers at 500 K and 700 K. Results showed that with a 500 K trigger, the most probable release altitude for demise decreased from 74 km to 70 km, with minor fragments surviving up to 72 km. With a 700 K trigger, it decreased to 72 km, with fragments surviving up to 74 km [52]. These results reinforce the use of demisable screws for components with housings to increase demisability.

Future activities under development include assessing the demisability of a larger KARMA-5 TG SADM, performing higher-fidelity test dummies and additional D4D iterations in simulations.

DLR Demisable SADM

In parallel, DLR is developing a demisable SADM with a primary focus on modifying the **BBU**. The main design modification is the integration of an **activated thermite blend**, to promote a controlled break up during re-entry. Testing has been conducted on thick-walled and thin-walled BBU geometries, partially filled with thermite (solution also studied for demisable RWs). A comparison between experimental and numerical data revealed:

- For the thick-walled BBU (50% filling), the initial temperature rise was well predicted by SCARAB, although ignition was simulated 16 s later than observed in the PWT. For the thin-walled BBU (26% filling, thermite and activated pellets), the ignition prediction only had a 1 s delay [61].
- Multiple ignition events were detected in tests with one of the peaks at 300 s, whereas SCARAB simulations released all the additional enthalpy at the first ignition event [61]. Despite this, the overall heat release profile was consistent between simulation and test.
- The progression of the combustion front in the sample was not immediate.

In both cases, numerical results captured pre-ignition heating trends accurately, but post-ignition temperature deviations suggest limitations in modelling combustion front propagation and pyrotechnic energy release. Since this activity started recently, more results and design modifications are underway, with the objective of reaching TRL 6 in the following years.

4.3.4. Propellant tanks

To enhance the demisability of satellite propellant tanks, research efforts have focused on modifying tank materials and structural configurations. This section presents demisable chemical propellant tanks, divided into large and small tanks, followed by demisable electric propellant tanks, also categorised into large and small configurations. Each subsection details the materials, structural changes, and demise outcome.

Large Chemical propellant tanks

ADS and Orbital ATK UK large Aluminium tank

The development of this large chemical propellant tank was led by Airbus Defense and Space (ADS) and Orbital ATK UK, **replacing Titanium by Aluminium**. The baseline material is AA2219 alloy for the Aluminium liner, overwrapped with Carbon. Alternative Al-Cu-Li, Al-Cu, and Al-Mg-Sc alloys were also investigated due to their lower melting temperatures and enhanced demisability. The design and features of this tank are [62]:

- Volume: 100 - 200 l.
- Diameter: < 600 mm.
- Shape: Spherical domes with variable-height intermediate rings.
- Operating Pressure: Maximum Expected Operating Pressure (MEOP) ~24 bar at launch, decreasing to 5.5 bar in blowdown mode.
- Expulsion Device: Diaphragm and Propellant Management Device.
- Propellants: Compatible with H₂O₂, Hydrazine (H₂N₄), NTO and derivatives.
- Break up Mechanism: **Bolted tank halves** enabling early structural failure (see Figure 54).
- Re-entry Performance:
 - Complete demise for release altitude ≥ 78 km.
 - Partial demise for release altitude of 65 km (30 - 45 % impacting mass remains).

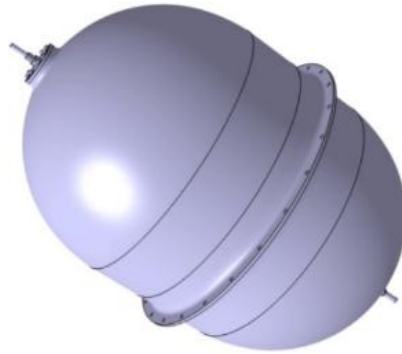


Figure 54: ADS and Orbital ATK UK large Aluminium tank with its bolted halves [62].

Simulations using DRAMA were conducted to assess the demisability under different conditions:

- Melting Temperature: This is the most significant factor affecting demise. A worst-case melting temperature increases the impacting mass by 9 % [62].
- Tank Size and Alloy Choice: No significant influence on demisability was observed for tank sizes between 100 - 200 l or between different Aluminium alloys.
- Titanium Tanks: Do not demise at all, reinforcing the need for Aluminium alternatives.

Moreover, a bimetallic adapter is recommended to facilitate integration with existing spacecraft systems. The mass penalty (4 kg heavier than Titanium) is deemed acceptable given the necessity for controlled re-entry.

MTA large Aluminium tank

The second demisable chemical propellant tank presented in this research was developed by MTA and has reached TRL 5/6. This tank is designed to achieve early break up during re-entry while keeping structural integrity for operations. The main **material** of the structure is **AA2219-T851 (Al-Cu alloy)**, and the tank incorporates an Ethylene Propylene Diene Monomer (EPDM) diaphragm [63], which is mounted to the lower half of the tank, as it can be seen in Figure 55.

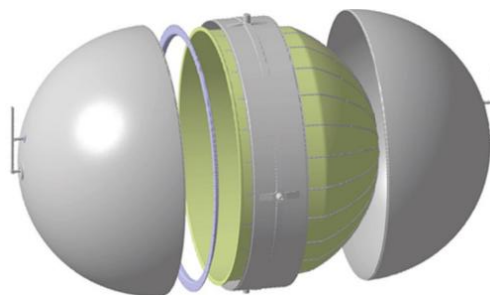


Figure 55: MTA large Aluminium tank with its EPDM diaphragm [63].

The volume of the tank is within the range of 177 - 200 l, with a spherical equivalent diameter of 600 mm and a total mass of ~ 15 kg. Structural load transfer is achieved through either equatorial mounting (via trunnions or an integrated Aluminium skirt) or polar mounting (using off-the-shelf bearings), the latter incurring an additional mass penalty of 1 kg. The tank shell is composed of **two hemispherical domes** and a **cylindrical section**, all fabricated from AA2219-T851, **welded** together using TIG welding to ensure structural integrity [63]. The hemispherical design, combined with a **reduced wall thickness**, promotes early break up upon atmospheric re-entry, thereby enhancing its demisability. The pole fittings, made of Ti6Al4V, serve as connection points while minimising the overall use of Titanium, which is less prone to demise.

The tank demise performance was evaluated in simulations for the baseline AA2219 tank of ~ 15 kg mass. It was observed that if it is released from an altitude of 78 km, it fully demises at 68.8 km altitude, confirming its enhanced break up characteristics. However, in less favourable conditions, 65 km release altitude, a ~ 5.8 kg fragment was predicted to survive. Overall, the minimum required release altitude for complete demise was determined to be ~ 74.3 km [63]. Additional findings include:

- The EPDM diaphragm showed high demisability due to its low char yield, though it demonstrated a higher heat of demise compared to metals.
- Larger tanks (approximately 200 l) demised at ~ 70 km when using a spherical geometry.
- Reducing the volume to 50 l would allow for a two-part integral design, minimising welds and reducing costs [63].

In the end, the MTA large chemical demisable propellant tank presents a viable solution for future satellite applications, with optimised demise characteristics and structural robustness. While further work is required to fully characterise its demisability, particularly through PWT tests, the TRL 5 rating confirms its advanced development.

ADS large CFRP tank

ADS, apart from the large Aluminium tank, also started the design and testing of a large chemical demisable COPV propellant tank. This design substitutes Titanium with a **thermoplastic liner and a CF overwrap** aiming to enhance demisability while maintaining structural integrity.

This design concept has a total volume of 200 l and is compatible with both standard and green propellants, including H₂O₂, LMP-103S and HAN. The tank shell consists of a Polyamide 6 thermoplastic liner, ensuring leak-tightness, and an overwrap of a Polyamide 12 matrix reinforced with either CF, Kevlar, or other organic fibres. The structural loads, including internal pressure and dynamic forces, are sustained by the composite overwrap. Based on past experience with similar tank volumes and propellant mass, equatorial mounting was preferred for structural integration, and for ensuring optimal load distribution and stability within the satellite. Moreover, the **liner thickness** in the cylindrical section has been **minimised** to 3 mm [62].

A preliminary mass evaluation was conducted for both CF and Kevlar tanks under two safety margin conditions (MEOP ×1.5 and MEOP ×2). Despite Kevlar's lower strength, the mass increase remained moderate, with Kevlar based tanks proving lighter than CF ones [62].

The demisability of the tank was studied through simulations, assessing survivability at a release altitude of 78 km. For the CF case, the liner melted completely, but 79 % of the overwrap mass remained. For the Kevlar case, the liner also melted, but 73 % of the overwrap survived.

Additional simulations assessed the impact of varying break up altitudes (reference altitude of 75 km, upper bound of 93.6 km, lower bound of 62.4 km and worst-case scenario of 65 km) [62]. For all cases, the thermoplastic liner fully melted. However, composite overwraps exhibited partial or complete survivability. For the CF overwrap, the thermoplastic matrix burned, but CF remained intact at all break up altitudes while for the Kevlar case, the matrix presented partial charring in the reference break up scenario, with Kevlar fibres largely intact.

As these results were less promising than the large Aluminium tank designed by Airbus, the efforts were focused on the metallic design instead of the composite one. Therefore, the large CFRP tank of ADS only reached TRL 3.

Small Chemical propellant tanks

Institute of Aviation small Aluminium tank

Part of the ongoing efforts to enhance tanks' demisability focuses on developing small propellant tanks. Specifically, the Institute of Aviation is developing a small chemical propellant tank that implements **material substitution** and **alternative manufacturing** techniques. Traditionally used Titanium alloys have been replaced with an Aluminium alloy, specifically the **AA6061**. Using this material, the tank was shaped using a **two-sheet welding** concept and an **incremental sheet forming** technique, keeping both structural integrity and manufacturability. Moreover, it is designed to accommodate monopropellants, primarily hydrazine, with a long term goal of transitioning to green propellants [64].

The two-sheet welding configuration consists of incrementally forming the AA6061 sheets into the desired shape and subsequently joining them using Friction Stir Welding (FSW) (see Figure 56). This approach provides several advantages over conventional Titanium forging, including reduced manufacturing complexity, lower recurrent costs and improved demisability.

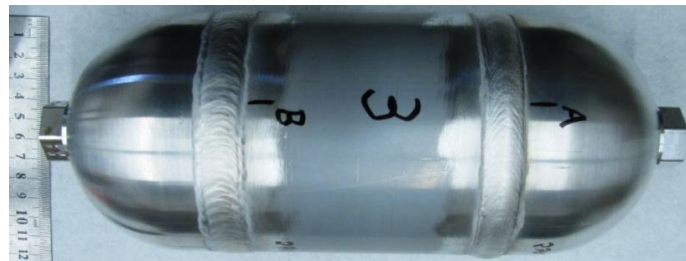


Figure 56: Institute of Aviation small Aluminium tank after FSW [64].

The tank volume is 40 - 52 l, with 52 l as a reference for demise simulations. The wall thickness and demise testing parameters remain to be determined according to the literature. This tank aims to achieve TRL 6, although the available literature researched by the author only justifies that it has reached TRL 3/4, indicating successful proof-of-concept validation through experimental demonstration in a controlled environment [64]. Further development stages will focus on structural integrity testing, compatibility assessments with monopropellants, and demisability verification through experimental and numerical modelling.

PEAK Technology GmbH small COPV tank

Another demisable small chemical propellant tank was developed by PEAK technology. This concept is a COPV tank with modifications to enhance its demisability. The baseline PEAK design consists of an **Aluminium liner** (EN AW 6082-A T651) **overwrapped with CFRP** (T800SC-24k-10E/RCX0245/28 \pm 2%). It has a volume of 30 l, a MEOP of 200 bar, an external diameter of 291 mm, and a structural mass below 6 kg [65]. The Aluminium liner consists of two identical halves with ovaloid domes, differing only in the boss port opening on one side (see Figure 57). These are machined from raw stock and welded together using **electron beam welding** under vacuum conditions. The CFRP overwrap consists of 10 layers, each with specific thicknesses and lay-ups, leading to a total thickness of 3.7 mm [65]. The winding process is done with a high-precision towpreg/tape winding system with a rotational axis and a 9-degree-of-freedom robotic arm.

To ensure representativeness in the PWT test, the tests were performed on a scaled down version of cylindrical geometry with a 50 mm diameter, 300 mm length, 1.5 mm liner thickness and 1.2 l volume. This tank version retains the fundamental COPV architecture, using a similar Aluminium liner and CFRP reinforcement.



Figure 57: PEAK small COPV tank illustration [65].

Simulations conducted by PEAK on the 1.2 l tank suggest an expected sequence of fragmentation events under representative re-entry conditions. The main takeaway was that all resin disappeared above 70 km release altitude, but there was CF left, classifying the tank design as not demisable. This was reinforced by simulations performed on the 30 l baseline tank, where almost all resin disappeared above 90 km of release altitude (20 km higher than for the 1.2 l baseline), but only about 5 % of the CF did so [65]. The reason for this behaviour was the resin, which did not degrade. Conversely it formed a protective layer that kept the strips from ablating acting as a heat shield.

As this design proved to be not compliant with demisability requirements, it reached TRL 4/5 and the research focus on new design modifications to improve demisability of the tank:

- **Burst collar:** Aiming to oxidise the fibres during re-entry. Tests showed removal of several layers with propellant grain demise, but the fibre strips option was more promising.
- **Strip tape Fibre Lay-Up:** Instead of a continuous filament winding, the CFRP overwrap would use 150 - 300 mm strip fibres, promoting fragmentation during atmospheric re-entry. This was observed to enhance demise.
- **Resin Modification:** The baseline resin was replaced with a new one that reduced char formation, ensuring that fibres detach rather than forming a solid residue. This has been identified as a critical factor influencing demise behaviour.

The proposed modifications necessitate material-level testing to validate the CFRP's thermal and mechanical properties pre- and post-exposure to high temperatures. Once material integrity is verified, system-level tests will be performed for acceptance and qualification.

Electric

Airbus DS small Xenon COPV tank

Demisable propellant tanks for electric propulsion are also necessary to achieve fully demisable platforms, and thus, there have been activities to develop these technologies. One such tank concept has been investigated by ADS incorporating materials and structural changes to enhance demisability. The design strategy involved **replacing Titanium by Aluminium**, in conjunction with a **COPV** structure to improve the demise of the tank while maintaining structural integrity and performance requirements.

Specifically, the tank has a metallic liner of Aluminium alloy 2219. The overwrap consisted of CFRP or Kevlar fibres, with two matrix options explored: thermoset epoxy and thermoplastic resin. While CF provide high strength and stiffness, their demisability remains under investigation. In contrast, Kevlar fibres offer better thermal degradation properties [64].

The tank was designed for a Xenon storage application, with a volume between 12 and 50 l. The tank was initially developed with the goal of achieving TRL 6; however, based on available data, the design currently remains at TRL 3 [64]. The studied configuration targeted an operational pressure suitable for Xenon storage in electric propulsion systems, with the liner providing the necessary gas containment and the composite overwrap ensuring structural reinforcement.

The demisability of the ADS tank was assessed through simulations, which predicted the complete demise of the Aluminium liner at a release altitude of 78 km. The composite overwrap exhibited partial ablation, with 25% of its mass lost and the resin component fully charring [64]. While these results indicate improvements in tank demise behaviour compared to conventional Titanium designs, the complete demisability of CF remains an open question that requires further investigation. Future work of ADS may focus on alternative fibre materials or hybrid solutions to ensure full ablation of all tank components.

Haydale Composite Solutions large Xenon COPV tank

Haydale Composite Solutions has been developing a propellant tank that uses a hybrid material composition to optimise structural performance while enhancing demisability. The tank consists of a **non-metallic liner** made of Nylon PA6, a **permeability barrier of Copper**, and an **outer composite shell** made of Kevlar 49-7100 impregnated with UF3376-100 epoxy resin (see Figure 58). The **boss** is the connection point for propellant flow and is **made of AA7075-T6** [64].

The non-metallic liner improves its ability to ablate during re-entry and eliminates the reliance on traditional metallic containment structures. The presence of a thin Copper layer ensures gas containment during operational use while also enhancing melting and vaporisation. The Kevlar-Epoxy shell has relatively low thermal stability, leading to pyrolysis and fragmentation under high heat flux conditions. And the Aluminium boss is expected to melt at approximately 660 °C, facilitating structural break up and further enhancing demisability.

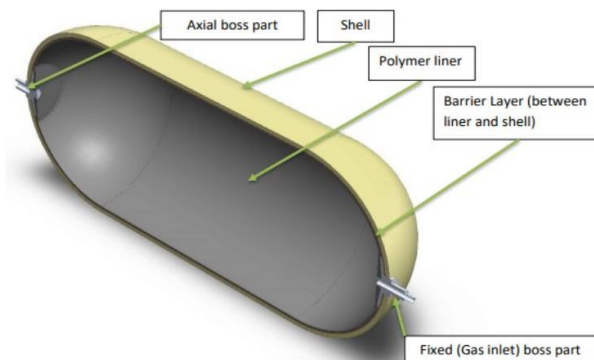


Figure 58: Haydale Composite solutions large hybrid composite tank illustration [64].

The propellant tank is intended for Xenon storage applications and is scalable to a volume range of 30 to 180 l. However, the primary design and analysis efforts have been conducted for a 100 l Xenon baseline tank, with a MEOP of 150 bar. According to simulations, it is compliant with demise requirements for a release altitude of 78 km [64]. This tank has reached TRL 6, indicating successful validation in a relevant environment.

While non-metallic composite tanks offer potential advantages in terms of reduced mass, lower manufacturing costs, and shorter production lead times, several challenges remain. One of the main concerns is ensuring that permeability requirements are met without the use of a fully metallic liner. The integration of the Copper barrier aims to address this issue, but further testing is necessary to validate its long-term performance in operational conditions.

PEAK Technology GmbH small Krypton COPV tank

Another small demisable electric tank is under development at the moment by PEAK Technology. As this is an activity that started recently, the tests results information is not yet available. The design concept studied consists of a 1 l tank selected as the baseline for full scale testing in PWT, to be scalable to a 30 l tank. Additionally, the relatively low production cost of a small scale tank enables testing across a broader range of conditions.

The tank structure consists of **two endcaps** with a thickness of 1.3 mm in the cylindrical section and an outer diameter of 90 mm, joined via **Electron Beam Welding** [66]. This design takes heritage from the chemical tank developed by PEAK Technology presented above, but adapted for Krypton compatibility. The tank is designed to be polar mounted on the bosses (see Figure 59). Prior to the filament winding process, the liner undergoes surface treatment to enhance adhesion between the liner and the composite overwrap. The overwrap is subsequently applied and cured in an autoclave.



Figure 59: PEAK small COPV Krypton tank illustration [66].

The **liner** is made of EN AW 6082 T6 **Aluminium**. Moreover, the **overwrap** is made of **CFRP**, with a final layup thickness of 1.88 mm in the cylindrical section. The overwrap burst pressure load is of 465 bar, which is 1.5 times the MEOP (310 bar) to be compliant with Krypton tank pressurisation requirements [66]. Additionally, to enhance demise, the design incorporates a **strip tape** concept, that demonstrated promising results in PWT testing with CFRP cylinders

So as to validate the demisability of the Krypton tank design, PWT tests on a 1 l tank with the strip tape concept are planned for April 2025, and simulations also considering the strip tape concept will follow just after. This will enable to assess if this Krypton tank design is truly demisable and increase its TRL level, currently being 4.

4.3.5. Reaction Wheels

Rockwell Collins demisable Reaction Wheels

Traditional RW designs have high CR due to the survivability of elements such as the BBU and flywheel. Building on previous research by Altran, Rockwell Collins has developed demisable RW designs integrating material and structural modifications to enhance break up while maintaining functional performance. Several strategies were used:

- **Material Substitution:** Replacing Stainless Steel components with Aluminium for less demisable elements such as the flywheel, upper threaded ring, and rotor flange, promoting earlier melting and reducing mass.
- **Structural Modifications:** Introducing weaker adhesive connections and temperature-dependent release triggers within the BBU to promote early break up.
- **Thermal Enhancement:** Exploring the use of thermite to assist in the BBU break up.

Three RW configurations were analysed, incorporating different materials and break up mechanisms. The first one was the RSI 68 SS (Stainless Steel RW with early break up mechanism, see Figure 60), consisting of:

- Maintained Stainless Steel flywheel but introduced an Aluminium upper threaded ring to facilitate early break up.
- Implemented adhesive failure mechanisms in the rotor flange and magnet carrier.
- Completely demised above 87 km release altitude, though with 160 g of surviving mass and 0.5 m² CA at 78 km [67].
- Achieved TRL 4, needing further refinements to optimise demisability.

Moreover, they developed an RSI 45 Al (Smaller Aluminium RW) where they:

- Used an Aluminium monoblock flywheel and other Aluminium components to enhance demise probability.
- Did not include early break up mechanisms and partially demised at 78 km release altitude, indicating a need for additional refinements [67].
- Achieved TRL 3/4 due to early-stage implementation and required further testing.

The last one was the RSI 68 Al (Aluminium RW, see Figure 60), consisting of:

- Replaced Stainless Steel flywheel with Aluminium monoblock flywheel.
- Introduced an Aluminium upper threaded ring to trigger shaft release at 900 K.
- Applied adhesive connection between the rotor flange and magnet carrier to fail at 490 K.
- Achieved complete demise at 78 km release altitude in simulations.
- Reached TRL 3/4, aiming for TRL 6 though further development data is unavailable [64].

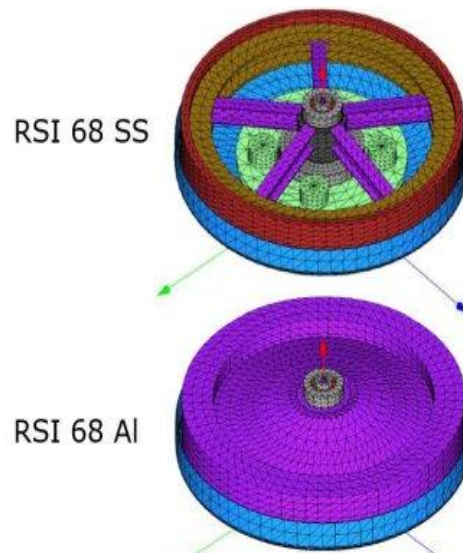


Figure 60: Demisable RWs Rockwell Collins illustration [64].

The development of these demisable RW demonstrates significant advancements in RW D4D strategies. The most effective approach combines material substitution, structural modifications and thermally activated disassembly to ensure lower CR while maintaining operational efficiency. Future work includes optimising thermite placement in the BBU, refining adhesive failure mechanisms and advancing designs to TRL 6.

4.3.6. Magnetorquers

LusoSpace demisable magnetorquer

Developing a demisable MTQ is a key building block for LEO platform above 500 kg. Traditional MTQs, particularly those exceeding 3.5 kg, tend to survive atmospheric re-entry due to shielding effects from the spacecraft and the MTQ housing. To address this, LusoSpace has conducted a series of design iterations to develop a demisable MTQ [68] whose design is hereby presented.

Several design configurations were assessed, considering the core composition (single or divided), core shape and different winding and potting approaches. The most significant improvement in demisability was achieved by promoting early separation of the core and increasing its exposure during re-entry. The MTQ design to enhance demisability consists of [68]:

- Using **more demisable materials for the core** (Hiperco50A), for the **external housing** (Aluminium 6082 shell that also provides structural support), and **eliminating internal housing** to reduce shielding effects.
- Use of **demisable polymer bolts** (PEEK fasteners) to promote early detachment.
- **Exposing 31% of the core** length to enhance thermal degradation (see Figure 61).
- **Excluding potting** materials to decrease thermal insulation and mass.

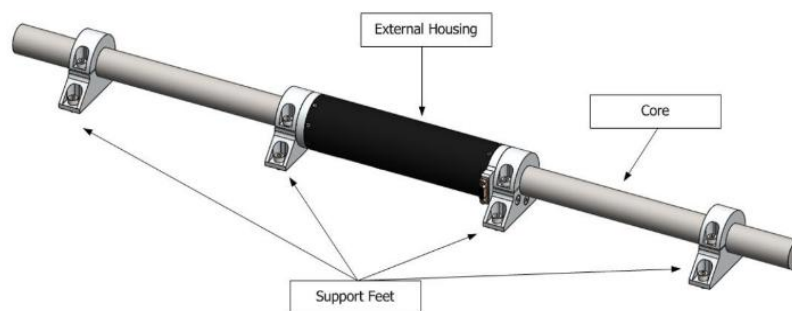


Figure 61: Demisable MTQ LusoSpace illustration [68].

The MTQ consists of a magnetic inductor, comprising a Copper coil and a Ferromagnetic core. The core is a cylindrical solid rod of 747 mm length and 25 mm diameter. The coil is a Copper wire wound around the core, of 162 mm length, 16 layers and 0.315 mm of wire diameter. It also has support feet of Aluminium 7075 that are attached with the PEEK fasteners [68], ensuring structural integrity while promoting demisability.

To assess the demisability of the MTQ, simulations were conducted. It was observed that the MTQ fully demises for release altitudes above 65 km, complying with demise requirements. More in detail, the core's early separation together with its increased exposure led to its complete disintegration. The housing fully demised before reaching ground, and the exclusion of potting and removal of internal shielding enhanced heat absorption despite the coil being of Copper (a high melting point material), promoting full demise [68].

Additionally, an alternative composite PEEK shell with an iron-cobalt core wrapped in Copper coils was evaluated. However, this configuration did not yield improvements in demisability due to the high shielding effects of the satellite and the nested MTQ structure. The CFRP components also exhibited prolonged resistance to melting.

The demisable MTQ of LusoSpace has reached TRL 5/6, with ongoing efforts to further refine its design and validate its performance through additional testing and analysis.

ZARM demisable magnetorquer

ZARM Technik has recently initiated the development of a new demisable MTQ concept. The design remains under development, and detailed information on the specific architecture, material selection and demisability is not yet available. However, it is known that this MTQ has reached TRL 6. This also represents an important step in broadening the range of demisable magnetorquer solutions. The availability of multiple providers working on demisable technologies is crucial to ensuring flexibility in satellite design, mitigating supply chain risks and enhancing adaptability. As the development progresses, further details regarding the ZARM demisable MTQ are expected to become available.

4.3.7. Optics

Thales Alenia Space demisable Spectrometer and Bipods

The development of demisable optical payload components is a critical aspect for demisability as previously explained. This advancements in demisable optics developed by TAS are hereby presented. A major limitation to achieve the demise of optical payloads are Ceramic spectrometer benches, which act as a thermal shield for attached components. Several design modifications were introduced to **replace the Ceramic bench with an Aluminium sandwich structure** to promote demise. The design iterations included:

- Titanium was replaced by **Aluminium-Silicon (AlSi40)** on **optical mounts, A-Frames, and bipod fittings** achieving a 40% mass reduction and improved demise.
- **Invar** was integrated into **large optical mounts and A-Frames**, with optimised designs reducing mass by 20% while maintaining stability.
- **3D-Printed Titanium and Invar** designs that enhanced exposure to the heat flux, increasing demise.
- Prisms and optical mounts were **split into smaller fragments**, while **glued connections** facilitated earlier separation, increasing thermal exposure [56].

Several simulations were conducted using SCARAB to evaluate the demisability of the different design configurations. The primary findings include [56]:

- Spectrometer Bench: Ceramic benches survived re-entry, shielding optical components. However, the Aluminium sandwich replacement enabled full demise.
- Mounts and Brackets: AlSi40 showed the best results, achieving full demise of optical mounts and A-Frames.
- Mirrors and Optics: Smaller mirrors (15 cm) generally demised, while bigger ones and some dichroic optics survived in certain scenarios. Interface weakening techniques helped release and expose them to higher heating.
- Cryostat and Electronic Components: Demised in optimised cases, with interface weakening further enhancing demise probability.
- Telescope Assembly: Material swaps reduced CA, though the scrambling window survived.
- Interface Weakening: Glued connections and composite blades promoted early break up.

The redesign of optical payload components by TAS demonstrated significant advancements in demisable optics. The best performing configuration (using AlSi40 for the spectrometer bench, all optical mounts, A-Frames and bipod fittings) achieved near-complete demisability [56]. However, low TRL was reached with this activity, and further research is required to increase it.

Demisable bipods were also investigated by TAS. Their proposed design implemented **AM** and the use of **flow holes** to enhance heat exposure. Simulations showed that the heating of legs and cutouts was of the same speed, with the legs demising slightly before the cutouts. In this case the TRL reached was 4, but further testing and technological development is required to validate the demisability and operational performance of these holes bipods. New activities for that purpose are to be started soon by ESA.

Belstead demisable Mirrors, Optical Payload Fixings and Support Structures

Belstead Research Limited has also performed research on optical components to enhance their demisability, including elements such as mirrors, optical payload fixings, and support structures. The design strategies used to enhance demisability aim to minimise undemisable fragments, use alternative materials with lower melting points or higher ablation rates and optimise joint and fixing structures using either adhesive or mechanically weakened joints to promote early break up.

Mirrors are a fundamental component of optical payloads, traditionally made of materials such as SiC. To improve demisability, alternative materials and designs have been developed:

- **CFRP Mirrors:** offer significant improvements in demisability due to their lower thermal resistance and enhanced fragmentation characteristics. These mirrors maintain the optical performance while ensuring that they burn up during re-entry. They have been flight-proven, thus having TRL 9 [57].
- **Smaller Beamsplitter Glass:** The use of smaller optical elements reduces the kinetic energy upon ground impact, minimising CR.
- **Contained Beamsplitter Glass:** Encapsulation techniques ensure Glass elements either fully demise or remain intact within a non-demisable structure.

The Optical Bench and Supporting Structures also play a crucial role in the overall demise behaviour of an optical payload. The traditional use of CFRP optical benches leads to the early separation of components, requiring additional considerations to ensure controlled fragmentation. Advancements from Belstead research include using:

- **Adhesive joints with high temperature failure paths:** designed to fail at high temperatures to enable early component separation. They have TRL 9 [57].
- **CFRP Main Bipods and Carbon-Carbon Telescope Barrels:** using materials with improved ablation characteristics, contributing to a more controlled demise. Both have TRL 9 as have been used in previous optical payloads with demonstrated space heritage.
- **Modular Optical Benches:** incorporate demisable connection points allowing controlled break up without compromising structural integrity during mission operations [57].

The effectiveness of these design modifications has been evaluated through Monte Carlo simulations and experimental validation campaigns. These tests have confirmed that:

- **Undemisable Joints Reduce Fragmentation Risks:** critical components either demise completely or reach the surface as a single entity. They are currently under testing to validate their demisability, having TRL 4.
- **Material Changes Enhance Thermal Response:** The shift from SiC to CFRP mirrors and structural elements improves demise without compromising performance.
- **Encapsulation methods for beamsplitter glass and focal plane assemblies prevent debris formation.** This has been indicated as with TRL 9 [57].

Since optical elements are different for each mission, depending on its objectives and requirements, further research in this field is required to provide a broad range of solutions. Therefore, ESA is starting activities soon on demisable brackets, and designing and assessing the demisability of CFRP benches.

4.3.8. Design for Containmentment

OHB Design for Containmentment methods

To evaluate alternatives further from D4D for non-demisable elements, activities have also been performed to develop D4C technologies. They focused on the identification, development, and validation of **containment** solutions for demise critical satellite components. OHB, with contributions from Belstead and DLR, investigated feasible containment methods and their integration into satellites to ensure compliance with CR and CA mitigation requirements.

Based on the identification of critical components, containment methods were classified into three categories: connections (or joints), enclosures, and hybrid solutions combining both concepts. A trade-off analysis identified four containment solutions for further study considering their system impact, CR reduction potential, reliability, and feasibility for testing.

The first concept involves **replacing the Aluminium Thermal Guard** around spectrometers with a non-demisable material (see Figure 62). The design considerations included:

- Ensuring thermal stability without compromising the spectrometer’s optical pathway.
- Using materials like **C/SiC or Tungsten alloys** to withstand extreme heat flux conditions.
- **Structural reinforcement** to prevent premature fragmentation due to thermal stress.

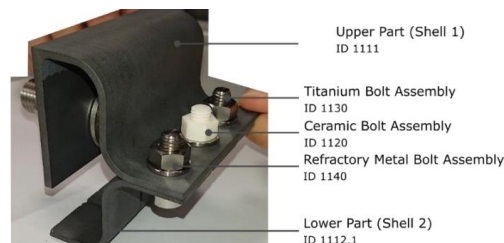


Figure 62: OHB D4C Spectrometer Thermal Guard [69].

Another containment approach was implemented by **modifying the optical bench material** to a non-demisable alternative (see Figure 63). The design criteria included:

- Matching the Coefficient of Thermal Expansion (CTE) of the optical bench with the mounting feet/bipods to minimise thermal stress-induced fractures.
- Evaluating material thickness, geometry, and exposure to high-velocity re-entry flow.
- Using **Ceramic bolts, Al₂O₃ or Molybdenum**, to ensure joint integrity during re-entry.

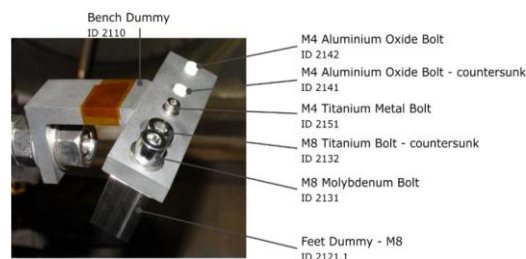


Figure 63: OHB D4C Optical Bench and Mounting Solutions [69].

The approach of **connecting feet/bipods by a tether** minimises modifications to spacecraft structures while integrating containment (see Figure 64). Considerations included:

- Use of high temperature resistant tethers of **Nextel 440 or Tungsten wires** to prevent premature detachment of bipods during re-entry.
- Evaluating tether length and attachment to optimise containment effectiveness.
- Studying failure modes at high heat flux and potential improvements to tether coatings.

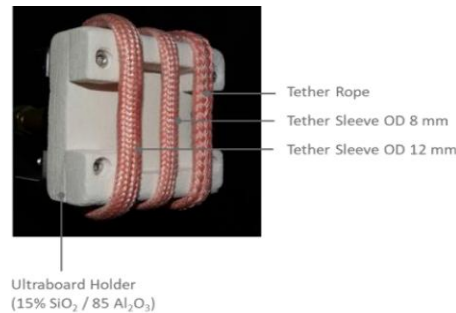


Figure 64: OHB D4C Feet/Bipods Connected by Tether [69].

The enclosure concept in a **net/cage** was introduced to mitigate the fragmentation of electronic units, which were previously modelled with inaccurate demisability assumptions (see Figure 65). Design aspects included:

- Developing **lightweight, high-temperature-resistant enclosures** using **Aluminium oxide reinforced fabrics**.
- Studying airflow blockage effects on contained electronic units to assess heat transfer and degradation dynamics.
- **Optimising the cage perforation pattern** to balance structural integrity and thermal shielding.

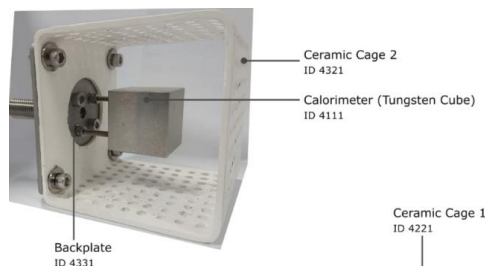


Figure 65: OHB D4C Electronic Units in a Net/Cage [69].

All the above-mentioned technologies were developed and tested until they reached TRL 3/4. The effectiveness of the four containment designs was assessed through DRAMA and SAMj simulations, which demonstrated a significant reduction in CA and fragment number for all D4C concepts. However, the Kinetic Energy of all designs was far above the 15 J [69] threshold established in the SDMR, thus, making them non-compliant on that side.

A PWT test campaign was conducted at the DLR L3K facility to validate the containment designs under high heat flux re-entry conditions. Observations from the tests include [69]:

- C/SiC Thermal Guards fractured earlier than expected, highlighting the need of other materials or alternate designs.
- Aluminium Oxide bolts exhibited thermal shock failure, pointing out the necessity of alternative fasteners.

- Tethers failed rapidly (~5 s to ~12 s), prompting investigations into alternative materials such as Tungsten wire.
- Cages displayed structural fractures due to thermal stress yet demonstrated promising heat blocking effects on enclosed components.

These results underscore the complexity of containment techniques and the need for further refinement in material selection and structural design. The findings demonstrate that while D4C is a viable approach to CA reduction, it is not for Kinetic Energy, and significant technological advancements are required to integrate these solutions into operational satellite systems.

Thales Alenia Space Design for Containment methods

TAS has also investigated D4C strategies. The D4C techniques identified have been categorised into four families: Regroup, Attach, Protect and Encapsulate. Through a trade-off analysis, the most promising methods (based on Regrouping, Specific Attachment, and Encapsulation) were selected for further development. The selection was based on their applicability across various satellite missions, effectiveness in reducing CA and Kinetic Energy, and feasibility in terms of mass, cost, and integration complexity. The technological enablers for containment designs, reached TRL 3/4 in this activity and include [41]:

- **Tether-based attachment:** A solution that connects surviving elements all together. Tethers made of **Tungsten** and **SiC** showed promise due to their high temperature resilience and oxidation resistance.
- **Encapsulation through structural modification:** Partial encapsulation concepts such as **cages and nets** were tested to balance heat flux exposure and elements retention.
- **Optimised interface materials:** Bolts, eyelets, and other joining elements were tested to assess their survivability and effectiveness in securing containment structures.

Experimental campaigns in the L3K PWT confirmed that certain high temperature materials, including Tungsten, SiC, and Molybdenum, exhibit controlled oxidation, making them viable candidates for containment applications. Conversely, materials such as Aluminium Oxide and Monolithic Alumina were found unsuitable due to thermal shock susceptibility and early melting.

A multi-criteria analysis was conducted to assess containment methods across several parameters, including CA reduction, Kinetic Energy variation, system impact, and feasibility of implementation. The results demonstrated:

- CA reduction: Tether-based attachment showed significant reductions, with optimised designs achieving up to 30 m² improvement in DRAMA simulations [41].
- Kinetic Energy impact: Encapsulation techniques increased Kinetic Energy due to added mass but could be optimised through selective exposure strategies.
- System integration feasibility: Architecture modifications and specific attachments were found to have minimal mass penalties and lower cost impacts compared to full encapsulation methods.

Testing of containment concepts highlighted key challenges, particularly regarding local heat flux concentration in joining elements such as eyelets. These areas experienced accelerated demise due to enhanced flow interactions, requiring design refinements. Overall, the results of TAS's D4C designs development show the feasibility of D4C solutions to reduce the CA. Nonetheless, they still do not comply with Kinetic Energy requirements. Specific attachment using tethers and selective encapsulation strategies emerged as the most effective methods, offering significant CA reduction while minimising system complexity.

5. D4D technology gaps and development roadmap

The research conducted in this thesis has provided a baseline from which to have a general understanding of component demise during atmospheric re-entry, allowing for the identification of critical components from the demise perspective. In parallel, an extensive review of D4D technologies has been performed, highlighting the current state of development and their potential to enhance satellite demisability. However, to achieve a demisable platform, several gaps remain.

This section aims to identify such gaps by analysing two aspects: first, components or factors that may influence demise but have not yet been studied, and second, critical satellite elements known to be non-demisable for which no D4D technologies have yet been developed. Based on this, a development roadmap is proposed to fill these gaps. This roadmap will focus on both increasing the TRL of existing D4D technologies and fostering the development of new solutions to ensure their availability to be used for a demisable satellite platform.

5.1. D4D gaps for fully demisable platform

The identification of D4D gaps is critical for developing a demisable satellite platform. Through the research conducted in this thesis, several components have been identified as either having an unknown or unstudied demisability, being recognised as critical from a demise perspective but lacking targeted D4D solutions. For other components, existing D4D technologies which require further development to reach higher TRLs have also been identified. These gaps represent the challenges that must be addressed to obtain a satellite design that complies with demise requirements.

5.1.1. Critical components with unstudied demisability

Several satellite components have not been studied in terms of their atmospheric re-entry behaviour. This lack of research introduces uncertainty regarding their demise performance and potential contribution to on-ground CR. Components falling in this category include:

- **Engines:** Their complex structures, including high temperature resistant materials and intricate internal configurations, make their demise behaviour difficult to predict accurately without further testing. Research has been performed on a small thruster, but no information is available for larger engines.
- **Fill and Drain Valve:** The structural integrity and material composition of these valves could result in partial or complete survival during atmospheric re-entry.
- **Large Antennas:** These components often include robust metallic structures and composite materials that are classified as not demisable.
- **Laser Communication Terminal:** Given the increasing use of laser communication in modern satellites, and their classification as non-demisable components, research is necessary to understand their demise behaviour and, from there infer, the optimal D4D strategies to increase their demisability.
- **Helicoils:** Identified in previous research as components requiring specific demise testing, helicoils may contribute to on-ground debris if not properly assessed.

5.1.2. Critical Components Without Existing D4D Technologies

Through the analysis conducted in this thesis, several satellite components critical from the demise perspective that currently lack dedicated D4D technologies have been identified. As this is a relatively recent field, and given budget constraints, D4D developments have so far focused on components with higher contributions to CR, like propellant tanks and RWs. While theoretical assessments suggested potential D4D strategies for the following components, no technological development activities have been made yet to improve their demisability: **Gyroscopes, Thrusters, Batteries, Electronic Cards and Boxes, Star Trackers** and **Balance Masses**. While solar arrays also fall into this category, it is important to note that their demisability, as assessed in previous studies, was found to be of low criticality. As a result, the lack of D4D developments for these components is a logical outcome rather than a technology gap.

The limited progress in D4D solutions for these components can be attributed to multiple challenges. Some of these systems, such as gyroscopes and star trackers, contain delicate optical and electromechanical elements, making redesign for improved demise non-trivial without affecting their performance. Batteries and balance masses, on the other hand, often use high density materials that inherently resist ablation, requiring alternative material solutions or controlled break up approaches.

5.1.3. D4D Technologies Requiring Further Maturation

The D4D technologies from Section 4.3 require further advancements to increase their TRL and ensure their effectiveness and integration into future satellite platforms. The list of the D4D technologies under development together with the TRL they have reached according to the information found in the literature review is presented in Table 3.

Table 3: D4D Technologies with their TRL and company that develops them.

D4D technology	TRL	Company
Structural panel	5	EPFL, RUAG, BComp
Joint Bolted and bonded Cleat	8	OHB
Adhesively Bonded Demisable Joint	4	OHB
Composite Insert	5	OHB
SMA bolts	7	OHB
Thermally Triggered Fastener Joint	6	TAS
Bolt with Internal Actuator	2/3	ADS
Bolt with External Actuator and Dual Thread Interfaces	2/3	ADS
Bolt with External Actuator and Insert Interface	2/3	ADS
Pin Puller Concept	2/3	ADS
Clamped Interface Concept	2/3	ADS
Clamped Interface with Radial Bracing	2/3	ADS
Thermite based Joint	2/3	HTG
Short CF/PEEK bolts	5/6	EPFL, RUAG, BComp
Demisable joints LEO Communication platforms	-	INVENT
SADM KARMA - 4/5 TG	6	KDA
Demisable SADM BBU modified and thermite	-	DLR
Large chemical Aluminium propellant tank	3	ADS and Orbital ATK
Large chemical Aluminium propellant tank	5	MTA
Large chemical CFRP propellant tank	3	ADS

Small chemical Aluminium propellant tank	3/4	Institute of Aviation
Small chemical COPV propellant tank	4/5	PEAK Technology
Large Xenon composite propellant tank	6	Haydale Composite Solutions
Small Xenon COPV propellant tank	3	ADS
Small Krypton COPV propellant tank	4	PEAK Technology
RW RSI 68 SS	4	Rockwell Collins
RW RSI 45 Al	3/4	Rockwell Collins
RW RSI 68 Al	3/4	Rockwell Collins
Demisable MTQ LusoSpace	5/6	LusoSpace
Demisable MTQ ZARM	6	ZARM Technik
Demisable Spectrometer	3	TAS
Demisable Bipods	4	TAS
CFRP mirror, adhesive joint, Carbon-Carbon barrel	9	Belstead Research Limited
Undemisable Joints	4	Belstead Research Limited
Encapsulation beamsplitter glass and focal plane	9	Belstead Research Limited
D4C Spectrometer Thermal Guard	3/4	OHB
D4C Optical Bench and Mounting	3/4	OHB
D4C Feet/Bipods connected by Tether	3/4	OHB
D4C Electronic Units in a Net/Cage	3/4	OHB
D4C Undemisable Tungsten or SiC tether	3/4	TAS
D4C partial encapsulation in cages and nets	3/4	TAS
D4C Undemisable joints	3/4	TAS

The relatively low TRL of most of these technologies highlights the need for further testing, validation and potential redesign to ensure they can be integrated into a demisable satellite platform. The identification of these gaps establishes the foundation for the development roadmap presented in Section 5.2. Addressing these gaps through targeted research and technology maturation is essential for achieving a satellite platform that is compliant with re-entry specific SDMR, mitigating the risk of surviving debris reaching the ground during atmospheric re-entry.

5.2. D4D proposed development roadmap

TRLs are a standard used to assess the maturity of technologies before they are fully deployed in space. Advancing a technology from an early concept (TRL 1-3) to a system that has been demonstrated in a relevant environment (TRL 7-8) is crucial for ensuring mission success, reducing risks, and meeting regulatory requirements. Developing a demisable satellite requires maturing multiple components to TRL 6, having tested them in relevant conditions, and ensuring they comply with SDMR and demise thresholds upon atmospheric re-entry.

Maturing all identified components and technologies reaching TRL 6 requires parallel advancements across multiple subsystems. Addressing current technology gaps through targeted research, prototyping, and relevant environment validation will enable future missions to comply fully with D4D requirements, reducing the risk of on ground casualties due to surviving debris. By following the subsequent roadmap, a demisable platform could be expected within the next 6 - 7 years, depending on the pace of technology maturation, and the accuracy of testing facilities and simulations to provide a representative enough re-entry environment for testing the components.

5.2.1. Engines and Fill and Drain Valves demise behaviour

To enhance the demisability of propulsion system components, this activity would study the break up and demise behaviour of engines and fill & drain valves. The goal is to identify failure mechanisms, evaluate material substitutions, and validate predictions through testing.

Proposed approach:

- Initial testing: Analyse structural integrity and material response via testing, including PWT tests on representative engine and valve breadboards and/or their critical elements.
- Material evaluation: Assess alternative materials with lower melting points.
- Final testing: Validate promising options through simulations and PWT campaigns.

Timeline: 2-3 years to reach TRL 3/4; the strategy for further maturation would depend on the test results.

5.2.2. Helicoils influence in demise

An activity to study helicoils demisability has been identified as necessary. It would study how helicoils affect demisability in bolted joints under re-entry conditions.

Proposed approach:

- Initial testing: Study the demise behaviour of helicoils and the fragmentation of bolted joints with helicoils in PWT tests.
- Analysis of results: Determine whether helicoils aid or hinder demisability, and develop the best strategy for future activities based on the results.

Timeline: ~ 2 years.

5.2.3. Antennas and Communication Payloads demise behaviour

As payload components, antennas and communication terminals are not essential for achieving a demisable satellite platform. However, understanding their demise behaviour is valuable for future missions that might include them and do not comply with SDMR regarding CR or demise. It is thus recommended in the roadmap to have an activity for characterising the break up and material response of these elements during atmospheric re-entry.

Proposed approach:

- Initial testing: Analyse structural integrity and material characteristics of antennas and LCTs via testing, including PWT tests on representative breadboards and/or their critical elements.
- Analysis of results: Identify predetermined weaker parts or failure points and assess structural redesigns exploiting these points to promote early break up during atmospheric re-entry.
- Material evaluation: Study lightweight composites and demisable materials as alternatives.
- Final testing: Validate promising options through simulations and PWT campaigns.

Timeline: 3 years to reach TRL 3/4.

5.2.4. Demisable Gyroscope

In Section 4.2.12 gyroscopes were identified as critical from the demise perspective, with multiple sub-components, particularly GFRP-based GEUs and Fused Silica sensor coils, having a high likelihood of survival during re-entry. Building on the heritage of these findings, an activity to develop a demisable gyroscope would be necessary in this roadmap. The development until TRL 6 is estimated to take around 4 to 5 years.

Phase 1: Redesign and Initial Testing

Proposed approach:

- Material and new designs evaluation: Study alternative materials for GEU cards to replace GFRP or Fused Silica sensor coils that maintain performance and investigate design modifications to promote early fragmentation.
- Initial testing: Validate the mechanical integrity and demisability of promising options through testing, simulations and PWT campaigns of initial prototypes.

Timeline: 1 - 2 years to reach TRL 3/4.

Phase 2: Design Optimisation and Component-Level Testing

Proposed approach:

- Design optimisation: Refine the most promising demisable gyroscope design from Phase 1 compliant with demise and operational requirements.
- Final testing: Validate the refined design performance, compliance with operational requirements and demise via full-scale testing including full-system PWT tests.

Timeline: 2 - 3 years to reach TRL 6.

5.2.5. Demisable Thruster

Thrusters are also critical from the demise perspective, with different survivability of their upper and lower sections, the influence of potting material and the high resistance of certain nozzles. This activity would build upon the results presented in Section 4.2.8. to develop a demisable thruster. The development until TRL 6 is estimated to take around 4 to 5 years.

Phase 1: Redesign and Initial Testing

Proposed approach:

- Material and new designs evaluation: Study alternative materials with lower melting temperatures for nozzles and thick-walled components and controlled failure points in critical points to promote early break up.
- Initial testing: Validate the mechanical integrity and demisability of promising options through testing, simulations and small-scale PWT campaigns of initial prototypes.

Timeline: 1 - 2 years to reach TRL 3/4.

Phase 2: Design Optimisation and Component-Level Testing

Proposed approach:

- Design optimisation: Refine the most promising demisable thruster design from Phase 1 compliant with demise and operational requirements.
- Final testing: Validate the refined design performance, compliance with operational requirements and demise via full-scale testing including full-system PWT tests.

Timeline: 2 - 3 years to reach TRL 6.

5.2.6. Batteries and Electronic Cards and Boxes demise enhancement

In Sections 4.2.4 and 4.2.5 ABSL batteries and electronic cards/boxes were identified as low to medium criticality regarding demise, depending on their size, shielding effects and material composition. This activity would consist of developing concepts to enhance batteries and electronic cards/boxes demisability for the largest equipment that presents the highest criticality. The development until TRL 6 is estimated to take around 5 to 6 years.

Phase 1: Redesign and Initial Testing

Proposed approach:

- Material and new designs evaluation: Study alternative materials to the Steel casings that would lead to an earlier demise without compromising mechanical integrity. Assess the use polyamide or paper-based PCBs as demisable alternatives to GFRP, reducing PCBs dimensions and optimising component placement to enhance thermal exposure. Investigate introducing controlled failure points to facilitate early break up of enclosures and PCBs.
- Initial testing: Validate the mechanical integrity and demisability of promising options through testing, simulations and small-scale PWT campaigns of initial prototypes.

Timeline: 1 - 2 years to reach TRL 3/4.

Phase 2: Design Optimisation and Component-Level Testing

Proposed approach:

- Design optimisation: Refine the most promising demisable battery and electronics cards and boxes designs from Phase 1 compliant with demise and operational requirements.
- Final testing: Validate the refined designs performance, compliance with operational requirements and demise via full-scale testing including full-system PWT tests.

Timeline: 2 - 4 years to reach TRL 6.

5.2.7. Demisable Star Tracker

Star trackers are critical due to their Titanium structures, Optical Barrel shielding, and bolted assembly. It is thus necessary an activity to develop a demisable star tracker. The development until TRL 6 is estimated to take around 4 to 5 years.

Phase 1: Redesign and Initial Testing

Proposed approach:

- Material and new designs evaluation: Study alternative materials to Titanium for the optical barrel and focal plane housing. Assess the applicability of demisable coating or inserts to promote earlier melting. Investigate material alternatives for lenses and optical components. Optimise bolted connections or lens mountings to promote earlier break up e.g. via demisable joints or adhesives.
- Initial testing: Validate the mechanical integrity and demisability of promising options through testing, simulations and small-scale PWT campaigns of initial prototypes.

Timeline: 1 - 2 years to reach TRL 3/4.

Phase 2: Design Optimisation and Component-Level Testing

Proposed approach:

- Design optimisation: Refine the most promising demisable star tracker design from Phase 1 compliant with demise and operational requirements.
- Final testing: Validate the refined design performance, compliance with operational requirements and demise via full-scale testing including full-system PWT tests.

Timeline: 2 - 3 years to reach TRL 6.

5.2.8. Demisable Balance Masses

Balance masses are potentially critical regarding demise due to their high density materials and internal placement, which limit exposure to the heat flux. Even if they are not used in all satellites, it would be interesting to have an activity that builds on past findings to develop demisable balance masses for future satellites that might use them and do not comply with the SDMR and CR threshold. The development until TRL 6 is estimated to take around 4 to 5 years.

Phase 1: Redesign and Initial Testing

Proposed approach:

- Material and new designs evaluation: Study alternative materials such as Aluminium or composites. Assess the use sintered or layer structures to enhance break up. Investigate controlled break up techniques for the masses and/or their attachments. On system level strategies the optimal location of balance masses would also be studied (including external mounting configurations), keeping in mind that this is not always possible because part of the objective of balance masses is to control the position of the Centre of Mass and thus their location cannot be modified without an impact.
- Initial testing: Validate the mechanical integrity and demisability of promising options through testing, simulations and small-scale PWT campaigns of initial prototypes.

Timeline: 1 - 2 years to reach TRL 3/4.

Phase 2: Design Optimisation and Component-Level Testing

Proposed approach:

- Design optimisation: Refine the most promising demisable balance mass design from Phase 1 compliant with demise and operational requirements.
- Final testing: Validate the refined design performance, compliance with operational requirements and demise via full-scale testing including full-system PWT tests.

Timeline: 2 - 3 years to reach TRL 6.

5.2.9. Demisable structural panels and joints development roadmap

Structural components and joints must be designed to promote early break up in order to enhance the demisability of a satellite. Demisable structural panels have reached TRL 5, while for joints depending on the design concept it varies between 3 to 8. Advancing to TRL 6 is expected to take around 2 to 4 years as an average, depending on TRL of the design concept.

Phase 2: Design Optimisation and Component-Level Testing

Proposed approach:

- Design optimisation: Refine the most promising demisable structural panels and joints designs from Sections 4.3.1. and 4.3.2. compliant with demise and operational requirements. For the structural panels, it could consist of hybrid CF-FF composite optimisation (fibre fraction, ply thickness adjustments). Alternative demisable resin systems with reactive fillers should be assessed too. The same rationale would be applied for improving the demisable joints designs.
- Final testing: Validate the refined design performance, compliance with operational requirements (e.g. vibration, shock tests) and demise via full-scale testing including full-system static and dynamic PWT tests and Interlaminar Shear Strength, face sheet shear, and tensile compression and bending tests.

Timeline: 2 - 3 years to reach TRL 6.

5.2.10. Demisable SADM development roadmap

A demisable SADM under development has already reached TRL 6, while the TRL of the other one remains unknown. Since TRL 6 has already been reached for at least one design, no detail roadmap is considered necessary. However, the feasibility of thermally triggered fasteners and break up strategies using thermite could be further researched to enhance demise even more.

5.2.11. Demisable Propellant tanks development roadmap

Demisable propellant tanks have reached varying TRLs: large Aluminium tanks are at TRL 5/6, CFRP tanks at TRL 3, and small Aluminium tanks at TRL 3/4. Advancing all of them to TRL 6 is expected to take 3 to 4 years depending on the tank. The roadmap proposed is a generalisation for all tanks, and the phases that apply for each type of tank depend on the TRL level.

Phase 2: Design Optimisation and Component-Level Testing

Proposed approach:

- Design optimisation: Refine the most promising demisable propellant tanks designs (at least one big and one small for chemical propulsion and the same for electric propulsion) from Section 4.3.4. compliant with demise and operational requirements. For Aluminium tanks, alternative alloys such as Al-Cu-Li or Al-Mg-Sc could be assessed. For CFRP tanks, fibre selection and resin modification should be explored to reduce char formation and enhance fragmentation.
- Final testing: Validate the refined designs performance, compliance with operational requirements and demise via full-scale testing including simulations and full-system PWT tests. Apart from the qualification tests necessary for any propellant tank, Aluminium tanks will undergo pressure cycling, vibration and weld integrity assessments, and CFRP tanks will focus on fibre fragmentation and burst collar testing to enhance break up.

Timeline: 3 - 4 years to reach TRL 6.

5.2.12. Demisable Reaction Wheels development roadmap

Rockwell Collins' demisable RW concepts have reached TRLs of 3/4. Advancing to TRL 6 will require a development roadmap spanning 3 to 4 years.

Phase 2: Design Optimisation and Component-Level Testing

Proposed approach:

- Design optimisation: Refine the RW designs from Section 4.3.5. compliant with demise and operational requirements. The placement of the thermal triggers for the BBU early release through adhesives and thermite should be optimised and further verified to balance break up reliability with functional stability.
- Final testing: Validate the refined design performance, compliance with operational requirements and demise via full-scale testing including simulations, vibrations and full-system PWT tests.

Timeline: 3 - 4 years to reach TRL 6.

5.2.13. Demisable Magnetorquer development roadmap

To advance the TRL of demisable MTQs from TRL 5/6 to a definitive TRL 6 it would be necessary to refine some design elements, conduct additional testing and validate performance in representative conditions, which can be grouped in one phase lasting 1 to 2 years. The necessary validations would include high-fidelity re-entry simulations to confirm full demise of the core, coil and housing, assessing the shielding effects from the satellite structure to determine the optimal placement of the MTQ (expected to be near the corners and edges).

Full-scale PWT tests would be necessary to validate the demisability assumptions as well as thermal vacuum, vibrations and shock tests. The structural integrity of the demisable MTQ should also be validated, focusing on the modified fasteners and core separation. Magnetic field testing would also be necessary to ensure no performance degradation from material substitutions.

5.2.14. Demisable Optics development roadmap

The development of demisable optics components is at varying TRLs. Advancing them to TRL 6 is expected to take 3 to 4 years for spectrometer optics, 2 to 3 years for bipods and optical benches, and additional research efforts for other components if needed. It is to be noted that CFRP mirrors, adhesive joints with high-temperature failure mechanisms, and Carbon-Carbon telescope barrels, have already been flight-proven and reached TRL 9.

Demisable Spectrometer Phase 2: Design Optimisation and Component-Level Testing

Proposed approach:

- Design optimisation: Refine the spectrometer design studying the use of AlSi40 for optical mounts, A-Frames and bipod fittings, and assessing options to promote early break up such as redesigning weaker structural points to promote fragmentation, using flued connections and implementing 3D printed parts.
- Final testing: Validate the refined design performance, compliance with operational requirements and demise via full-scale testing including full-system PWT tests.

Timeline: 3 - 4 years to reach TRL 6.

Demisable Bipods Phase 2: Design Optimisation and Component-Level Testing

Proposed approach:

- Design optimisation: Refine the bipods design from Section 4.3.7. using strategies such as AM to integrate flow holes that enhance thermal exposure and keep structural integrity, and promoting earlier fragmentation of bipods legs.
- Final testing: Validate the refined design performance, compliance with operational requirements and demise via full-scale testing including simulations, vibrations and full-system PWT tests.

Timeline: 2 - 3 years to reach TRL 6.

Demisable Optical Bench Phase 2: Design Optimisation and Component-Level Testing

Proposed approach:

- Design optimisation: Refine the Optical Bench design from Section 4.3.7 considering material trade-offs or improving the adhesive used to early break up.
- Final testing: Validate the refined design performance, compliance with operational requirements and demise via full-scale testing including simulations, vibrations and full-system PWT tests.

Timeline: 2 - 3 years to reach TRL 6.

5.2.15. Design for Containment development roadmap

Most of the identified D4C technologies in Section 4.3.8. remain at TRL 3/4, requiring further research to reach TRL 6. It is estimated that this development would take between 3 to 4 years.

D4C Spectrometer Thermal Guard Phase 2: Design Optimisation and Component-Level Testing

Proposed approach:

- Design optimisation: Refine the Spectrometer Thermal Guard design from Section 4.3.8. since the design using C/SiC and Tungsten demonstrated premature fragmentation. Material optimisation and structural reinforcement would be recommended.
- Final testing: Validate the refined design performance, compliance with operational requirements and failure mode via full-scale testing including simulations, shock resilience tests and full-system PWT tests.

Timeline: 3 - 4 years to reach TRL 6.

D4C Optical Bench Phase 2: Design Optimisation and Component-Level Testing

Proposed approach:

- Design optimisation: Refine the D4C Optical Bench from Section 4.3.8 to address the thermal stress-induced fractures, optimising material thickness and geometry of bolts.
- Final testing: Validate the refined design performance, compliance with operational requirements and failure mode via full-scale testing including simulations, vibrations and full-system PWT tests.

Timeline: 3 - 4 years to reach TRL 6.

D4C Tether Phase 2: Design Optimisation and Component-Level Testing

Proposed approach:

- Design optimisation: Refine the Tether design from Section 4.3.8. considering alternative materials such as Tungsten, Nextel 440 and SiC to enhance thermal resistance. Explore concepts to avoid localised heat flux concentration.
- Final testing: Validate the refined design performance, compliance with operational requirements and failure mode via full-scale testing including simulations, vibrations and full-system PWT tests.

Timeline: 3 - 4 years to reach TRL 6.

D4C Net/Cage Phase 2: Design Optimisation and Component-Level Testing

Proposed approach:

- Design optimisation: Refine the net/cage design from Section 4.3.8. via investigating lightweight and high temperature resistant enclosures with optimised perforation patterns to balance heat transfer and structural integrity.
- Final testing: Validate the refined design performance, compliance with operational requirements and failure mode via full-scale testing including simulations, CFD and full-system PWT tests.

Timeline: 3 - 4 years to reach TRL 6.

5.3. Scalability and mass production

To transition from TRL 6 to full operational deployment, considerations of scalability and mass production are necessary. Once D4D technologies reach TRL 6, their integration into satellite platforms must be assessed to ensure adaptability across different missions. The ability to scale these technologies efficiently is critical.

A key aspect of scalability is ensuring that small scale prototypes tested in PWT facilities are representative of their full scale counterparts. For instance, propellant tanks, often tested in 1l breadboard configurations, must be designed with specific shape, length, and material characteristics that allow results to be extrapolated to larger tanks. This approach enables efficient validation of D4D technologies avoiding the need of full scale experimental campaigns for each configuration and also reducing costs. It is to be noted that full scale technologies have higher mass than the small breadboards, so ensuring proper representativity when scaling them down in their design as well as in the PWT test conditions, is critical to understand how would the full scale technologies behave during re-entry and confirm their demise.

Beyond technical scalability, mass production poses additional challenges in terms of cost, manufacturability, and supply chain integration. Adapting demisable solutions to high production rate environments requires the standardisation of materials and processes. However, manufacturing techniques such as AM, may introduce trade-offs. While AM allows for design flexibility and rapid prototyping, conventional manufacturing techniques remain more cost-effective for high volume production, highlighting the need of a balance between customisation and efficiency.

To ensure seamless integration into different satellite platforms, demisable solutions must be considered from the early design stages. The adoption of modular and adaptable demisable components enables their application across several spacecraft sizes, from small to large

platforms. However, scaling up demise optimised architectures may require additional thermal and structural reinforcements, particularly for larger spacecraft where higher mass and heat flux interactions impact re-entry behaviour. Moreover, the spatial distribution of critical components varies across platforms, which might require tailored demise strategies that preserve effectiveness without imposing excessive mass or cost penalties.

Ultimately, the development of scalable and mass producible demisable satellite technologies aligns with the space industry trend toward sustainable and cost-efficient satellite manufacturing. The findings of this research provide a foundation for future studies focused on optimising demisable technologies for mass production while maintaining compliance with CR and kinetic energy requirements. Further research should explore automated manufacturing approaches, material supply chain optimisations, and mission specific scalability constraints to enable the widespread adoption of D4D satellite designs.

Despite efforts to validate demisable technologies through PWT testing and simulations, uncertainties remain regarding how components behave in real re-entry conditions. DRACO mission plays a crucial role to address these gaps by observing the demise and fragmentation of the satellite in situ. Equipped with onboard sensors, DRACO aims to collect real time data on the thermal and structural response of critical components, including demisable elements such as the PEAK Krypton tanks. By correlating these observations with existing PWT tests and simulations data, DRACO will enhance the accuracy of demise predictions and consequently improve the scalability of demisable designs. This approach will refine models used in satellite development, ensuring that scalable, demisable solutions remain effective in real scenarios.

6. D4D implementation in DRACO mission and scientific return

The DRACO mission represents a key step in the advancement of D4D, as it is a dedicated platform to study satellite demise processes in atmospheric re-entry conditions. Unlike previous approaches that relied heavily on ground based testing and computational models, DRACO will provide in situ observational data, offering first-time information into satellite break up, ablation, and material behaviour during re-entry. This data is critical for refining models and simulations, validating and correlating demise on ground testing, and reducing uncertainties in satellite design aimed at minimising space debris risks.

DRACO aims to mimic a representative small satellite undergoing an uncontrolled re-entry scenario. It comprises three main elements as presented in Figure 66: (i) the Platform, which serves as the re-entry vehicle, designed with representative structural and subsystem components; (ii) the Instrument, which records and transmits re-entry data to the ground for analysis; and (iii) the Objects of Interest, which are specific satellite components and materials subjected to demise observations.

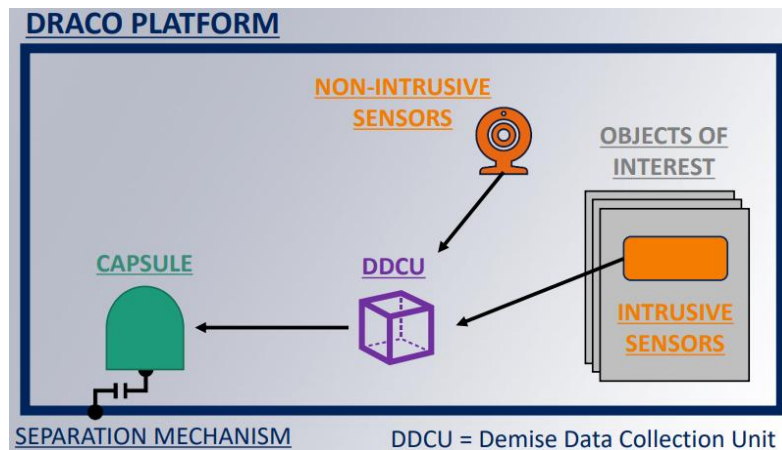


Figure 66: DRACO Design platform concept [36].

The mission follows a structured sequence of phases: launch, orbital, and re-entry, with a controlled shallow re-entry trajectory (starting from ~500 km altitude) that aims to mimic the natural deorbiting process of satellites. During re-entry, DRACO will use sensors, including thermocouples, strain gauges, infrared cameras, and spectrometric markers, to capture parameters such as temperature evolution, mechanical stresses, and fragmentation events. A re-entry capsule will ensure data recovery by transmitting it to ground during descent, in which a parachute is used.

By systematically analysing the behaviour of different materials and spacecraft elements under extreme aerodynamic heating and structural loads, DRACO will contribute significantly to the optimisation of D4D strategies, technologies and testing. The mission's findings will not only enhance the accuracy of current re-entry simulations but also help refine ground testing, ensuring more reliable and efficient satellite designs that comply with space sustainability policies.

6.1 DRACO Objects of Interest

The Objects of Interest (OoI) onboard DRACO are satellite components and materials specifically chosen to be monitored during their demise. These items, embedded within the satellite structure, will be observed and studied during the re-entry to assess their thermal and mechanical degradation. The information gained from their behaviour will play a fundamental role in understanding the atmospheric re-entry physics and refining D4D strategies and validating simulations and models.

The DRACO mission aims to include the following OoI:

- **Demisable COPV Tank:** A propellant tank of 1 l volume from PEAK (presented in Section 4.3) designed for enhanced demise, tested against a conventional propellant tank to compare their respective behaviours.
- **COPV Tank:** A representative propellant tank also from PEAK, used as a benchmark to understand the effectiveness of D4D improvements.
- **Sample Materials:** A selection of materials, including both traditional and demisable alternatives, to evaluate their demise characteristics. These materials will be tested in a PWT beforehand to establish a baseline for their expected re-entry behaviour to be correlated with the data acquired in situ during DRACO's re-entry.
- **Marker Materials:** Blocks of, and components embedded with, spectroscopic markers to facilitate optical tracking and compositional analysis during re-entry.
- **Platform Panels and Structural Elements:** Representative spacecraft structural components to study the break up behaviour of the satellite. A non-demisable panel, designed to survive until lower altitudes (~60 km) will be included in the platform to support the OoI during the observation phase.

Each OoI is expected to be instrumented with at least three thermocouples and two strain gauges to measure temperature gradients and structural deformations. Thermocouples will be positioned at varying depths within materials to capture detailed thermal profiles, while strain gauges will monitor mechanical stresses and potential fracture points. Due to the extreme conditions of re-entry, the reliability of strain gauges at this environment remains an open question, making this an important experimental validation for future studies.

The COPV tanks will be designed at a representative scale to ensure accurate flight model extrapolation. Their integration will consider typical satellite configurations to prevent artificial failure modes. Additionally, a spectroscopic marker will be included within the COPV tank to provide an optically identifiable signature detectable from both DRACO's onboard cameras and an airborne campaign.

The sample materials will include at least four different compositions, comparing traditional spacecraft alloys with alternative demisable materials. These materials will be arranged in different layouts (e.g. satellite walls, thin coupon arrays, cylindrical samples) to explore a range of possible failure modes. Their characterisation will follow ESA DIVE Guidelines (ESA-TECSYE-TN-018311), ensuring consistency with broader research efforts in spacecraft demise studies.

6.2 Spectroscopic markers characterisation

Spectroscopic markers play a crucial role in DRACO, serving as diagnostic tools to identify and track the evolution of specific species during atmospheric re-entry. These markers correspond to spectral emission lines associated with atomic, ionic or molecular transitions, which can be observed and analysed to infer physical conditions such as temperature, composition and density. Their characterisation is essential for accurately modelling and interpreting the observed spectra, particularly in the context of satellite demise studies. The emissions spectra of common materials are presented in Figure 67 for reference.

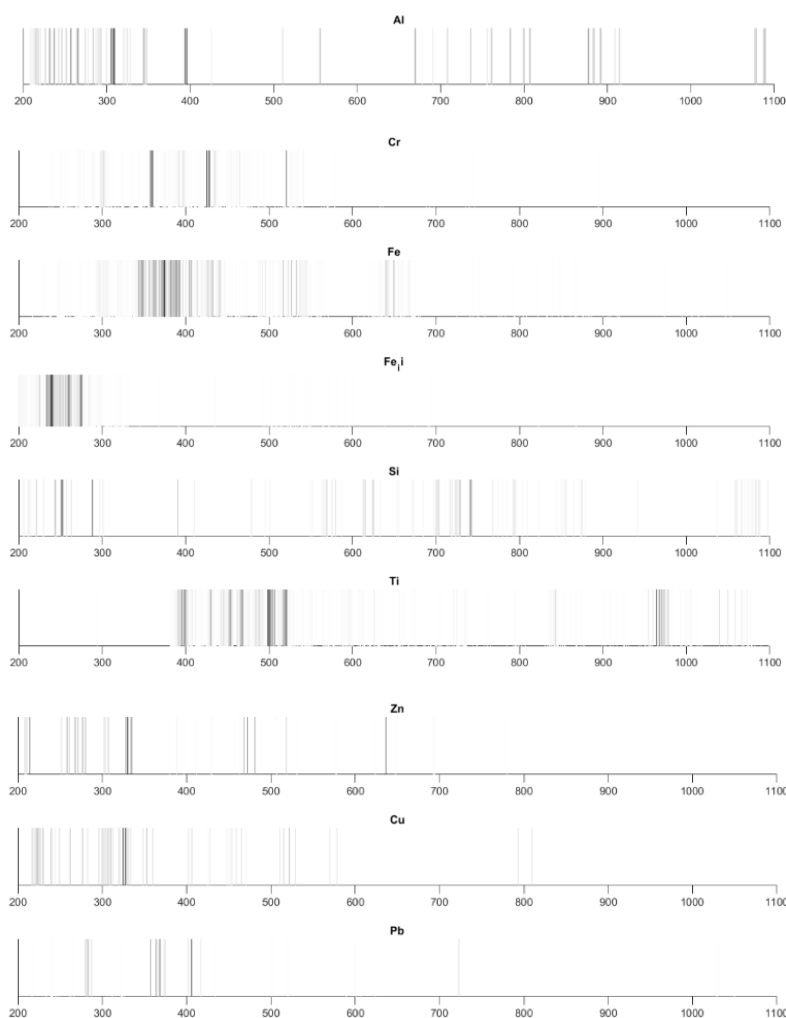


Figure 67: Emission spectra of common materials in the Ool and in the markers [70].

Spectroscopic markers can be categorised into three main types:

- **Atomic Markers:** correspond to electronic transitions of neutral atoms, producing emission lines in the ultraviolet, visible, and infrared regions of the spectrum. They include Fe, Si and Al, relevant due to their presence in satellite structural materials.
- **Ionic Markers:** at high temperature, atoms become ionised, generating additional spectral features. Ionic species such as O^+ , N^+ and Fe^+ are of particular interest, as they provide information about the plasma state and ionisation dynamics during re-entry.
- **Molecular Markers:** Diatomic molecules such as CN, SiO, and AlO exhibit characteristic band structures in their emission spectra. These molecules are useful for identifying chemical recombination and dissociation processes occurring at lower temperatures.

Within the context of DRACO, to support marker characterisation, a dedicated spectroscopic database was developed. This database serves as a reference for spectral line predictions based on physical parameters. To enhance its applicability, additional species were incorporated, as listed below [71]:

- Atomic Species: H, He, Li, C, N, O, Na, Mg, Al, Si, K, Ca, Ti, V, Cr, Mn, Fe, Ni, Cu, Zn, Mo, Xe, Ba, Hg.
- Ionic Species: C^+ , N^+ , O^+ , Si^+ , Ca^+ , Fe^+ , N_2^+ .
- Molecular Species: N_2 , CN, MgO, SiO, AlO, CaO, TiO.

This selection was made to include species with a high probability of being present, as well as those capable of producing strong spectroscopic signals. The inclusion of ionic species was particularly important given the elevated temperatures expected during re-entry. Data sources for this database include the NIST Atomic Spectra Database (Version 5.11) for atomic transitions and publicly available repositories such as SPARK for molecular species.

The selection of spectroscopic markers depends on the specific objectives of an observation campaign. For DRACO, the ideal markers must provide strong, unambiguous signatures to minimise overlap with emissions from standard satellite materials and thus enable reliable tracking of material evolution during re-entry. Moreover, they should be released in a controlled manner to enable time resolved tracking of material ablation and demise.

6.2.1 Integration of Ool: COPV tanks

As part of the DRACO mission, the integration of a COPV tank from PEAK Technology has been investigated to enhance the understanding of its demise behaviour under real operating conditions. This effort focused on embedding thermocouples and a spectroscopic marker within the tank to collect temperature data and facilitate remote tracking of the tank during re-entry.

6.2.1.1 Thermocouples integration in COPV tanks

A thermocouple is a temperature sensor that measures temperature through a junction of two different metals. When this junction experiences a temperature difference, it creates a voltage that can be interpreted to measure temperature. This is known as the Seebeck effect, a phenomenon in which a temperature difference between two dissimilar electrical conductors or semiconductors produces a voltage difference between the two substances. This occurs when heat is applied to one of the materials, causing heated electrons to flow toward the cooler one. Thermocouples are widely used due to their simplicity, durability and broad temperature range. They come in various types, suitable for different temperature ranges and environments.

- Type K: Suitable for temperatures from 95 °C to 1260 °C. It is good practice to protect this type of thermocouple with a suitable metal or ceramic protecting tube, especially in reducing atmospheres. In oxidising atmospheres, tube protection is not always necessary when other conditions are suitable; however, it is recommended for cleanliness and general mechanical protection.
- Type J: Suitable for temperatures from 95 °C to 760 °C. It may be used exposed or unexposed where there is a deficiency of free oxygen.
- Type T: Suitable for temperatures from - 200 °C to 350 °C. It can be used in either oxidising or reducing atmospheres, though for longer life a protecting tube is recommended.

- Type E: Suitable for temperatures from 95 °C to 900 °C. At cryogenic temperatures it is not subject to corrosion.
- Type N: Nickel-based thermocouple alloy, suitable for temperatures from 650 °C to 1300 °C. It provides better resistance to oxidation at higher temperatures than for Type K.
- Type R and S: Suitable from operating temperatures around 900 °C until up to 1450 °C. They are easily contaminated and require protection.
- Type B: Suitable for very high temperatures from 1370 °C up to 1700 °C. It is easily contaminated and requires protection.

Among these thermocouples, Type K and Type N were identified as suitable candidates for DRACO due to their high temperature resilience, robustness, and ability to withstand oxidising environments. Their integration within the COPV tank requires careful consideration of attachment methods to ensure measurements that do not compromise structural integrity, needing accurate placement, secure attachment, and survivability through manufacturing and re-entry. To address this, several mounting techniques have been evaluated:

- **Adhesive Attachment:** High-temperature epoxy adhesives, such as 3M's 2216, offer secure bonding while withstanding thermal cycling.
- **Kapton Tape:** Provides sufficient adhesion but requires validation under dynamic conditions to ensure stability.
- **Encapsulation within Composite Layers:** Embedding thermocouples within the composite layers during lay-up ensures integration but necessitates careful routing to avoid exposure to external flow.

It was concluded that to optimise placement, thermocouples should be routed internally within the composite layers or secured through small, encapsulated holes. This prevents direct exposure to flow, minimising the risk of premature failure. Additionally, routing paths must account for the need to extract sensor cables from the vacuum bag during manufacturing. The expected operational range of thermocouples has been reviewed based on previous test campaigns, with failure typically occurring between 1200 °C and 1600 °C.

To optimise data collection, the positioning of thermocouples has been considered. Ideally, they will be located at different tank depths and positions to capture temperature gradients, providing data about the thermal response of material layers. Another consideration for the layout is for it to align with on ground test campaigns and simulations to allow data comparability.

After all these considerations, it was proposed to use a layout for embedding thermocouples in the COPV tanks of DRACO, as similar as possible to that used in the PEAK COPV tanks on-ground testing to enable data comparability. Based on previous research, high-temperature thermocouples should be embedded at different laminate depths, lengths, and orientation positions to measure heat transfer accurately. The specifications of PEAK's COPV tank and its manufacturing process have to be considered. The manufacturing of the tank follows a process involving an Aluminium liner with CFRP overwrap. The liner is fabricated by welding two machined Aluminium halves under vacuum conditions, followed by sandblasting for enhanced adhesion. The CFRP overwrap consists of ten layers, applied using a robotic tape winding system while maintaining internal pressure to ensure fibre tension. The final structure undergoes curing in an autoclave and autofrettage to introduce residual compressive stress in the liner. Since the laminate thickness exceeds 3 mm, a three-step winding process with subsequent curing in the autoclave is necessary. Additionally, compaction and pre-curing are required after approximately 1 mm of laminate, facilitating the integration of thermocouples at different depths [72].

For scientific measurements, it is recommended to integrate four type-K thermocouples with a 0.5 mm diameter during sample manufacturing. However, since the cured raw parts undergo post-machining and trimming to the correct dimensions, thermocouple realignment within the tube may be necessary. This could lead to breakage due to the thermocouples' brittleness, as observed in previous tests, where two out of six samples experienced thermocouple failures [72].

Since a rotating electrical connector is not feasible for the small thermocouple signals and wireless connections cannot be used in the ionising/EM-emitting environment, an encapsulated data-logger within the samples presents an attractive alternative. This data-logger is a stand-alone recording device that logs temperatures from four thermocouples onto an SD card, or in the case of DRACO, to the Demise Data Collection Unit (DDCU). It is designed to fit inside rotating probes and is thermally protected, along with wiring, using an aluminium oxide-based ceramic cloth/paper with a total thickness of approximately 3 mm [72]. The outermost ceramic paper layer should be implemented before integrating the thermocouples, as shown in Figure 68. Residual voids inside the tube will be filled with ceramic paper/cloth material after data-logger installation.



Figure 68: Data-logger circumferential layer ceramic paper [72].

It is to be noted that a small hole has to be drilled through the tube, through which the feeler ends will be guided and positioned. The hole has to be also hermetically sealed, and the wires must remain inside the tube throughout the manufacturing process. The proposed thermocouple placements based on a coordinate system following the axis direction and tubular angle are presented in Table 4 and Figures 69 a and b.

This configuration aims to provide a temperature gradient during the test time using TC1, TC2 and TC4, while TC3 would provide additional information on eccentric heat distribution.

Table 4: Proposed thermocouple Positions for COPV PEAK Tank.

TC #	Position x [m]	Tubular Angle α [°]	Application Time	Depth
1	150	0	Before 1st winding step	On Al liner
2	150	180	After 1st winding step	1/3 laminate depth
3	225	180	After 1st winding step	1/3 laminate depth
4	150	270	After 2nd winding step	2/3 laminate depth

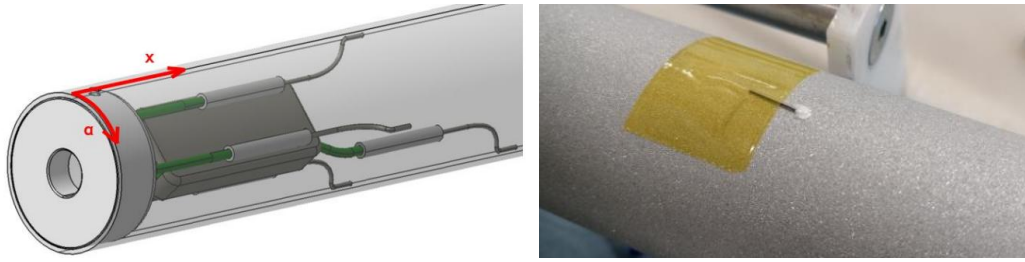


Figure 69 a and b: Thermocouple placement coordinate system and thermocouple application on Al liner, respectively [72].

6.2.1.2 Spectroscopic markers integration in COPV tanks

In addition to thermocouples, the integration of a spectroscopic marker in the COPV tanks of DRACO has been explored to enable remote detection of the tank during demise. Potassium and Sodium were identified as potential candidates due to their strong spectroscopic signatures in the visible spectrum, although further research on this selection is still to be performed and outside of the scope of this MSc thesis. These markers would facilitate tracking via on board or airborne optical instruments, enhancing observational capabilities.

Several integration methods for the marker were assessed, considering factors such as structural impact, manufacturing complexity, chemical compatibility, cost, and detectability. The five identified options included:

- **Integration into the Weld Joint:** Incorporating the marker material directly into the electron beam welding process of the Aluminium liner. While this method ensures the marker is securely embedded, it presents challenges related to weld integrity and even distribution of the marker.
- **Embedding Between CFRP Layers:** Introducing the marker material between the CFRP layers during the lay-up process. This method ensures wide distribution but may compromise structural integrity and demise due to added layer thickness.
- **Coating the Outer Liner Surface:** Applying a thin layer of the marker material to the Aluminium liner before CFRP overwrapping. This allows for gradual marker release but requires strong adhesion and compatibility with both the liner and CFRP.
- **Incorporating the Marker in a Matrix Material:** Mixing the marker with a polymer or resin and embedding it within specific locations in the tank. This provides better control over marker placement but adds complexity to the manufacturing process.
- **Using Marker-Infused Fibres:** Integrating marker-infused fibres directly into the CFRP overwrap. This option allows for an even marker distribution with minimal impact on structural integrity but requires assessment of fibre manufacturing processes and cost.

A trade-off analysis was conducted to rank these methods based on compliance with the scientific requirements of DRACO, including structural impact on the tank, integration manufacturing complexity, customisable marker distribution, chemical compatibility between the marker and tank materials, cost, and how easy it would be to detect the marker based on its integration. The weight of each of the parameters is included in Table 5, together with the scores assigned to each of them, 1 being the worst compliance and 5 the best. It is to be noted that the weights and scores given are subject to the review of PEAK Technology and might be modified in the future based on the results the manufacturers obtain in the activity for the tank development.

Table 5: Trade-off marker integration manufacturing options.

	Weight (%)	Weld Joint integration	Between CFRP layers	Outer liner coating	Marker-matrix	Marker-Infused fibres
Structural Impact	25	2	2	3	4	4
Manufacturing Complexity	15	3	2	4	2	3
Marker Distribution	10	1	4	5	4	4
Chemical compatibility	20	2	3	3	4	4
Cost	5	4	3	4	4	2
Scientific objectives detectability	25	1	4	4	2	4
Scores		1.9	2.95	3.65	3.2	3.75

The highest-scoring options were **marker-infused fibres** and **outer liner coating**. These methods offer the best balance between detectability, structural integrity, and feasibility. Further investigations outside the scope of this MSc thesis will focus on assessing chemical compatibility, optimising marker concentration, and verifying adhesion properties.

The integration of thermocouples and spectroscopic markers in the COPV tank offers a promising approach to study the demise behaviour of COPVs under real re-entry conditions. The selected marker integration methods provide a balance of feasibility and scientific value. Future work outside of the scope of this thesis will involve refining specifications for marker-infused fibres, testing chemical compatibility and manufacturing prototype tanks for validation.

6.2.2 Software tool PRODUCERS simulations

PRODUCERS is a software tool designed to simulate the spectral signatures of a re-entering satellite as it undergoes demise and fragmentation. It provides predictions of radiation emissions based on the satellite material composition, trajectory and fragmentation dynamics. It utilises input data from DRAMA (re-entry analysis tool introduced in Section 3.4) and PADRE (a spacecraft definition framework) to estimate emissions resulting from various physical processes, including:

- Grey body emission from main fragments.
- Shock layer radiation due to air species in assumed equilibrium conditions.
- Radiation from species released into the boundary layer by demising components.
- Grey body emission from particles stripped from fragments.
- Radiation from gaseous species released from those particles.

The aim of PRODUCERS is to assist in the study of atmospheric re-entries by simulating the expected spectral emissions observed from ground-based or airborne campaigns. The tool helps refine re-entry observation strategies and validates physical models of spacecraft demise [73].

The objective of the author of this thesis was to set up and validate PRODUCERS as a support engineering tool. Specifically, to deploy the software and conduct simulations replicating data acquisition from the Cluster II re-entry airborne campaign. While confidentiality restrictions prevent the inclusion of the Cluster II results, this section presents findings based on the example case included in the software package.

A PRODUCERS analysis follows a structured workflow, illustrated in Figure 70. It consists of:

- Defining the Satellite Model: The vehicle description (vehicle.xlsx) is created in PADRE, specifying materials and potential emission species.
- Generating the Trajectory: A DRAMA re-entry simulation is executed to provide trajectory and fragmentation data.
- Importing Data into PRODUCERS: The DRAMA output, along with the PADRE generated vehicle definition, are loaded into PRODUCERS.
- Running the Simulation:
 - Phase 1 - Broad Spectral Overview: This step generates preliminary results covering the entire spectral range, identifying key features.
 - Phase 2 - Refined Spectral Analysis: Based on Phase 1, this step zooms into specific spectral regions for higher resolution analysis.
- Post-Processing & Validation: Results are compared with observational data for verification.

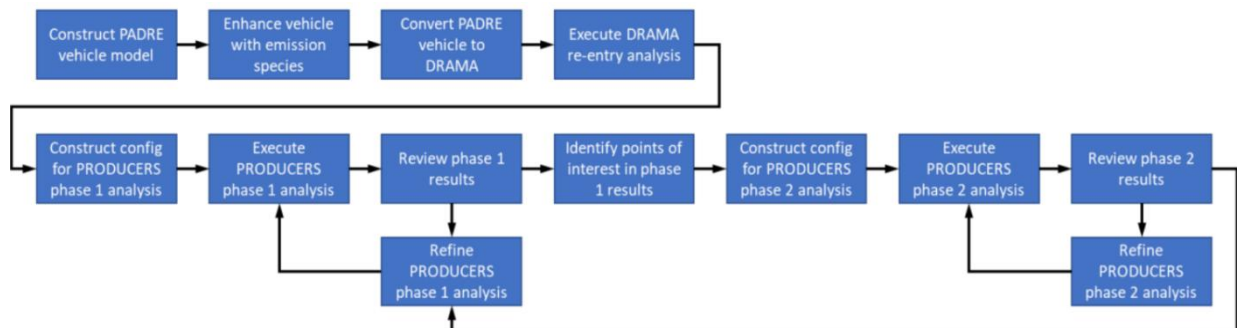


Figure 70: PRODUCERS analysis process workflow [73].

PRODUCERS executes several tasks for understanding the radiative properties of re-entering satellites:

- **Grey body emission calculation:** The tool estimates thermal radiation emitted by the main satellite fragments based on their material properties and temperature. This emission is vital in determining how visible the object will be in different spectral bands.
- **Shock layer radiation estimation:** By analysing the heated air surrounding the satellite, PRODUCERS computes the radiation emitted by ionised and excited atmospheric species. An equilibrium shock layer forms around a re-entering fragment when the airflow is compressed and heated to high temperatures due to the object's supersonic velocity. In this state, the shock layer reaches thermochemical equilibrium, meaning the ionisation, dissociation, and excitation of air species balance out over time. This allows for the estimation of temperature, density, and molecular composition, which are critical for understanding re-entry heating, ablation, and radiation effects. An example of the results for the Shock Layer temperature is presented in Figure 71 where each colour represents each of the air species for each fragment as a function of time. This step is essential to understand the high energy emissions that could be observed by remote sensing instruments.

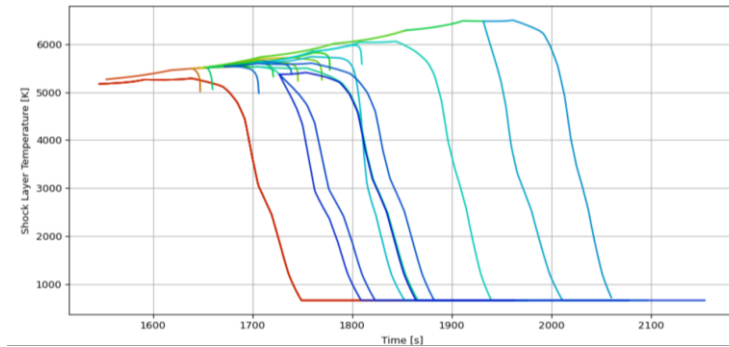


Figure 71: Example EquilibriumShock Shock Layer Temperature Plot PRODUCERS [73].

- **Material specific radiation contributions:** PRODUCERS models how components made of different materials, such as Aluminium, Titanium, and Carbon, contribute to the overall emission spectrum. This enables the identification of specific emission lines that could be used to infer material composition.
- **Fragmentation influence on emissions:** The tool considers how breaking apart into smaller pieces affects thermal radiation and shock layer emissions. Fragment gas emission refers to the release of gases from a fragment during re-entry. The emission depends on the fragment's temperature and mass loss rate, with spectral markers indicating the presence of different species. A key parameter, as it directly influences emissions, is the indicative radiance, presented in Figure 72. The different colours represent distinct spectral emissions from various gas species. For example, blue may indicate atomic oxygen (O), red for nitrogen (N₂), and green for ionised nitrogen (N₂⁺).

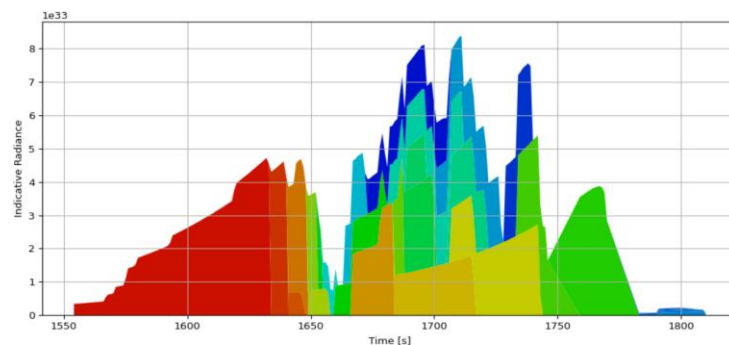


Figure 72: Example FragmentGasEmission Indicative Radiance Plot PRODUCERS [73].

- **Particle and gas emission analysis:** As the satellite disintegrates, particles and gases are released. PRODUCERS estimates their radiation contribution, which is important for characterising the full re-entry emission profile.
- **Observer specific spectral predictions:** Depending on the chosen observation method (ground based or airborne), PRODUCERS adjusts the spectral calculations to simulate what a real observer would detect. This is critical for mission planning and sensor positioning optimisation.
- **Generate demise timeline:** This task produces a table of events within a DRAMA trajectory. This includes the start and finish of each simulation within the trajectory, the start and completion of object demise within a simulation and the start and finish of radiation of marker species. Each line in the table shows when each of the objects is demising and the emissions it has, as illustrated in Figure 73.

Visualisation of object demise as a function of time

- Green = period of demise with no gaseous emission
- Blue = period of demise with gaseous fragment emission
- Red = period of demise with both fragment and particle gaseous emission

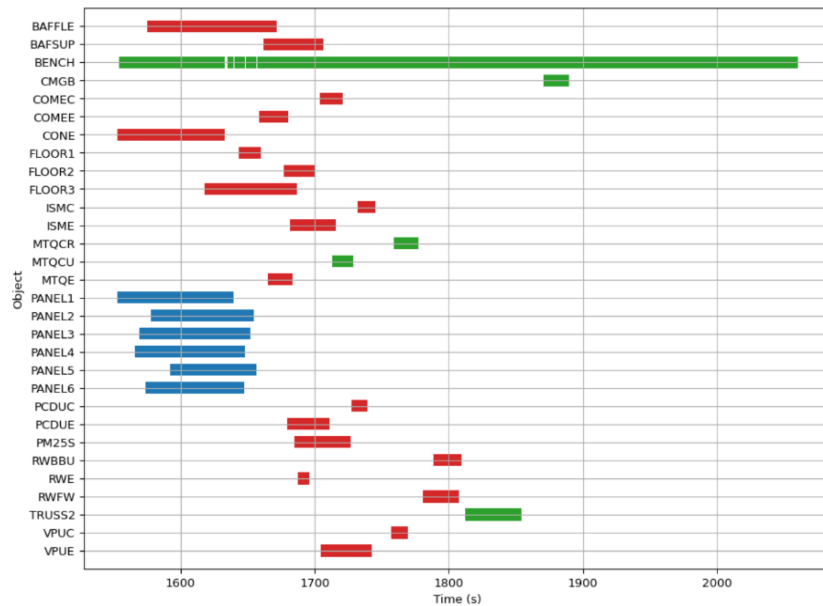


Figure 73: Example GenerateTimeline Object Demise Timeline PRODUCERS [73].

Originally, PRODUCERS required manual input of aircraft trajectory points, which was impractical for real airborne campaigns involving thousands of data points. To streamline this process, the author of this thesis implemented a function that automatically imports trajectory data from a .dat file. This script reads latitude, longitude, timestamps, and datetime values, eliminating manual entry and reducing errors. This modification enables efficient airborne campaign simulations, making PRODUCERS more applicable to real observation missions.

The results obtained with PRODUCERS simulation tool are relevant for multiple reasons:

- **Re-entry observation planning:** By predicting spectral characteristics, researchers can optimise sensor placement and observation strategies.
- **Material identification:** The emission lines help to remotely identify satellite materials during re-entry.
- **Validation of demise models:** Comparing PRODUCERS output with observed data supports the refinement of satellite demise models.
- **Airborne and ground based observation feasibility:** The simulations provide insight into which spectral features are best captured from an aircraft, guiding campaign planning.

The next step is to correlate Cluster II airborne observation data with PRODUCERS results to refine the software further. This is not included in the present document as it was not possible to curate Cluster's II re-entry data before the end of the author's internship. Once this data is available and the correlation with the simulations results is performed, it will enhance PRODUCERS predictive accuracy and allow it to support future re-entry campaigns, such as DRACO, in determining optimal aircraft trajectories and spectral observation windows.

6.3 Cameras' location

DRACO will be equipped with four cameras, each strategically positioned to capture critical aspects of the satellite's demise during atmospheric re-entry. These cameras play a crucial role in gathering visual data, which will be used to correlate and validate re-entry simulation models and on ground testing and improve our understanding of satellite fragmentation dynamics.

The placement of the cameras is determined by the scientific objectives of DRACO (shortly presented in Sections 6 and 6.1) and the derived requirements. The aim of DRACO's cameras allocation is for each camera to comply with a specific function while capturing high-speed fragmentation events data:

- **Camera 1:** to record the **structural break up** of the satellite, focusing on a **corner** of the structure as the highest heat flux is expected to be there.
- **Camera 2:** to record the **structural break up** of the satellite, focusing on an **edge** of the structure as one of the highest heat fluxes is expected to occur there.
- **Camera 3:** Directed at **material samples** attached to the spacecraft. This setup enables real-time observation of the thermal and mechanical degradation of various materials.
- **Camera 4:** Directed at the **tanks** to study their demise as Ool and verify the demisability of the demisable tank designed to verify D4D technologies and compare them with non-demisable critical ones.

Due to the technical specifications of the cameras and the need to maximise scientific return, determining their optimal placement and orientation was a necessary task. To achieve this, simulations were conducted using the EVENT SIMULATOR software tool [74], which allowed for an analysis of different camera positions and angles to ensure the best possible coverage of the satellite's demise.

6.3.1 Software tool EVENT SIMULATOR simulations

EVENT SIMULATOR is a software tool designed to predict the response of an instrument embedded on a re-entering satellite as it fragments and demises. The software integrates data from DRAMA and PADRE to simulate how components interact with environmental conditions during atmospheric re-entry. Due to confidentiality about DRACO platform design and re-entry parameters, the DRAMA simulations and CAD of the satellite are not presented in this thesis as they are not necessary for the reader to interpret the results obtained with EVENT SIMULATOR. This enables the simulation of various instrument responses, including sensors and cameras, under different re-entry conditions [74]. The software executes four tasks, each providing information about the spacecraft's demise:

- **Task 1 calculateDDCUConnectivity:** evaluates the connectivity of the instruments. It models how the DDCU stays connected to sensor boxes and sensors during the fragmentation process, helping to assess data continuity and potential sensor failures. An example is presented in Figure 74, where the connectivity of sensors to the DDCU is presented at almost 120 km of altitude and around 45 km of altitude after starting re-entry for a case studied for DRACO. It can be seen that the connectivity at 45 km is much more reduced as expected.

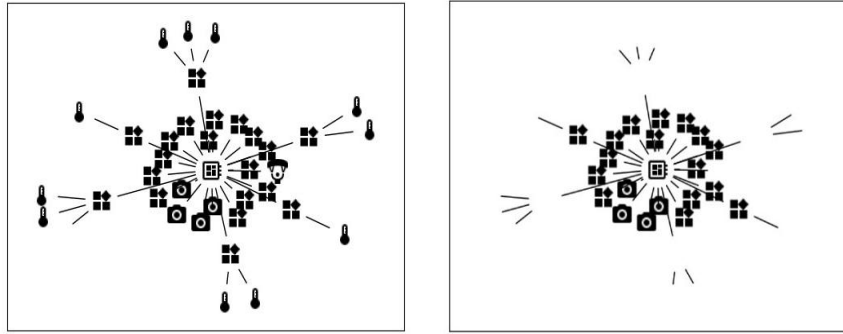


Figure 74: DDCU connectivity of a DRACO re-entry study case at around 120 km and 45 km of altitude respectively.

- **Task 2 calculateComponentThermalResponse:** simulates the thermal response of satellite components, predicting temperature profiles throughout re-entry. It aids to understand how each material endures demise and when structural failures might occur.
- **Task 3 calculateInstrumentResponse:** analyses the response of intrusive sensors, including thermocouples, pressure sensors and strain gauges. It provides data on mechanical stress, thermal loads and sensor survivability.
- **Task 4 calculateCameraResponse:** models the cameras' ability to capture the satellite's demise. It considers parameters such as Field of View (FoV), focal distance, clipping planes and light sources to evaluate the optimal camera placements and orientations.

To optimise the positioning and orientation of the cameras onboard DRACO, a series of simulations were conducted using EVENT SIMULATOR after deploying the tool. The workflow is presented in Figure 75 and followed these steps:

- **Definition of the satellite:** The structural and material composition of DRACO was described using spreadsheets following the PADRE format.
- **Importing DRAMA re-entry data:** The trajectory and fragmentation predictions generated by DRAMA were imported into EVENT SIMULATOR.
- **Execution of camera response simulations:** The "calculateCameraResponse" task was executed to analyse different camera placements and orientations.

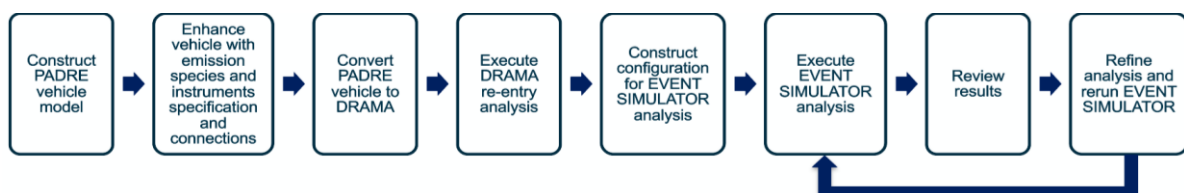


Figure 75: EVENT SIMULATOR's workflow.

Several parameters influencing camera performance were modified for these simulations, to represent the cameras that will be on board of DRACO. Those parameters include the FoV, focal point and clipping distances. Moreover, since this task also generated videos of what the camera would record during the demise, the step size was modified, to reduce simulation time and control frame rendering frequency while keeping enough scientific accuracy for the task purpose.

One of the outputs of this task was the camera mesh data. As the mesh data was in .VTP format, it was converted to .STL using PyVista. These files were then imported into a CAD software for further visualisation and analysis as presented in Figure 76, where the 'pyramid' shapes in green represent the FoV of the camera to understand what it would record in each orientation, allowing for a faster iteration of its positioning and orientation.

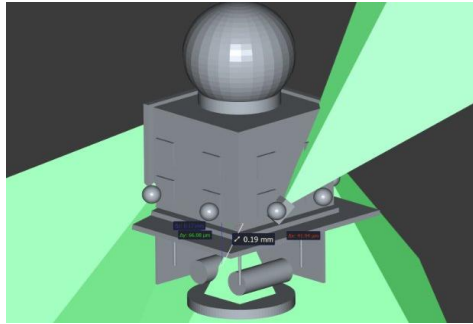


Figure 76: DRACO simplified CAD with the FoV of the on-board cameras in green with the tanks' camera on the centre of the mid-panel looking downwards.

To optimise the camera setup, multiple iterations were performed with different positioning and orientations. Several configurations were tested, including:

- **Camera on top of the mid-panel, looking downwards:** provided a clear view of the top part of the tanks, but failed to fully capture the demise of both tanks due to the limited FoV. As illustrated in Figure 76, only the part of the tanks closer to the centre of the satellite in the X-Y plane is comprised by the FoV of the camera.
- **Camera at the structure corners:** allowed for a broader perspective but still did not allow for a complete view of both tanks (see Figure 77), for the given tanks' location.
- **Camera on the middle an edge of the mid panel:** this placement still did not fully capture both tanks simultaneously within the current FoV as seen in Figure 78.

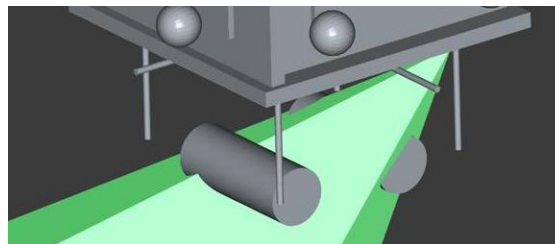


Figure 77: DRACO simplified CAD with the tank on-board camera at the corner of the lower box of the platform.

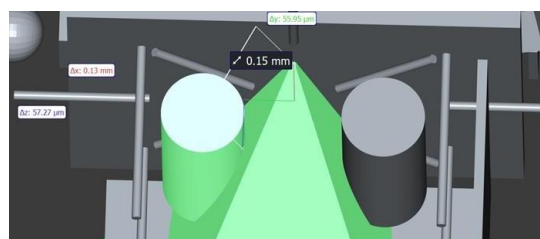


Figure 78: DRACO simplified CAD with the tank on-board camera at the middle of the lower side of the mid-panel.

The results of these simulations revealed that no single configuration could fully record both tanks due to the constraints of the selected camera's FoV and tanks location. As a result, this limitation has been taken into account in the ongoing reassessment of the tanks' placement within the DRACO. Adjustments to their location are being considered to ensure the best possible scientific return from the available camera perspectives.

The findings from the EVENT SIMULATOR simulations highlight the complexity of demise observation and underscore the importance of an iterative approach in optimising instrument placement within the DRACO mission. By refining the camera placements using EVENT SIMULATOR, DRACO's imaging system will provide the highest possible scientific return.

7. Conclusions

This thesis explored several aspects of the demise behaviour of satellites' elements under uncontrolled atmospheric re-entry conditions. The findings and conclusions presented herein contribute to the development of satellite platforms that enhance demisability, improving existing designs and promoting the creation of new ones tailored for compliance with evolving space sustainability regulations. Given the increasing relevance of D4D in the European space industry, the research of this thesis holds relevance for future satellite development efforts.

The thesis first provided an overview of the current state of space debris, emphasising the urgent need for sustainable EoL management strategies. Various approaches to mitigating debris generation were reviewed, highlighting the D4D solution. As D4D is a recent field where industrial competition limits publicly available information, a literature review was conducted to establish a knowledge base on existing research, technological developments and best practices.

One of the key contributions of this thesis is the investigation of strategic approaches to designing demisable satellite platforms. The study examined critical design parameters such as external shape, thickness, ballistic coefficient and material selection, factors that significantly influence re-entry behaviour. Through this analysis, critical components with high survivability rates during re-entry were identified, aligning with findings in existing literature. These include propellant tanks, RWs, MTQs and mechanical joints among others, each requiring specific demisability enhancements to ensure disintegration before reaching the Earth's surface.

To address these challenges, the thesis reviewed demisable technologies under development and proposed a development roadmap to advance their maturity. The roadmap outlines the steps and estimated timeframes for achieving a demisable satellite platform, offering a pathway for future research. Integrating AM was also explored to optimise mass and cost while enhancing demisability, making scalable and mass producible solutions more viable.

A significant portion of this research has also contributed directly to the DRACO mission, which aims to improve understanding of satellite demise behaviour through in situ re-entry observations. Despite extensive testing in PWT facilities and advanced simulations, significant uncertainties remain regarding the actual break up processes and material interactions during atmospheric re-entry. DRACO seeks to bridge this gap by using onboard sensors to measure in-flight demise and fragmentation dynamics, providing crucial data to refine existing re-entry models. The research included in this thesis played a role in integrating Ool, such as the PEAK tanks and spectroscopic markers into DRACO, helping validate their performance under real conditions and maximising the scientific return of this mission. Once DRACO is launched, correlating its flight data with PWT and simulation results will also contribute to improving the scalability of demisable technologies and refining methodologies for future missions.

Ultimately, the findings of this thesis align with the broader industry goal of developing fully demisable satellite platforms that comply with SDMR while maintaining cost-effectiveness and operational reliability. By assessing critical components demisability, providing a state-of-the-art of available D4D technologies, laying the groundwork for D4D implementation in identified gaps and for the maturation of existing technologies, and contributing to DRACO's scientific objectives, this research supports the long-term sustainability of space activities. The proposed advancements in demisable technologies and manufacturing processes pave the way for future satellite platforms designed to ensure safe re-entry, reinforcing the importance of integrating demisability into the early stages of spacecraft development.

Bibliography

- [1] ESA Space Debris Mitigation WG, ESA Space Debris Mitigation Compliance Verification, Noordwijk, 2023.
- [2] ESA, “Reentry and Collision avoidance,” [Online]. Available: https://www.esa.int/Space_Safety/Space_Debris/Reentry_and_collision_avoidance. [Accessed January 2025].
- [3] ESA, “The current state of space debris,” 12 October 2020. [Online]. Available: https://www.esa.int/Space_Safety/Space_Debris/The_current_state_of_space_debris. [Accessed January 2025].
- [4] United Nations, “The 17 Goals,” [Online]. Available: <https://sdgs.un.org/goals>. [Accessed January 2025].
- [5] E. S. Agency, “Clean Space,” [Online]. Available: https://www.esa.int/Space_Safety/Clean_Space/Clean_Space2. [Accessed January 2025].
- [6] NASA, State-of-the-Art Small Spacecraft Technology, 2023.
- [7] N. V. Patel, “Satellite mega-constellations,” 2 April 2020. [Online]. Available: [https://www.technologyreview.com/technology/satellite-mega-constellations/..](https://www.technologyreview.com/technology/satellite-mega-constellations/) [Accessed January 2025].
- [8] Orbiting now, “Orbiting now,” [Online]. Available: <https://orbit.ing-now.com/>. [Accessed March 2025].
- [9] A. A. Looten, DESIGN FOR DEMISE APPLIED TO SPACECRAFT STRUCTURAL PANELS AND EXPERIMENTS FOR CLEARSPACE-ONE PLATFORM, Lausanne, 2024.
- [10] A. Thompson, “The Kessler Syndrome,” 21 January 2021. [Online]. Available: <https://spacecentre.co.uk/blog-post/the-kessler-syndrome/>. [Accessed January 2025].
- [11] ESA, “Active debris removal,” 20 February 2023. [Online]. Available: https://www.esa.int/Space_Safety/Space_Debris/Active_debris_removal. [Accessed January 2025].
- [12] J. McDowell, “Space Activities in 2021,” 03 January 2022. [Online]. Available: <https://www.planet4589.org/space/papers/space21.pdf>. [Accessed January 2025].
- [13] M. Panasovskyi, “Debris from the Soviet Kosmos-1408 satellite destroyed by the Russian ASAT missile poses a threat to Starlink,” 11 August 2022. [Online]. Available: <https://gagadget.com/en/science/156722-debris-from-the-soviet-kosmos-1408-satellite-destroyed-by-the-russian-asat-missile-poses-a-threat-to-starlink/>. [Accessed January 2025].

- [14] D. J. Kessler and B. G. Cour-Palais, "Collision frequency of artificial satellites: The creation of a debris belt," *Journal of Geophysical Research: Space Physics*, vol. 83, no. A6, pp. 2637-2646, 1 June 1978.
- [15] ESA, "ESA's Space Environment Report 2022," 22 April 2022. [Online]. Available: https://www.esa.int/Space_Safety/Space_Debris/ESA_s_Space_Environment_Report_2022. [Accessed January 2025].
- [16] INTER-AGENCY SPACE DEBRIS COORDINATION COMMITTEE, "IADC Space Debris Mitigation Guidelines," 2007.
- [17] ESA, "8th European Conference on Space Debris - links for media," [Online]. Available: https://www.esa.int/Space_Safety/Space_Debris/8th_European_Conference_on_Space_Debris_-_links_for_media. [Accessed January 2025].
- [18] C. Fuglesang, "Lecture 3, The Space Environment, SD2905 Human Spaceflight," Stockholm, 29-1-2024.
- [19] ESA, "CLEAN SPACE," [Online]. Available: <https://technology.esa.int/program/clean-space>. [Accessed January 2025].
- [20] U. Gotzig, E. Zaccaria and M. Wurdak, "DEORBIT AND CLEAN SPACE – WHAT WE NEED FROM A SPACE PROPULSION POINT OF VIEW," in *2nd International Conference on Flight Vehicles*, Heilbronn, 2022.
- [21] ESA, "CleanSat | Passivation," 05 March 2019. [Online]. Available: https://www.esa.int/ESA_Multimedia/Images/2019/03/CleanSat_Passivation. [Accessed January 2025].
- [22] J. Delaval, "ON THE ATMOSPHERIC IMPACT OF SPACECRAFT DEMISE UPON REENTRY," 11 August 2022. [Online]. Available: <https://blogs.esa.int/cleanspace/2022/08/11/on-the-atmospheric-impact-of-spacecraft-demise-upon-reentry/>. [Accessed January 2025].
- [23] FCC, Space Innovation; Mitigation of Orbital Debris in the New Space Age, Washington D.C., 2022.
- [24] P. Minacapilli, S. Campo Pérez, F. Criado Zurita, G. De Zaiacomo, I. Pontijas and B. Bastida Virgili, "TOWARDS A DESTRUCTIVE RE-ENTRY ASSESSMENT CONTAINER," in *chez 2nd International Conference on Flight Vehicles, Aerothermodynamics and Re-entry Missions & Engineering (FAR)*, Heilbronn, 2022.
- [25] ESA, "BURNING UP A MAGNETORQUER IN A PLASMA WIND TUNNEL," 23 April 2019. [Online]. Available: <https://blogs.esa.int/cleanspace/2019/04/23/burning-up-a-magnetorquer-in-a-plasma-wind-tunnel/>. [Accessed January 2025].
- [26] L. Grassi, "Design for Demise techniques for medium/large LEO satellites reentry," in *7th European Conference on Space Debris*, Darmstadt, 2017.

- [27] J. Amos, "UK 'knitted satellite' will see Earth day or night," 05 May 2023. [Online]. Available: <https://www.bbc.com/news/science-environment-65483204>. [Accessed January 2025].
- [28] ESA, "Laser communication terminal," 05 June 2015. [Online]. Available: https://www.esa.int/ESA_Multimedia/Images/2015/06/Laser_communication_terminal. [Accessed January 2025].
- [29] J. Delaval, "THE RE-ENTRY BREAK-UP EXPERIMENT ASSESSMENT," 22 November 2018. [Online]. Available: : <https://blogs.esa.int/cleanspace/2018/11/22/the-re-entry-break-up-experiment-assessment/>. [Accessed January 2025].
- [30] ESA, "ATV's fiery break-up to be seen from inside," 17 July 2014. [Online]. Available: https://www.esa.int/Enabling_Support/Space_Engineering_Technology/ATV_s_fiery_break-up_to_be_seen_from_inside. [Accessed January 2025].
- [31] ESA, "Salsa's last dance targets reentry over South Pacific," 26 January 2024. [Online]. Available: https://www.esa.int/Enabling_Support/Operations/Salsa_s_last_dance_targets_reentry_over_South_Pacific. [Accessed January 2025].
- [32] ESA, "Cluster reentry explained: world's first targeted reentry," 08 September 2024. [Online]. Available: https://www.esa.int/esatv/Videos/2024/09/Cluster_reentry_explained_world_s_first_targeted_reentry. [Accessed February 2025].
- [33] T. Rongier and I. Sgobba, "Space Safety is No Accident," *Springer International Publishing, Cham*, no. ISBN 978-3-319-15981-2 978-3-319-15982-9, 2015.
- [34] GmbH, Aerospace & Advanced Composites, "AAC - WRK-Facility-Description-l2R0.pdf," April 2020. [Online]. Available: <https://www.aac-research.at/wp-content/uploads/2023/01/WRK-Facility-Description-l2R0.pdf>. [Accessed February 2025].
- [35] O. Chazot, C. O. Asma, J. Thoemel, S. Paris and S. C. Tirtey, "Utilization of infrared thermography to investigate atmospheric entry aerothermodynamics of space vehicles at von Karman Institute," in *9th International Conference on Quantitative InfraRed Thermography*, Krakow, 2008.
- [36] P. Minacapilli, F. Criado Zurita, S. Campo Pérez, J. De Zaiacomo, I. Pontijas and B. D'Andrea, "Addressing DRACO mission phase A design challenges," in *Clean Space Industry Days*, Noordwijk, 2022.
- [37] T. Schleutker, B. Esser and A. Gülhan, "CHARDEM, Tests on baseline materials in re-entry environment, Final Report," 2015.
- [38] A. Fagnani, B. Helber, O. Chazot, A. Hubin, P. Laha and L. Walpot, "In situ multi-band apparent emissivity measurements of aerospace materials in inductively coupled plasma flows," *Infrared Physics & Technology*, p. p. 105301, 2024.

- [39] J. Beck and a. et, "Characterisation of materials and structures under re-entry conditions (COPPER) - Final Report," 2023.
- [40] J. Beck and a. et, "SPACECRAFT OBJECT RISK EVALUATION DATABASE (SCORED): FINAL REPORT," 2024.
- [41] J. Beck, T. Schleutker, M. Weihreter, T. Lips, P. Laurenti and A. Sita, "Demise for Containment Executive Summary," 2023.
- [42] T. Schleutker, A. Gülhan, S. Röddecke, E. Kaschnitz, J. Beck and R. Close, "On Demisable Fiber Reinforced Plastic Composites," in *Clean Space Industry Days*, Noordwijk, 2023.
- [43] T. Schleutker, A. Gülhan, S. Röddecke, E. Kaschn and J. Beck, "Development of Demisable Fiber," in *Clean Space Industry Days*, Noordwijk, 2022.
- [44] B. Lockett, "Final Report D4D-OnE: Platform Optics and Electronic equipment demise," 2024.
- [45] O. U. e. H. Najaf, "Thermal protection systems for space vehicles: A review on technology development, current challenges and future prospects," *Acta Astronautica*, vol. 176, no. ISSN 0094-5765, pp. 341-356, 2020.
- [46] E. Venkatapathy, B. Laub, G. Hartman, J. Arnold, M. Wright and G. Allen, "Thermal protection system development, testing, and qualification for atmospheric probes and sample return missions. Examples for Saturn, Tital and Staradust-type sample return..," *Advances in Space Research*, vol. 44, no. 1, pp. 138-150, 2009.
- [47] M. Trisolini, H. G. Lewis et C. Colombo, «Demisability and survivability sensitivity to design-fordemise techniques,» *Acta Astronautica*, vol. 145, pp. 357-384, 2018.
- [48] J. Beck, I. Holbrough and T. Schleutker, "The Revolutionary Design of Spacecraft through Holistic Integration of Future Technologies - ReDSHIFT Final Report," 2018.
- [49] Thales Alenia Space Italy, "D4D Final Report," 2016.
- [50] D4DBB Team (OHB, INVENT, DLR, Blestead, Fluid Gravity, HTG), "TN11 Final Report D4D Breadboarding," 2019.
- [51] A. Gülhan and T. Schleutker, "Demisable Solar Array Driving Mechanism Final Presentation," 2021.
- [52] N. Eggen, "Demisable SADM," 2021.
- [53] A. Caiazzo, J. Beck, T. Schleutker, T. Soares and L. Innocenti, "Plasma Wind Tunnel Demisability Testing of Spacecraft Equipment," in *First International Orbital Debris Conference*, Sugar Land, Texas, 2019.
- [54] D. Riley, I. Pontijas Fuentes, J.-C. Meyer, G. Proffe and T. Lips, "Multi-Disciplinary Assessment of Design for Demise Techniques: Final Report and Executive Summary," Harwell, 2017.

- [55] J. Beck, I. Holbrough and T. Schleutker, "CHARACTERISATION OF BEHAVIOUR OF CRITICAL ELEMENTS IN RE-ENTRY CONDITIONS: FINAL REPORT," Ashford, 2019.
- [56] S. Bianchi, "Study on demisability of optical payloads (D4OP), Executive Summary Report," 2017.
- [57] J. Beck, N. Joiner, S. Bainbridge and P. Doel, "STUDY ON DEMISABILITY OF OPTICAL PAYLOADS: D2 DESIGN FOR DEMISE TECHNIQUES FOR OPTICAL PAYLOADS," 2017.
- [58] J. Beck, A. Caiazzo, B. Ganzer, T. Lips, P. Laurenti, B. Lockett, T. Schleutker, T. Soares, D. Wischert and L. Suriani, "Re-entry safety: Analysis and Plasma Wind Tunnel testing of design for containment techniques to reduce on-ground casualty risk," 2021.
- [59] S. Kraus, M. Flach and A. Sylvaïn, "BB06: Early Breakup Structures Executive Summary," 2016.
- [60] T. Lips, "Executive Summary Report: Spacecraft demise during re-entry expedited using various exothermic reactions (SPADEXO)," 2023.
- [61] A. Finazzi, F. Maggi, C. Paravan, D. Daub, S. Dossi, A. Murgia, T. Lips, G. Smet and K. Bodjona, "Thermite-for-Demise (T4D): Preliminary assessment on the effects of a thermite charge in arc-heated wind tunnel experiments," in *Aerospace Europe Conference 2023 – 10TH EUCASS – 9TH CEAS*, 2023.
- [62] Airbus DS GmbH, "BB05 Demisable Metallic Propellant Tank Final Report," 2016.
- [63] H. Lange and C. Bauer, "Demisable metallic propellant tanks Executive Summary," 2021.
- [64] A. Caiazzo, "Design for Demise - Technologies ESA Accademy," Noordwijk, 2021.
- [65] M. Schleiffelder, "Demisable Tanks for LEO satcoms: Final Report," 2021.
- [66] S. Hartl, "Preliminary Tank Design Requirements," Holzhausen, 2024.
- [67] S. Bonavita, H. and P. , "CLEANSAT'S TECHNOLOGY ASSESSMENT AND CONCURRENT ENGINEERING IN SUPPORT OF LEO PLATFORM EVOLUTIONS," 2016.
- [68] A. Amador, J. Castanheira and P. Coelho, "Public Executive Summary CleanSat Demisable Magnetorquer Study," 2016.
- [69] B. Ganzer and B. Lockett, "Executive Summary Report D4C-Containment," 2022.
- [70] L. Theuns and et al, "Characterization of off-stagnation point pyrolysis in plasma flow using optical measurement techniques," 2015.
- [71] D. Evans, J. Merrifield, H. Whitehouse, N. Donaldson, J. Beck, I. Holbrough, A. Pagan, J. Oswald, M. Winter, G. Herdrich and M. Lino da Silva, "Spectroscopic Response of Break-up Fragments to the Re-entry Environment - Final Report," Emsworth, 2024.
- [72] M. Schleiffelder, "Strip Tape PWT - Testplan Demisability Tanks for LEO SatComs," Holzhausen, 2021.

[73] J. Beck, I. Holbrough and J. Merrifield, "SOFTWARE USER MANUAL FOR RADIATIVE OBSERVATION PREDICTION IN RE-ENTRY," Ashford, 2023.

[74] A. Flinton, "Generic Breakup Instrument: Event Simulator Software User Manual - Issue 2," Emsworth, 2024.

Appendix

The following Tables 6 and 7 provide a summarised overview of the demise behaviour analysis conducted as part of this thesis. They summarise the main findings previously presented including the **demise behaviour** of satellite components, the **critical drivers** for demise, an assessment of each component’s **overall demisability criticality**, and a selection of proposed D4D concepts to enhance demise.

Component	Demise behaviour	Critical Drivers	Demisability	D4D Ideas
Structural Panels 🏠	Adhesive softening, panel peeling and core collapse	Adhesive degradation, material thermal response	High (but key for altitude release of inner components)	<ul style="list-style-type: none"> - Panel free designs - Early break up - Topology optimisation
Joints 🔩	Screws loosen or fail, and cleats weaken	Thermomechanical load and rotation effects	Medium	<ul style="list-style-type: none"> - Aluminium or SMA screws - Printed cleats - Damping rubbers
Solar Arrays ☀️	CFRP ablation, core melts and early cell detachment	CFRP layer burn off, aerodynamic loads	High	<ul style="list-style-type: none"> - Weak points for early fragmenting (if necessary)
SADM ⚙️	Progressive melting and failure, and early detachment of small Steel parts	Local heating in driveline cavity, Steel material	Medium	<ul style="list-style-type: none"> - Use more demisable materials - Design for early gear break up
Batteries 🔋	Casing melts, GFRP fails, and faster fragmentation for higher spin rates	Casing material, GFRP recession, rotation speed	Medium (Small cells demise, large do not)	<ul style="list-style-type: none"> - Replace/enhance GFRP break up - Use predesigned weak points
Electronics 📡	PCB oscillation, delamination and housing melt off	GFRP behaviour, and shielding effects	Medium	<ul style="list-style-type: none"> - Use predesigned weak points - Size reduction - Replace GFRP: limited feasibility
Propellant Tanks 🚰	CFRP chars and acts as a heat sink, and Titanium survives	Material: Titanium’s high melting point	Very Low	<ul style="list-style-type: none"> - Use more demisable materials - Pyro-cutting (high risk) - Thermite coatings (mass risk)
Thrusters 🔥	Lower half demises faster than upper, and potting outgassing delays heat transfer	Material thickness, potting behaviour, and nozzle material	Medium: depends on material and half	<ul style="list-style-type: none"> - Use more demisable materials - Thinner sections - Redistribute potting

Table 6: Summary of demise behaviour of components part 1.

Component	Demise behaviour	Critical Drivers	Demisability	D4D Strategies
Balance Masses ⚖️	Survive due to high mass/density Aluminium masses tend to demise	Material type (Steel vs Aluminium), mass, internal vs external placement	Medium: Steel or Aluminium masses	<ul style="list-style-type: none"> - Smaller units with demisable containers - External mounting and AM
Reaction Wheels (RW) 🌀	Staged demise: housing fails first, then internal Al parts melt, flywheel and motor survive	Material conductivity, structural layout, and motor heat sink effect	Low: housing demises; motor, BBU and flywheel survive	<ul style="list-style-type: none"> - Use Al for inertial rims - Use CuBe for flywheels - Glued parts for break up
Magnetorquers (MTQ) 🧲	CFRP housing ablates layer by layer Copper windings poor conductivity Core melts at high flux	Core and housing material, exposure time and location, insulation effects	High: depends on release altitude	<ul style="list-style-type: none"> - Replace Steel with Nickel - External placement - Improve heat transfer
Gyroscopes 🌀	Multiple subcomponents survive Fused Silica sensor coils and GFRP cards resist heat Low Kinetic Energy but high CA	Use of Fused Silica, GFRP, and compact design	Low: high survivability	<ul style="list-style-type: none"> - Replace GFRP by demisable materials - Promote early break up
Star tracker 🌟	Structural detachment, but Titanium parts survive Lenses flow out rather than break	Size, material (Ti, Borosilicate), rotation, and helicoil failure	Low: small partially demise, large ones survive	<ul style="list-style-type: none"> - Use demisable materials - Promote early break up - Reduce size if feasible
Optical Payloads 📡	Mirrors and lenses survive Mounts materials and compact design affect break up Shock impingement drives heating	Material resistance, mounting rigidity, shape/size, and shielding	Low: Mirrors/lenses survive; fixings and baffles may demise	<ul style="list-style-type: none"> - Use demisable materials - Use orifices and AM - Weaken interface points - Adhesive joints

Table 7: Summary of demise behaviour of components part 2.

Moreover, in Figure 79 it is presented an infographic that allows to visualise the proposed roadmap for achieving a demisable satellite platform. The roadmap outlines in two phases the milestones and development steps, from the redesign and initial testing of critical components to the integration and full-level testing of D4D technologies. This roadmap aims to provide a structured approach to maturing demisable solutions and supports the broader goal of aligning satellite design with emerging space sustainability regulations, such as ESA’s SDMR.

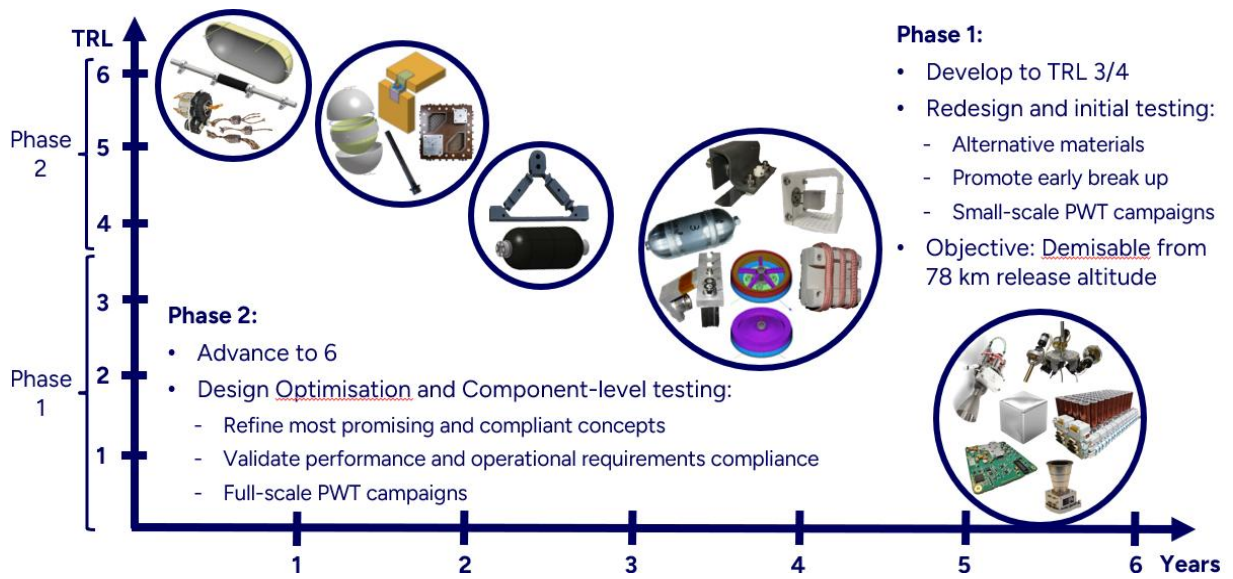


Figure 79: D4D development roadmap for a demisable satellite platform.

(This is the end of the thesis)

TRITA – SCI-GRU 2025:041.

Stockholm, Sweden 2025

www.kth.se